Characterization of the plant-derived isotopic proxies for precipitation reconstruction in the tropics

विद्या वाचस्पति की
उपाधि की अपेक्षाओं की आंशिक पूर्ति में प्रस्तुत शोध प्रबंध

A thesis submitted in partial fulfillment of the requirements of the degree of Doctor of Philosophy

द्वारा /By
अमृता साईश्री/ Amrita Saishree

पंजीकरण सं ./ Registration No.: 20183580

शोध प्रबंध पर्यवेक्षक / Thesis Supervisor: Dr. Shreyas Managave

भारतीय विज्ञान शिक्षा एवं अनुसंधान संस्थान पुणे
INDIAN INSTITUTE OF SCIENCE EDUCATION AND RESEARCH PUNE
2024

Dedicated to my grandparents

Late Birabara Lenka

Late Kananbala Lenka

DECLARATION

I declare that this written submission represents my ideas in my own words and where others' ideas have been included, I have adequately cited and referenced the original sources. I also declare that I have adhered to all principles of academic honesty and integrity and have not misrepresented or fabricated or falsified any idea/data/fact/source in my submission. I understand that violation of the above will be cause for disciplinary action by the Institute and can also evoke penal action from the sources which have thus not been properly cited or from whom proper permission has not been taken when needed.

Date: January 13, 2024

Amrita Saishree

Roll No. 20183580

CERTIFICATE

Certified that the work incorporated in the thesis entitled **"Characterization of the plant-derived isotopic proxies for precipitation reconstruction in tropics"** Submitted by **Ms. Amrita Saishree** was carried out by the candidate, under my supervision. The work presented here or any part of it has not been included in any other thesis submitted previously for the award of any degree or diploma from any other University or institution.

Date: January 13, 2024

(Dr. Shreyas Managave)

Supervisor

Associate Professor,

Earth and Climate Science,

Indian Institute of Science Education and Research (IISER) Pune

Dr. Homi Bhabha Road, Pashan, Pune-411008, India.

ACKNOWLEDGEMENTS

I extend my heartfelt gratitude to my supervisor, Dr. Shreyas Managave, without whom the successful completion of my Ph.D. work would not have been possible. His mentorship has not only contributed significantly to my intellectual development but has also shaped me into a more resilient and resourceful individual. In addition to being an exceptional supervisor, he has played the role of a compassionate friend during the inevitable challenges that arise while pursuing a Ph.D. As I reflect on the culmination of my Ph.D. journey, I realize that his influence will endure as a positive force in my career and life.

I express my sincere appreciation to Research Advisory Committee (RAC) members, Prof. Prasanta Sanyal and Prof. Deepak Barua, for their insights, expertise and constructive feedback, which have enriched the quality of my research. I am grateful of the opportunity to have collaborated with Prof. Prasanta Sanyal, who hosted me at Stable Isotope Laboratory of the Indian Institute of Science Education and Research Kolkata (SILIKA), IISER Kolkata, where I carried out a significant amount of laboratory work. I extend my gratitude to Prof. Deepak Barua for his support in facilitating the successful execution of the outdoor experiment and field measurements carried out at IISER Pune. His expertise in plant biology provided valuable insights and guidance at every stage of the experiment.

I am thankful to prof. M.G. Yadava for his pivotal role in conducting isotopic analysis of water samples at PRL, Ahmedabad. I extend my sincere appreciation to Prof. Ansgar Kahmen for his generosity in addressing my queries over emails particularly concerning the intricacies of the isotope-labelling experiment. I am grateful to Mr. Anil Sutar from the horticulture unit at IISER Pune for his assistance in arranging and tending to the plants during the experiment.

I express my gratitude to Dr. Girish Jathar for helping with the sample collection for the precipitation gradient investigation.

I express my deep gratitude to IISER Pune for granting me an institute fellowship during the tenure of my doctoral research. A special thanks to the director of IISER Pune for fostering an enriching academic environment and offering me the privilege of being hosted as a Ph.D. student.

The successful completion of this thesis work owes much to the conducive research environment provided by the department of Earth and Climate Science (ECS) at IISER Pune. My sincere thanks to all faculty members and colleagues for their constant support throughout my doctoral research.

I extend my heartfelt gratitude to my lab mate Salam Maheshwori Devi who has been a sister to me throughout my Ph.D. journey. Her unwavering support, encouragement and familial warmth made the challenges of doctoral studies more manageable. I am also thankful to my lab mates Sindoora. P and Sushant Rauthan whose contributions have been instrumental in fostering a warm and positive lab environment. The stimulating discussions, collaborative spirit, enthusiasm and friendly demeanor of all the lab members at the biogeochemistry lab have significantly contributed to overall well-being and productivity within lab.

I am grateful to Dr. Vijayananda Sarangi for assuming the role of an elder brother during my tenure conducting laboratory work at IISER Kolkata. He taught me the lab protocols and utility of various instruments with great patience. His guidance not only enhanced my technical skills but also contributed significantly to the smooth progression of my laboratory work. I am thankful to Mahesh Da for his invaluable support during my sample analysis work at IISER Kolkata.

I would like to thank my friends, Shilpi, Samparna and Dikshya for their unwavering support in every stage of my life. I am truly thankful for the depth of our friendship and the positive impact it has had on me.

Lastly, my heartfelt gratitude goes to my parents Mr. G. B. Singh, Mrs. Bijayalaxmi Singh and my sister Ipsita Saishree, for their patience and continuous support. Their encouragement, understanding, and sacrifices have been the bedrock of my Ph.D. journey and their love has been a constant source of inspiration.

CONTENTS **Page**

LIST OF FIGURES

LIST OF TABLES

Abstract

Proxy-based paleoclimate reconstructions provide climate data extending back to thousands to millions of years. These reconstructions not only contribute to our understanding of the past climate but also play a crucial role in validating climate models that can be used to project future climate changes. For past precipitation reconstructions, a variety of climate proxies are used. However, the reconstructions are often qualitative, limiting their applicability. To quantify past precipitation variability, it is essential to apply a transfer function to the climate proxies. This requires characterization of the response of the climate proxies and the establishment of an empirical relationship between their response and concurrent precipitation. This thesis work focuses on characterizing various plant-derived isotope proxies widely utilized for past precipitation reconstructions, viz. (i) the hydrogen isotopic composition (δD) of leaf wax *n*-alkanes and *n*-alkanoic acids, (ii) plant-derived carbon ($\delta^{13}C$) and δD isotopes in soil and plants. The emphasis is on characterization of the plant-derived proxies from the tropical climate.

Quantifying the hydrogen isotope fractionation between leaf wax compounds and source water (ε_{app}) is a prerequisite for leaf wax-based paleo-hydrological studies. However, the characterization of the ε_{app} values, mostly done in field-based studies, are predominantly carried out in northern mid-latitude regions as compared to that in the tropics. Further, the ε_{app} values estimated in field-based studies are often associated with inherent uncertainties that could stem from (i) incorrect source water δD values, (ii) species-effect, and (iii) varying climatic conditions (as in transect studies). Hence, to characterize the ε_{app} values in the tropics and to decouple the factors affecting the variability of ε_{app}, an outdoor experiment was conducted wherein four evergreen and three deciduous angiosperm trees were grown under similar climatic conditions for 85 days with water of known δD value (−2‰). The ε_{app} values in the studied species were −119 ± 23‰ (n = 14) for *n*-alkanes and −126 ± 27‰ (n = 12) for *n*-alkanoic acids of chain lengths C_{31} and C_{30}, respectively. Inter-species variabilities in ε_{app} values that are consistent with previous field and transect studies were observed. As the plants were grown under similar climatic conditions and irrigated with water of the same δD value, the variability in ε_{app} values observed here suggested that the species-specific hydrogen isotopic fractionation likely has a dominant control over the uncertainty in the community-averaged ε_{app}values. Further, the ε_{app} values of

deciduous and evergreen species showed no systematic differences, suggesting that changes in the relative proportion of these taxa may not affect the community-averaged ε_{app} and the reconstructed δD values of paleo-precipitation in angiosperm tree-dominated catchments.

The climatic parameters controlling the hydrogen isotope composition (δD) of leaf-wax *n*-alkanes and *n*-alkanoic acids, used widely in paleohydrologic research, are fairly known. However, the climatic parameters of exactly which period (i.e. early or entire period of the leaf's lifespan) these biomarkers represent is unclear. A longer duration experiment was conducted, wherein, tropical deciduous and evergreen species were grown with the normal (δD = −2‰) water followed by the isotopically-labeled water (δD = 1000‰) during a growing season. The observed differences between the δD values of *n*-alkanes (and *n*-alkanoic acids) of the leaves collected later and prior to the application of the isotopically-labeled water were 38 ± 38‰ (and 32 ± 42‰). These differences were much smaller than the corresponding expected differences that varied from 272 ± 118 to 547 ± 127 for *n*-alkanes and 272 ± 118 to 547 ± 133‰ for *n*-alkanoic acids, indicating insignificant (7-9%) production of these biomarkers in the mature leaves of deciduous and evergreen species. The δD analysis of *n*-alkanes and *n*-alkanoic acids of new leaves emerging during the next growing season in deciduous species indicated minor incorporation of the previous year's photosynthates in the leaf wax pool of the current year's mature leaves. The overall positive correlation between the δD values of *n*-alkanes and *n*-alkanoic acids (r^2= 0.7, n = 60, $p < 0.05$) indicated synchronous synthesis of these biomarkers. Unlike inferences from extra-tropical studies, this work suggests the δD records of both biomarkers are biased towards the climatic conditions prevailing during the early stages of the leaf's growth. The climate models aimed at reproducing the leaf wax δD-based hydroclimatic reconstructions should consider this bias.

Precipitation plays a crucial role in controlling the $\delta^{13}C$ and δD values of plants. The organic matter derived from plants, when integrated into the soil and sedimentary archives, carries valuable information about past precipitation conditions. In this study, the possibility of establishing a relationship between various plant-derived isotopic proxies and precipitation amount was explored along a precipitation gradient ~500 to 3700 mm/yr in western peninsular India. It was observed that the $\delta^{13}C$ values of soil organic matter ($\delta^{13}C_{SOM}$) and *n*-alkanes ($\delta^{13}C_{alk}$) in soil exhibited a negative correlation with the precipitation amount. The calibration equation derived from $\delta^{13}C_{SOM}$ values and precipitation amount provides a means for past precipitation

reconstruction from $\delta^{13}C_{SOM}$ values of paleosols in western peninsular India. The $\delta^{13}C_{alk}$ values of different *n*-alkane homologues in soil correlated negatively with the precipitation amount, as did the $\delta^{13}C_{SOM}$; measurement of $\delta^{13}C_{alk}$ values in soil (which is analytically more challenging) may not be necessary for paleo precipitation reconstruction, as their interpretations would yield outcomes similar to that derived from the $\delta^{13}C_{SOM}$ studies. The δD values of *n*-alkanes (δD_{alk}) in soil showed a positive correlation with precipitation amount, contrary to the expected negative correlation arising due to the 'amount effect' in tropical precipitation. This discrepancy indicated the influence of local vegetation composition (i.e. tree vs grasses) on the measured δD_{alk} values in soil. Therefore, a vegetation composition correction might be necessary before reconstructing the δD values of precipitation from the measured δD_{alk} values in various archives. The $\delta^{13}C$ values of C_4 grasses were positively correlated with precipitation amount indicating an influence of precipitation on the end-member $\delta^{13}C$ values of C_4 grasses. However, the observed sensitivity for this dependence was low: 0.07 ± 0.03 ‰ per 100 mm of precipitation. The low sensitivity implies that minor fluctuations in precipitation amount may not significantly impact the $\delta^{13}C$ values of C_4 grasses. In such cases, the use of uncorrected (i.e. modern) $\delta^{13}C$ values of C_4 grass end-member may not introduce significant error in the vegetation reconstruction studies from western peninsular India.

Chapter 1
Introduction

1.1 Introduction

Sustained global warming is anticipated to have far-reaching effects on the Earth's climate system. It has been predicted that global warming will increase the variability of precipitation, extreme wet and dry weather, climate events and seasons in the future (IPCC, 2023). The assessment of climate models employed for projecting future climate scenarios is often based on their capacity to reproduce past climate conditions (Flato et al., 2013). By assessing their performance in replicating past conditions, efforts can be made to refine and improve these models, making them valuable tools for understanding and addressing the complex challenges posed by climate change. To capture the full range of past climate variability, researchers rely on a combination of short instrumental records and paleoclimate data (Armstrong et al., 2020). Instrumental records, which typically span the last century, provide a detailed and accurate account of climatic parameters such as temperature, and precipitation at a high temporal resolution. However, instrumental climate data is of too short duration to assess the natural climate variability; it also cannot reveal climate during different mean states of climate. This necessitates the need to have pre-instrumental climate data. Proxy-based paleoclimate reconstructions provide climate data extending back to thousands to millions of years, thereby increasing the temporal scope of climate analysis.

For past precipitation reconstructions various marine and terrestrial climate proxies have been used. The marine proxies mainly constitute the chemical composition of marine sediments (Haug et al., 2001; Hendy et al., 2015; Martinez-Ruiz et al., 2015, Du et al., 2021) and the isotopic composition of corals (Sun et al., 2005; Shen et al., 2005), foraminifera (Burton and Vance, 2000; Tiwari et al., 2006). The terrestrial proxies such as the isotopic composition of stalagmites (McDermott, 2004; Mattey et al., 2008; Dayem et al., 2010; Cai et al., 2015), leaf wax derived biomarkers (Hou et al., 2008; Sachse et al., 2012; Feakins et al., 2016) and tree-rings (Managave et al., 2011; Morales et al., 2012; Yang et al., 2014) have been used. Pollen assemblage preserved in sediments has also yielded information on past precipitation (Guiot et al., 1993; Bonnefille and Chalie, 2000; Chevalier et al., 2020).

Although the climate proxies have yielded important information about the past climate variability and factors controlling it, the qualitative nature of the reconstructed climate has been

one of the limitations. The quantitative reconstructions of past climate not only help to assess the extent of variation in the past climate but also provide an opportunity to test the veracity of the climate models (Haywood et al., 2019; Liu et al., 2020). To quantify the past precipitation variability, the transfer or calibration functions (Rozanski et al., 1997; Ramesh, 2001) are necessary. The estimation of transfer or calibration functions often involves establishing an empirical relationship between the response of the proxies and concurrent precipitation (Terwilliger et al., 2008; Feakins et al., 2016; Stein et al., 2021). However, regional climate variations and their effect on various proxies can influence the transfer functions in different geographical areas. This underscores the necessity for region-specific calibrations between proxies and climate variables.

One of the important utilities of proxy-based past climate reconstructions is in testing the veracity of climate models by checking whether the models correctly reproduce the reconstructed past climate variability. Before such validation exercise is carried out it is important to know the climate of which season the proxy-based reconstructions represent. The correlation of yearly response of the climate proxies which are annually resolved (e.g. tree-ring width) with monthly climate parameters (such as temperature or precipitation) of concurrent years often reveals that the former do not reflect annual climatic conditions but conditions during certain month(s) (Fritts et al., 1991). This bias towards the climatic conditions of a particular season is called seasonality in the proxy response. However, because of the limited span of instrumental climate records, an alternative approach is needed to decipher the seasonality in the proxies revealing centennial-scale variability (e.g. the hydrogen isotopic composition (δD) of the leaf wax compounds in lake sediments).

1.2 Leaf wax compounds

Plant leaf wax compounds are useful proxies for providing insights into the past climate (Liu and Huang, 2005; Tierney et al., 2008; Hren et al., 2010; Tipple and Pagani, 2010; Collins et al., 2013). The outer surfaces of plant leaves have a protective cuticular wax layer which is a complex mixture predominantly comprised of various long-chain compounds such as *n*-alkanes, *n*-alkanoic acids, *n*-alkanols, phytol, sesquiterpenes (Chikaraishi et al., 2004). These compounds are preserved in a variety of geological archives, including lake sediments, peat bogs, and marine

sediments. The widespread occurrence of leaf wax compounds in terrestrial plants, their resistance to degradation (Bush and McInerney, 2013) and isotopic exchange below 100°C (Sessions et al., 2004) makes them suitable for studying past climate changes over different spatial and temporal scales.

1.2.1 δD of leaf wax n-alkanes and n-alkanoic acids

The δD values of leaf wax *n*-alkanes and *n*-alkanoic acids reflect the δD values of precipitation (δD_{precip}) (Sachse et al., 2012; Tipple and Pagani, 2013; Feakins et al., 2016) which is used to estimate the variability in past precipitation amount and atmospheric circulation (Konecky et al., 2011; Feakins et al., 2019; Ghosh et al., 2020; McGrath et al., 2021, Managave et al., 2023). The δD signature of water taken up by plants from soil is influenced by δD value of precipitation. The transported water is then utilized for the synthesis of leaf wax *n*-alkanes and *n*-alkanoic acids. However, several steps involved in the process fractionate the hydrogen isotopes (Sachse et al., 2012) (Fig. 1.1). The source water undergoes evaporative enrichment in deuterium in the leaf during transpiration; the extent of enrichment depends mainly upon the relative humidity and leaf temperature (Roden et al., 2000). The final leaf water that is used in the synthesis of organic molecules, the biosynthetic water pool, is the mixture of evaporatively enriched leaf water and the xylem/source water. Finally, the synthesis of *n*-alkanes and *n*-alkanoic acids leads to the isotopic fractionation that favors hydrogen over deuterium. The net fractionation between the source water and leaf wax *n*-alkanes and *n*-alkanoic acids δD values is termed as apparent fractionation (ε_{app}).

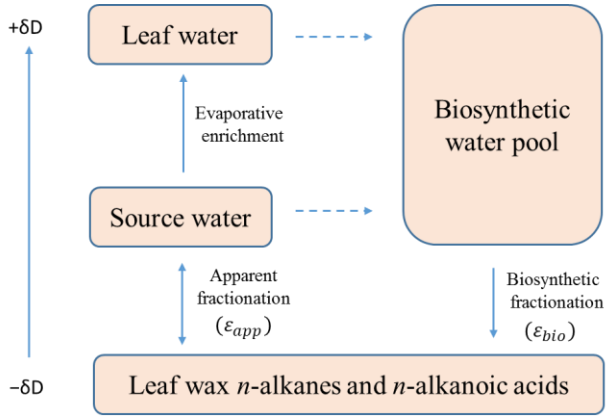

Fig. 1.1 Schematic illustration of δD fractionations during leaf wax synthesis.

1.2.2 ε_{app} of leaf wax n-alkanes and n-alkanoic acids

For quantitative assessment of paleo-precipitation variability or atmospheric circulation, a reliable estimation of the hydrogen isotopic fractionation between the leaf wax compounds and precipitation (ε_{app}) is essential.

Previous field (Chikaraishi et al., 2004; Hou et al., 2007; Sachse et al., 2009; Gao et al., 2014; Sachse et al., 2015; Freimuth et al., 2017; Huang et al., 2018) and transect studies (Sachse et al., 2006; Feakins and Sessions, 2010; Tipple and Pagani, 2013; Feakins et al., 2016; Berke et al., 2019; O'Connor et al., 2020) have reported ε_{app} values of different climatic regimes. However, not only the factors influencing uncertainty associated with ε_{app} is not constrained well but also the global ε_{app} dataset is strongly biased towards Northern Hemisphere mid-latitude biomes (Sachse et al., 2012). The estimation of ε_{app} values for *n*-alkanes and *n*-alkanoic acids at a local and regional scale is desired for reliable reconstruction of paleo-precipitation δD values (Feakins and Sessions, 2010; Daniels et al., 2017; Berke et al., 2019; Liu and An, 2019; Corcoran et al., 2022). Fewer studies encompassing different regions of tropical latitudes exist (Fig. 1.2). Using ε_{app} values of Northern Hemisphere mid-latitude biomes might lead to a systematic bias in the reconstructed δD_{precip} values at tropical biomes.

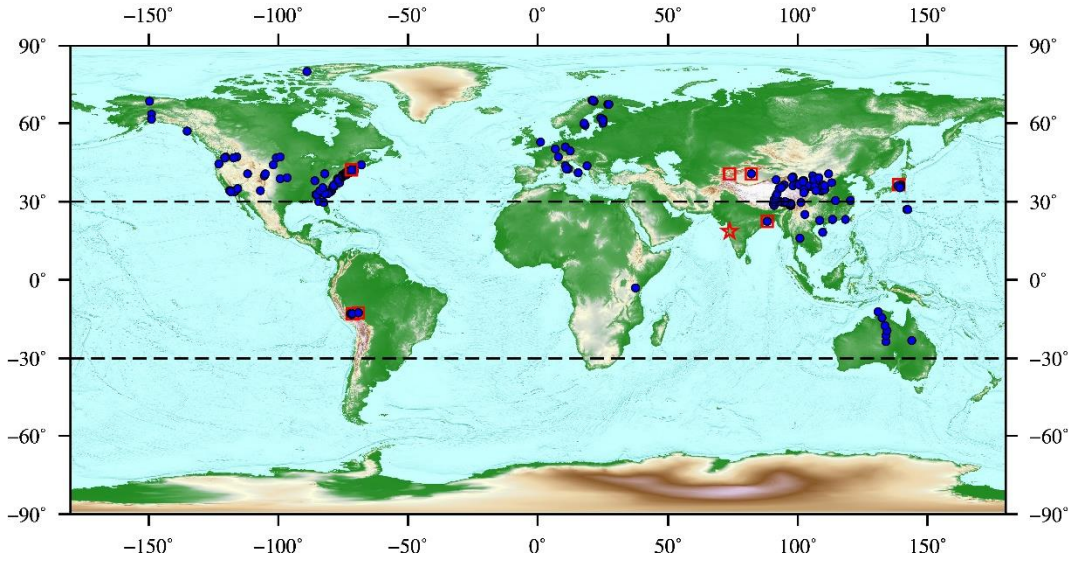

Fig. 1.2. Distribution of plant leaf wax *n*-alkanes (blue circles) and *n*-alkanoic acids (red squares) hydrogen isotope studies. The star symbol marks this study. Data source: Sachse et al., (2012);

Yang et al., (2021); Duan et al., (2014); Feakins et al., (2016); Friemuth et al., (2017); Griepentorg et al., (2019); Liu and An, (2019); Roy and Sanyal., (2022).

The estimation of ε_{app} values involves measuring the δD values of leaf wax compounds and contemporaneous precipitation/source water (Hou et al., 2007; Pedentchouk et al., 2008; Sachse et al., 2009; Tipple and Pagani, 2013; Daniels et al., 2017; O'Connor et al., 2020). In most studies where ε_{app} values of modern vegetation were reported, the source water δD values were assumed to be similar to that of environmental water bodies i.e., lakes, streams, rivers and groundwater (Douglas et al., 2012; Duan et al., 2012; Freimuth et al., 2017; Daniels et al., 2017). Studies (Li et al., 2019; Corcoran et al., 2022) have also considered the interpolated δD_{precip} values derived from the Online Isotopes in Precipitation Calculator (OIPC) (Bowen and Revenaugh, 2003) that uses the Global Network of Isotopes in Precipitation (GNIP) data. However, estimated ε_{app} values may show systematic offsets due to the assumption of the incorrect source water δD values which could stem from interpolation of δD_{precip} values (Ladd et al., 2021). The depth-dependent variation in the δD values of soil water (White et al., 1985; Garcin et al., 2012) and limited knowledge about the rooting depth of different plant species might also lead to an assumption of incorrect source water δD values. These limitations underscore the need for experimental work using source water with known δD values for determining the absolute ε_{app} of a region.

In addition to δD values of the source water, the ε_{app} values are affected by (i) the species effect (i.e., the influence of a given species on the extent of evaporative enrichment of the leaf water in deuterium, and on the isotopic fractionation between leaf water and leaf wax compounds; the latter called as biosynthetic fractionation, ε_{bio}) and (ii) ambient climatic conditions such as relative humidity. Differences in leaf phenology, morphology and stomatal characteristics contribute to differential leaf water enrichment (Grice et al., 2004; Smith and Freeman, 2006; Liu and Yang, 2008; Diefendorf et al., 2011; Gao et al., 2015). The plausibility of ε_{bio} influencing community-averaged ε_{app} values has also been realized (Gamarra et al., 2016). Relative humidity, leaf temperature and the isotopic composition of atmospheric water vapor also influence the enrichment of the heavier isotopes in the leaf water (Flanagan et al. 1991; Farquhar and Lloyd, 1993) and consequently the ε_{app} values. In transect studies, where both plant species, as well as

external environmental conditions, vary, assessing the relative influence of the species effect and external conditions on ε_{app} is often challenging. Hence, an experimental study involving different plant species grown under similar environmental conditions and with water of known δD value may better constrain the species effects on the ε_{app} values.

The global dataset on δD value of the leaf wax compounds is also biased towards *n*-alkanes (Sachse et al., 2012). Only a few studies have dealt with both *n*-alkanes and *n*-alkanoic acids in the leaf waxes of the same plants (e.g., Chikaraishi and Naraoka, 2007; Feakins et al., 2016; Freimuth et al., 2017; O'Connor et al., 2020; Yang et al., 2021). It has been suggested that *n*-alkanes preserve climate signatures of the early growing season and *n*-alkanoic acids preserve signatures of the entire growing season (Freimuth et al., 2017; Yang et al., 2021). Knowing the ε_{app} values of both *n*-alkanes and *n*-alkanoic acids could provide us with the past seasonal as well as annual hydroclimatic variability. Furthermore, in the absence of site-specific ε_{app} values of *n*-alkanoic acids, ε_{app} values of *n*-alkanes and an average alkane–acid offset occurring during biosynthesis reported for a different region have often been used (e.g. in Konecky et al., 2016). Therefore, direct estimation of ε_{app} of different leaf wax compounds and their offset for a given biome would further enhance the robustness of reconstructed δD_{precip} values from that biome.

The influence of monsoonal rainfall on the Indian economy is well-established (Mooley & Parthasarathy, 1983; Gadgil, 2003). Understanding of the rainfall variability during different mean states of climate in the past can help in constraining the response of monsoonal rainfall to the current climate change. Various proxies have been used to reconstruct past monsoonal rainfall variability (Morrill et al., 2003; Ramesh et al., 2010; Misra et al., 2019; Banerji et al., 2020). The importance of leaf wax δD as a proxy for reconstructing past monsoonal variability has been highlighted (Sarkar et al. 2015; Ghosh et al., 2020; McGrath et al., 2021; Managave et al., 2023). However, the lack of region-specific ε_{app} values has hampered the accurate estimation of δD_{precip} (Mangave et al., 2023). Further, studies based on pollen records have reported vegetation shifts between evergreen to deciduous taxa (Kumaran et al., 2013; Prasad et al., 2014) owing to monsoonal rainfall variability. The effect of such a shift in the vegetation on community-scale ε_{app} values is not known.

1.2.3 Seasonality in leaf wax δD records

The δD values of leaf wax *n*-alkane (Liu and Huang, 2005; Hren et al., 2010; Tipple and Pagani, 2010; Collins et al., 2013; Ghosh et al., 2020) and *n*-alkanoic acid (Tierney et al., 2008; Konecky et al., 2011; McGrath et al., 2021; Managave et al., 2023) have been extensively used for reconstruction of centennial to millennial-scale climate variability. The δD variability of past precipitation have been reconstructed employing these biomarkers (e.g. Konecky et al., 2011; Feakins et al., 2019; McGrath et al., 2021; Managave et al., 2023). Various isotope-enabled Global Circulation Models (GCMs) can simulate water isotopic composition of the precipitation (Sturm et al., 2010). The leaf wax-based reconstructed δD_{precip} values thus allow validation of the outputs of the isotope-enabled GCMs simulations (Knapp et al., 2022). The leaf wax-based reconstructed δD_{precip} values could potentially be used to test the outputs of water-isotope-enabled global circulation models [e.g. ECHAM5-wiso (Werner et al., 2011); isoGSM (Yoshimura et al., 2008); CAM3iso (Sturm et al., 2010), SPEEDY-IER (Dee et al., 2015), CAM5 (Nusbaumer et al., 2017), LMDZ-iso GCM (Risi et al., 2010)].

However, ambiguity exists regarding the seasonality in these records. Sachse et al., (2010) and Tipple et al., (2013) have reported the early growing season bias i.e. the δD record reveals the climatic conditions prevailing during the early growing season whereas Huang et al., (2018) and Sachse et al., (2009) suggested that the δD records integrate the climate conditions of the entire growing season. Further, a few studies (Freimuth et al., 2017; Yang et al., 2021) have observed the δD records of *n*-alkanes are biased toward the early growing season whereas, that of *n*-alkanoic acids are not biased towards any particular season. The effect of carryover of photosynthates (Sessions, 2006; Tipple et al., 2013) from the end of the growing season of a year to the beginning of the growing season of the next year on seasonality is not fully known. The effect of vegetation type (i.e. deciduous vs evergreen) and climatic regime (i.e. temperate vs tropical) on the seasonality in the δD records of *n*-alkanes and *n*-alkanoic acids is also not clear.

The leaf wax compounds are known to reflect δD values of the source water (Feakins et al., 2016; Tipple and Pagani, 2013; Sachse et al., 2012) and ambient climatic conditions (Smith and Freeman, 2006; Feakins and Sessions, 2010; Tipple et al., 2015) prevailing during their synthesis. Therefore, the timing of *n*-alkanes and *n*-alkanoic acids synthesis in the leaf determines

the climate of which season their δD records preserve (Kahmen et al., 2011; Sachse et al., 2015; Huang et al., 2018). The seasonal variation in the abundance of leaf wax compounds and their isotopic compositions can be used to reveal the timing of leaf wax production (Tipple et al., 2013; Yang et al., 2021). However, the utility of the former in this context is limited as is it affected by factors such as wind ablation (Freimuth et al., 2017), temperature stress, intense UV radiation and insect attacks (Shepherd and Griffiths 2006; Jetter et al., 2006). Temporally varying δD values of the leaf wax compounds have been used to reveal seasonality in their production (Tipple et al., 2013; Freimuth et al., 2017; Huang et al., 2018; Yang et al., 2021). However, the leaf wax δD variability in the periodically sampled leaves that flushed together could stem from the inter-leaf δD variability (up to 38‰; Hou et al., 2007) and/or synthesis of the new wax (with different δD values). When the former is larger, the leaf wax δD variability in the periodically collected leaves may not unambiguously prove the production of new leaf wax. Further, in a region where the factors controlling δD values of the leaf wax compounds do not vary significantly (e.g. aseasonal tropical forest), a constant δD value of the leaf wax compounds might not rule out continuous synthesis of the leaf wax.

The efficacy of the experiments involving isotopically-labeled source water in studying seasonality in the production of *n*-alkanes in a tree (Kahmen et al., 2011) and *n*-alkanes and *n*-alkanoic acid in a grass (Gao et al., 2012) has been demonstrated. A short-duration (50 days) experiment on one temperate tree species, wherein a pulse of tracer water was applied for 7 days, showed that the *n*-alkane pool, once formed, does not change subsequently (Kahmen et al., 2011). However, experiments of longer duration are necessary to assess the production of *n*-alkane and *n*-alkanoic acids in mature leaves if the turnover rate of these compounds is slow. Further, the suggestion that *n*-alkanes and *n*-alkanoic acids reflect climatic conditions during the early and entire growing seasons, respectively (Freimuth et al., 2017; Yang et al., 2021) has not been verified in experimental studies.

As with the investigation that estimated ε_{app}, most of the investigations regarding seasonality in *n*-alkane and *n*-alkanoic acid δD records have been carried out in temperate (Sachse et al., 2009; Sachse et al., 2010; Tipple at al., 2013; Freimuth at al., 2017) and sub-tropical regions (Yang et al., 2021; Huang et al., 2018); seasonality in tropical δD records is not known.

1.3 Plant-derived climate proxies and their relationship with precipitation

1.3.1 Carbon isotopes of C_3 and C_4 plants

The two major categories of vegetation are C_3 and C_4 plants. While the former constitutes trees, the latter are mostly grasses. For carbon fixation during photosynthesis, these plants use different pathways: C_3 (Calvin cycle) and C_4 (Hatch-Slack) pathways. Owing to this, the C_3 and C_4 plants fractionate carbon isotopes differently and thus have distinct carbon isotope ($\delta^{13}C$) signatures (Cerling et al., 1997). Typically, the $\delta^{13}C$ values of C_3 plants vary from −20‰ to −37‰ in C_3 plants (Kohn, 2010), whereas it varies from −9‰ to −16‰ in C_4 plants (Wynn and Bird, 2008).

The atmospheric moisture-influenced factors (such as relative humidity and stomatal conductance) play a significant regulatory role in controlling the $\delta^{13}C$ of plants (Farquahar, 1983; Weiguo et al., 2005; Cordon et al., 2013; Diefendorf et al., 2010). The precipitation amount influences relative humidity which in turn controls the stomatal conductance. Hence the precipitation amount can indirectly influence $\delta^{13}C$ of plants. Therefore, $\delta^{13}C$ values of plants have been utilized for past precipitation reconstructions (Liu et al., 2005; Galy et al., 2008; Youfeng et al., 2008; Ortiz et al., 2021).

To understand the effect of precipitation variability on $\delta^{13}C$ values of plants, many investigations have been carried out (Weiguo et al., 2005; Swap et al., 2004; Stevenson et al., 2005; Hartman and Danin, 2010). Typically, the $\delta^{13}C$ values of C_3 plants show a negative correlation with precipitation amount (Kohn et al., 2010). However, the correlation between $\delta^{13}C$ values of C_4 plants with precipitation amounts can be positive (Murphy and Bowman, 2009; Basu et al., 2015), negative (Ma et al., 2012; Weiguo et al., 2005) or zero (Swap et al., 2004; Hartman and Danin, 2010).

1.3.2. C_3 and C_4 vegetation composition

The C_4 plants can thrive in water-limited ecosystems because of their high water use efficiency compared to C_3 plants. Therefore, the relative proportion of trees and grasses at a location is influenced mainly by precipitation amount, especially at low altitudes (Sage et al.,

2003). At the high-altitude sites temperature may exert an additional influence by hindering the establishment of native trees in the grassland (Joshi et al., 2020).

1.3.3 Carbon isotopes of the soil organic matter ($\delta^{13}C_{SOM}$) and reconstruction of past vegetation composition

The organic materials derived from plants are integrated into the soil. Therefore, the $\delta^{13}C$ signatures of plants growing at a location influence the $\delta^{13}C$ of soil organic matter ($\delta^{13}C_{SOM}$). As the $\delta^{13}C$ values of C_3 and C_4 plants are distinct, the $\delta^{13}C_{SOM}$ values are utilized for reconstructing past vegetation composition which in turn gives an idea about concurrent precipitation. For quantitative paleovegetation reconstructions from $\delta^{13}C_{SOM}$, an isotope mass balance equation is utilized (Vidic and Montanez, 2004; Nordt et al., 2008; Yang et al., 2015), with the end members being the $\delta^{13}C$ values of C_3 and C_4 plants. However, the end member $\delta^{13}C$ values may vary spatially or temporally, depending on the regional $\delta^{13}C$ values of the plants (Basu et al., 2015) or variations in $\delta^{13}C$ values of plants with respect to changes in climate conditions (Wang et al., 2008; Yang et al., 2015; Sarangi et al., 2021). Selection of appropriate end member $\delta^{13}C$ values requires the knowledge of region-specific $\delta^{13}C$ values of C_3 and C_4 plants and their variations with climate parameters including precipitation amount.

1.3.4 Carbon isotopes of long-chain n-alkanes ($\delta^{13}C_{alk}$) preserved in soil

The carbon isotopes of long-chain *n*-alkanes ($\delta^{13}C_{alk}$) preserved in soil are used to understand precipitation variabilities (Diefendorf and Freimuth, 2017). The $\delta^{13}C_{alk}$ values are derived from terrestrial plants only and thus are robust representations of the vegetation of a region compared to $\delta^{13}C_{SOM}$, as the latter may incorporate signatures from heterogeneous organic inputs (Baczynski et al., 2016; Basu et al., 2019). Therefore, establishing a regional quantitative relationship between the $\delta^{13}C_{alk}$ values in soil and precipitation would help in the reconstruction of past vegetation composition and precipitation.

1.3.5 Hydrogen isotopes of long-chain n-alkanes (δD_{alk}) preserved in soil

The hydrogen isotopic compositions of the plant leaf waxes (δD_{alk}) are known to preserve δD_{precip} (Huang et al., 2004; Hou et al., 2008; Sachse et al., 2012; Tipple and Pagani, 2013; Feakins et al., 2016). The δD_{alk} values are integrated into the soil when the plants shed their leaves. Thus,

the δD_{alk} values preserved in marine and lacustrine sediments have been used extensively to reconstruct past precipitation isotope variability (Pagani et al., 2006; Shuman et al., 2006; Niedermeyer et al., 2010; Konecky et al., 2011). Although a large number of studies have examined plant δD_{alk} values (Chikaraishi et al., 2004; Sachse et al., 2006; Smith and Freeman, 2006; Hou et al., 2007; Sachse et al., 2009; Feakins and Sessions, 2010; McInerney et al., 2011; Gao et al., 2014; Tipple and Pagani, 2013; Duan et al., 2014; Sachse et al., 2015; Feakins et al., 2016; Friemuth et al., 2017; Huang et al., 2018; Berke et al., 2019; Griepentorg et al., 2019; Liu and An, 2019; O'Connor et al., 2020; Yang et al., 2021; Roy and Sanyal., 2022), relatively few studies have investigated δD_{alk} values in soil (Chikaraishi and Naraoka, 2006; Krull et al., 2006; Jia et al., 2008; Rao et al., 2011; Zech et al., 2015; Hermann et al., 2017; Lu et al., 2020; Aichner et al., 2021). Depending on the vegetation and climate of a region, the δD_{alk} values in soil may vary. Understanding the variability of δD_{alk} values in soil with precipitation amount in a region can help in their effective utilization for precipitation reconstructions.

1.3.6 Calibrating $\delta^{13}C$ values of the plant-derived climate proxies against precipitation

For calibrating the isotopic composition of the plant-derived climate proxies, modern plants and soil are sampled from various places and their isotopic response is calibrated against local precipitation. The correlations between $\delta^{13}C$ of modern C_3 and C_4 vegetation with precipitation amounts have often been leveraged for quantitative reconstructions of past vegetation (Zhang et al., 2003; Wang et al., 2008; Sarangi et al., 2021) and precipitation amount (Youfeng et al., 2008) from the $\delta^{13}C_{SOM}$ preserved in sediments and paleosols.

A global compilation of variations of modern $\delta^{13}C_{SOM}$ values with precipitation amount has been provided by Stein et al., (2021). However, as the compiled dataset consists of data points from C_3-dominated ecosystems, the past precipitation using this dataset can be quantified only for the periods between post-Devonian (~420 Ma) to the Miocene (~23 Ma). Nevertheless, regional modern $\delta^{13}C_{SOM}$ signatures of ecosystems consisting of both C_3 and C_4 vegetation have also shown a significant correlation with precipitation amount (Stevenson et al., 2005, Lee et al., 2005; Ma et al., 2012; Feng et al., 2008). For utilization of $\delta^{13}C_{SOM}$ values as a paleo-precipitation proxy post-expansion of C_4 plants, deriving regional calibrations between modern $\delta^{13}C_{SOM}$ values and precipitation amount are necessary.

The sites having a precipitation gradient give an opportunity to establish a quantitative relationship between plant-derived isotopes and precipitation amount (Swap et al., 2004; Stevenson et al., 2005; Feng et al., 2008; Murphy and Bowman, 2009; Hartman and Danin, 2010, Kohn, 2010; Ma et al., 2012; Basu et al., 2015). In India, many regional rainfall gradients exist due to the direction of the monsoon winds (Garrigues, 1999). However, very few isotope correlation studies (Basu et al., 2015; Kirkels et al., 2022) have been done so far in India.

1.4 Thesis work

The previous sections highlight the importance of paleoclimate studies and underscores the need for quantitative paleoclimate reconstructions. The stress was given to the isotopic composition of plant-derived proxies with special emphasis on δD of the leaf wax derived compounds and $\delta^{13}C$ of vegetation and SOM. The objectives of this thesis work were (i) to estimate ε_{app} of tropical plants, (ii) to decipher seasonality in δD records of *n*-alkanes and *n*-alkanoic acids, and (iii) to explore the possibility of establishing a quantitative relationship between plant-derived isotopic proxies and precipitation amount along precipitation gradient.

The following is a brief outline of various thesis chapters.

Chapter 2 deals with the experimental approaches employed to fill the research gaps highlighted earlier. In the beginning, the details of an outdoor experiment wherein different plant samplings were grown with water of known isotopic composition are given. This is followed by the details of the selection of the sampling locations along the precipitation gradient. The chapter also includes the procedures employed for the extraction and quantification of leaf wax *n*-alkanes and *n*-alkanoic acids from plants and soil samples, along with their subsequent hydrogen and carbon isotope measurements. The procedure followed for the carbon isotopic measurements of the bulk soil organic matter and C_4 grasses is provided.

Chapter 3 characterizes the abundance and isotopic composition of different homologues of *n*-alkanes and *n*-alkanoic acids in tropical angiosperm trees. The intra-species, inter-species and inter-vegetation type variability in δD and ε_{app} values are reported. The ε_{app} values of *n*-alkanes and *n*-alkanoic acids for the tropical species are suggested and the factors affecting the variability of ε_{app} are elucidated. The chapter also discusses the effect of relative variations in evergreen and

deciduous species in the catchment on the community-averaged ε_{app} values of *n*-alkanes and *n*-alkanoic acids.

Chapter 4 deals with the seasonality issue in the δD records of *n*-alkanes and *n*-alkanoic acids. The results of an outdoor experiment wherein various tropical species were irrigated with isotopic tracer (δD ~1000‰) water are discussed. The measured and expected δD values of *n*-alkanes and *n*-alkanoic acids in mature leaves after application of the isotopically enriched water are used to assess the seasonality in δD records. The effect of the transfer of photosynthates from a year to the next year on seasonality in δD records of leaf wax derived compounds of deciduous plants is also discussed.

In Chapter 5, the results and implications of an exercise aimed at calibrating the plant-derived climate proxies against precipitation are given. The variability in the $\delta^{13}C$, $\delta^{13}C_{alk}$ and δD_{alk} values in soil along a precipitation gradient of ~500-3700 mm/yr in western peninsular India is reported. Variability in the grass species, and their bulk $\delta^{13}C$ and $\delta^{13}C_{alk}$ along the precipitation gradient are also reported.

Chapter 2
Methodology

This thesis is focused on characterizing various plant-derived isotope proxies for past precipitation reconstruction. One of the proxies widely utilized for quantitative assessment of paleo-precipitation variability is the hydrogen isotopic composition (δD) of leaf wax compounds. To reconstruct the δD values of the past precipitation based on the leaf wax δD records and ensure their robust interpretation, knowledge of the hydrogen isotopic fractionation between the leaf wax compounds and precipitation (ε_{app}) is necessary. As emphasized in chapter 1 (Section 1.2.2), there is a necessity to assess the ε_{app} values in an experimental setting. Most of the evaluations of ε_{app} values have been conducted in natural field-based or transect studies where uncertainties in ε_{app} values may arise from inaccurate source water δD values, species-effect and variations in climate conditions. Further, the available ε_{app} dataset is biased towards northern mid-latitude regions (Fig. 1.2 in Chapter 1). In this study, the assessment of the ε_{app} values of tropical angiosperm trees was conducted in an outdoor experimental setting. The trees were grown under the same natural climate condition using water with a known δD value. This experiment not only served to evaluate tropical ε_{app} values but also helped in recognizing the uncertainties associated with species effect in the tropics.

For meaningfully using past precipitation conditions revealed from the leaf wax δD records, it is crucial to understand the seasonality associated with the leaf wax δD records. Here, seasonality refers to the biasness of the leaf wax δD records towards a particular season or time of the year. Although field studies have been conducted to elucidate seasonality in leaf wax δD records, certain limitations are associated with them (detailed discussion in Section 1.2.3 of chapter 1). An effective approach to understanding the seasonality in leaf wax δD records involves tracking the period of synthesis of the leaf wax compounds by isotopically labelling the source water. In this context, here, to monitor the synthesis of new leaf wax compounds, seven tropical angiosperms were irrigated with normal water for 85 days and subsequently with isotopically-labeled tracer water (δD ~1000 ‰) for 110 days. The rationale behind designing this experiment is discussed in section 2.1.3. In deciduous plants, photosynthates are transferred from the end of one growing season to the beginning of the next growing season. The effect of the transfer of photosynthates on the seasonality of leaf wax δD records derived from tropical deciduous plants is also explored in this study. The details of the experiment are provided in section 2.1.

For the quantitative reconstruction of past precipitation, calibration equations of isotopes of plants and soil organic matter with precipitation amount are commonly employed. To establish these equations, plant and soil samples are collected from diverse locations and are correlated with the local precipitation. Sites featuring gradients in local precipitation present an opportunity to formulate regional calibration equations. In this study, plant and soil samples were collected along a precipitation gradient in western peninsular India. The objective was to understand the variability of (i) the C_4 grass species, (ii) $\delta^{13}C$ values of C_4 grasses, (iii) $\delta^{13}C_{alk}$ values of grasses, (iv) $\delta^{13}C_{SOM}$ values, (v) $\delta^{13}C_{alk}$ values in soil, and (vi) δD_{alk} values in soil, in relation to precipitation amounts. The details of the locations of the transect are provided in section 2.2.

Overall, this chapter is organized into four distinct sections. The first section (2.1) provides a detailed explanation of the outdoor experiment conducted to estimate ε_{app} values of tropical angiosperms and to explore the seasonality associated with the leaf wax δD records in the tropics. The second section (2.2) focuses on the geographical locations and the sampling process for plants and soil along the precipitation gradient in western peninsular India. The third (2.3) and fourth (2.4) sections are dedicated to analytical protocols employed in this study.

2.1 Outdoor experiment to estimate ε_{app} values and to understand seasonality associated with leaf wax δD records in the tropics

2.1.1 Climate of the experiment site

An outdoor experiment was conducted at the Indian Institute of Science Education and Research Pune, Pune, India. The experiment site (18°32'44.9"N 73°48'30.0"E) experiences a semi-arid monsoonal climate with an annual rainfall of ~ 800 mm. The region receives most of its rainfall during the summer monsoon from June to September during which the relative humidity is higher (> ~78%) and temperatures vary from 25 °C to 28 °C (Fig. 2.1).

2.1.2 Plants selected for the experiment

Seven angiosperm trees including three deciduous (*Tectona grandis*, *Haldina cordifolia*, *Sterculia urens*) and four evergreen species (*Syzygium cumini*, *Callophylum inophyllum*, *Memecylon umbellatum* and *Diospyros malabarica)* were chosen (Fig. 2.2). These species are

found in forests around Pune (Deshpande et al., 1993) and the saplings of them were available in local nurseries. The plants were approximately 2-3 years old when the experiment commenced.

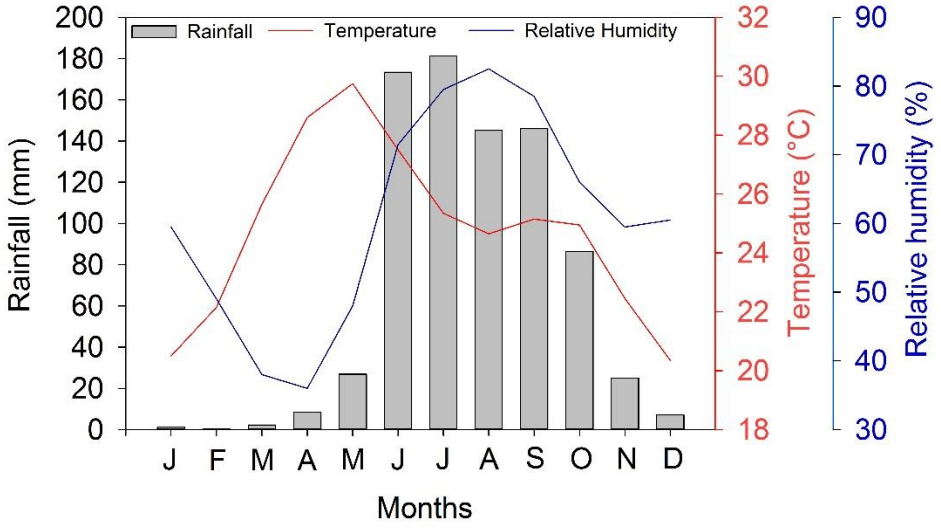

Fig. 2.1. Monthly rainfall, temperature and relative humidity in the study area. [Data source: India Meteorological Department *Climatological Normals*: (1981 - 2010)]

2.1.3 Concept of experiment design

It is well known that leaves develop a protective layer of wax upon sprouting to mitigate transpirational water loss. The wax layer is composed of many compounds which are preserved in soils and sediments. The δD values of leaf wax compounds reflect the δD values of water (usually precipitation) that was utilized for their synthesis and serve as a proxy for past precipitation. A critical questions arise here are (i) how much hydrogen isotopic fractionation occurs between the source water (~precipitation) and the leaf wax compounds (ε_{app} values) and (ii) if the δD values of precipitation vary throughout the year, do the leaf wax δD values capture this variation, or do they reflect the δD values of precipitation of a specific period only? Addressing the second issue entails understanding the period of leaf wax synthesis. If the leaf wax compounds are synthesized only during a particular period of the year, their δD values would reflect the δD values of precipitation of that particular period. If the leaf wax compounds are synthesized throughout the growing season, their δD values would record annually integrated δD values of precipitation.

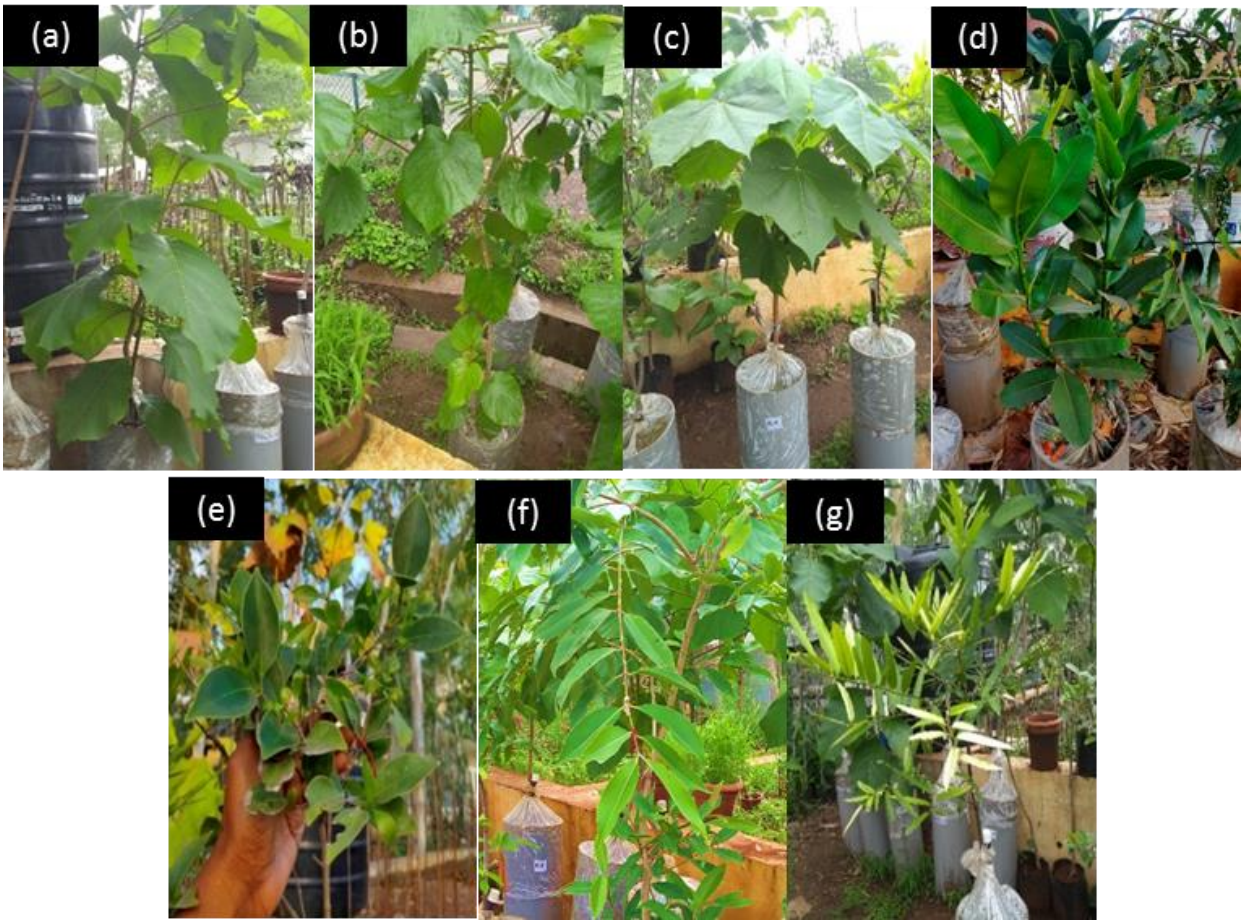

Fig. 2.2. The deciduous [(a) *Tectona grandis*, (b) *Haldina cordifolia*, (c) *Sterculia urens*] and evergreen [(d) *Callophylum inophyllum*, (e) *Memecylon umbellatum*, (f) *Syzygium cumini*, (g) *Diospyros malabarica*] plants studied in the experiment.

In this part of the study, the objective was to answer the two questions raised in the previous paragraph. We conducted our experiment to primarily study the δD values of mature leaves of the tropical angiosperm trees, initially irrigating the plants with normal tap water (δD = −2‰) and subsequently irrigating them with the deuterium-labeled tracer water (δD = 1000‰). The ε_{app} values were determined when the plants were irrigated with normal tap water. Should there be a replenishment of leaf wax compounds in the mature leaves, their δD values would reflect the δD signature of deuterium-labeled tracer water.

2.1.4 Irrigation regimes and sampling

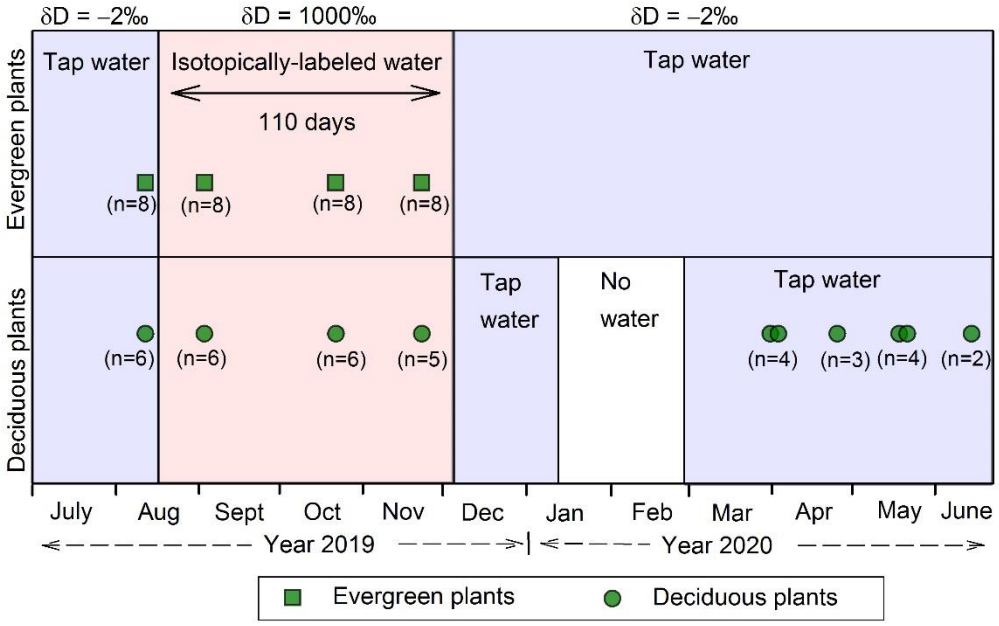

Fig. 2.3. A schematic illustration of the irrigation regime employed and sampling carried out in this study. The purple and beige colors indicate the period of application of normal and tracer water, respectively. After the leaf-shed, the deciduous species were not irrigated for 47 days (from the 13th of January 2020 to the 29th of February 2020). The squares and circles indicate the day of collection of the leaves; the associated numbers in the parenthesis indicate the number of trees sampled on a given day. In the growing season of 2020, new leaves of only deciduous species were collected.

The plants were grown under similar natural climate conditions and irrigated with the same source water. Two irrigation regimes were employed in year 2019: the first (from the 19th of May to the 15th of August) with normal tap water (δD = −2‰) and the second (from the 17th of August to the 5th of December) with deuterium-labeled tracer water (δD = 1000‰) (Fig. 2.3). The pots were properly sealed to avoid an influx of precipitation or groundwater (Fig. 2.4).

The mature leaf samples were collected during both irrigation regimes (Fig. 2.3). The first set of leaves was collected on the 12th of August. This set of leaves was utilized to assess the ε_{app} values of the tropical angiosperm trees. Leaf sampling was continued during the subsequent

months when the plants were irrigated with deuterium-labeled tracer water. The leaf collection dates were the 3rd of September, the 22nd of October and the 23rd of November. All the four sets of leaf samples were used to understand the seasonality associated with leaf wax synthesis. The maturity of the sampled leaves was ensured by their lower position on the stem and periodic measurement of the leaf length and leaf mass per unit area (LMA) (details in Section 2.1.5.1).

To evaluate the carryover of photosynthates from one growing season to the next in deciduous species, new leaves emerging at the beginning of the next growing season (i.e. from ~ April to June, 2020) were collected (Fig. 2.3). After 5th December 2019, the plants were irrigated with the normal water to flush out the isotopically-labeled water from the soil. The shedding of leaves for different deciduous species happened over a period of ~3-4 months (i.e. from December to March). The plants were not irrigated for 47 days (from 13th January 2020 to 29th February 2020). We resumed watering with the normal tap water (once in four/five days) during the bud break period (March for the majority of the plants) (Fig. 2.3).

Fig. 2.4. Pots sealed to prevent the influx of rain or ground water.

2.1.5 Field measurements

2.1.5.1 Leaf maturation

To select the mature leaves in deciduous species, leaf growth measurements (length measured in one of the fixed dimensions) (Fig. 2.6) and leaf mass per unit area (LMA) analysis (Fig. 2.5, 2.6) were carried out. The plants took ~10 to 64 days and ~32 to 82 days for attaining

saturation in leaf growth and LMA, respectively. The tracer water was applied 145 days after the leaf flush in the majority of the plants which was greater than the periods the plant took to attain maturity. In the case of evergreen species, thicker leaves lying at a lower level on a branch were considered mature and were sampled.

Fig. 2.5. Multiple parts of the leaves sampled to ensure the representative LMA value. For example, (a) *Haldina cordifolia,* and (b) *Sterculia urens*.

2.1.5.2 Climate and leaf parameters

If the plants utilized the deuterium-labeled tracer water to synthesize new leaf wax compounds, they would show enriched δD values of leaf wax compounds. To calculate the expected δD values of leaf wax compounds, it was essential to model the leaf water δD values. The modelling process relied on measurements of various climate and leaf parameters across various months.

Relative humidity data were obtained from a nearby (~1 km) Indian Meteorological Department (IMD) station records while temperature was measured in the field using a thermometer (Table 2.1). The stomatal conductance was measured using a leaf porometer (Decagon SC-1) (Table 2.2). The correlation between the air and leaf temperature for various plants established using thermistors (Ecomatik LAT-B2) was used to estimate the leaf temperature and e_i. A cryogenic trap method (Deshpande et al., 2013) was used to get an idea about the monthly variability of the δD values of atmospheric water vapor. Table 2.1 gives the δD values of source water and atmospheric water vapor considered for various months.

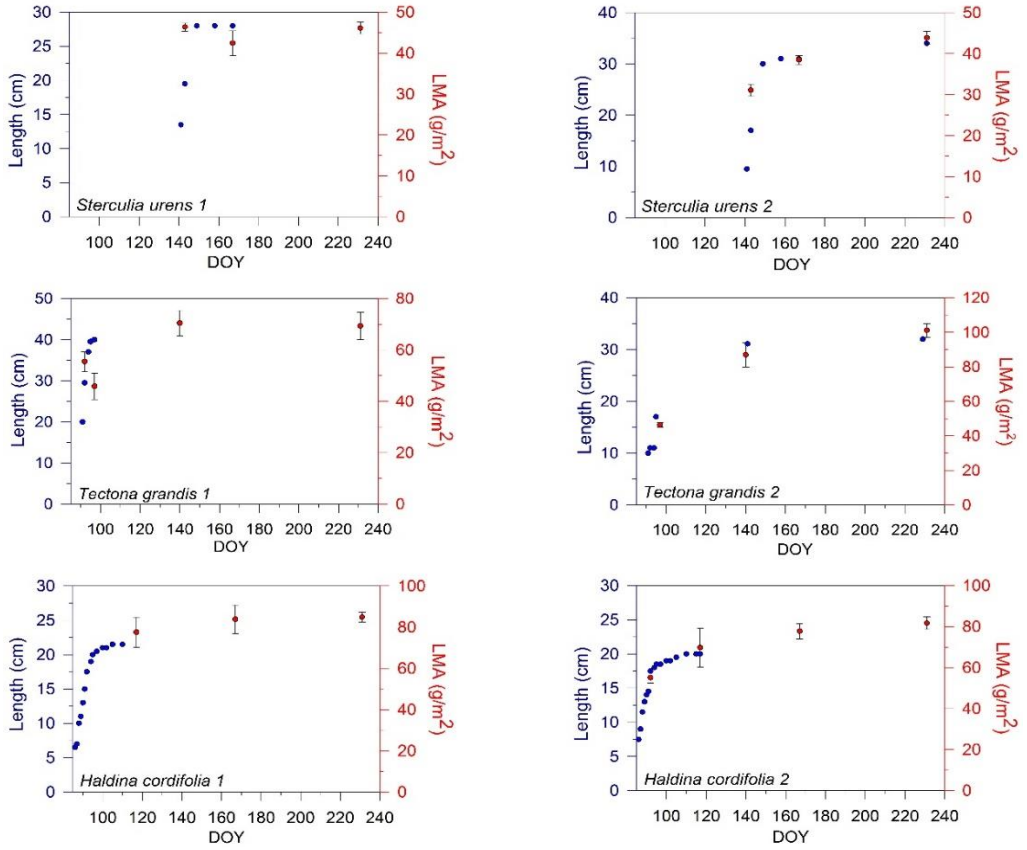

Fig. 2.6. Leaf lengths (blue circles) and LMA (red circles) variation in deciduous leaves.

Months	Barometric Pressure (KPa)[@]	Temperature (°C)[#]	Humidity (%)[$]	$\delta D_{atm\ vapor}$ (‰)[&]	$\delta D_{source\ water}$ (‰)
August	94.4 ± 0.3	28.7 ± 2.0	82.0 ± 10	-61 ± 6	−2 ± 1
September	94.5 ± 0.3	27.1 ± 2.0	78.0 ± 10	-61 ± 6	1000 ± 2
October	94.8 ± 0.3	29.6 ± 1.9	64.0 ± 12	-76 ± 8	1000 ± 2
November	95.0 ± 0.3	28.1 ± 0.7	58.0 ± 9	-118 ± 12	1000 ± 2

Table 2.1. Climate parameters used as inputs for leaf water modeling.

[@] Monthly mean values from IMD station data

[#] Daily measurements from 9 to 12 pm

[$] Daily IMD measurements from 9 to 12 pm; for August it is climatological mean.

[&] Measured periodically. δD values of September were considered for August

	Stomatal conductance (mol m^{-2} s^{-1})						
	Tg	*Hc*	*Su*	*Dm*	*Mu*	*Ci*	*Sc*
Aug	0.5 ± 0.1	0.6 ± 0.2	0.7 ± 0.3	0.4 ± 0.1	0.6 ± 0.3	0.3 ± 0.1	0.5 ± 0.1
Sept	0.5 ± 0.1	0.6 ± 0.2	0.7 ± 0.3	0.4 ± 0.1	0.6 ± 0.3	0.3 ± 0.1	0.5 ± 0.1
Oct	0.5 ± 0.1	0.7 ± 0.1	0.6 ± 0.2	0.4 ± 0.04	0.6 ± 0.07	0.7 ± 0.1	0.8 ± 0.5
Nov	0.4 ± 0.02	0.4 ± 0.09	0.3 ± 0.08	0.3 ± 0.04	0.4 ± 0.08	0.4 ± 0.09	0.6 ± 0.01

Table 2.2. Measured stomatal conductance values used as inputs for the leaf water δD modeling.

2.2 Precipitation gradient study

2.2.1 Field locations

To understand the variability of isotopes of plants and soils with precipitation amounts, a precipitation gradient transect spanning over ~85 km in western peninsular India was selected. The transect ranged from 18°48'E, 74°23'N (Bhuleshwar) to 18°39'E, 73°39'N (Tamhini) encompassing a precipitation range from ~500 to 3700 mm/yr, respectively (Fig. 2.7). In the study area, most of the rainfall occurs during summer monsoon i.e. from June till September. The precipitation data was obtained from IMD gridded rainfall data (Pai et al., 2014). The available IMD data was of 0.25° resolution and had been re-gridded to 0.01° resolution using a bicubic interpolation method.

The Tamhini region has a humid climate with tropical forest vegetation whereas Bhuleshwar region experiences a semi-arid climate with tropical shrub/grassland vegetation (FAO, 2000). Trees were the predominant vegetation in high precipitation region (i.e. L-1) whereas grasses were dominant in low precipitation region (L-8) (Fig. 2.8). In the intermediate precipitation locations, both trees and grasses were observed.

2.2.2 Sampling of soil and grasses

Soil and grass samples were collected from eight locations along the transect (L-1 to L-8; Fig. 2.7). Locations with minimum anthropogenic interference were chosen for sampling. After

removal of the litter layer, soil samples were collected from two depths: 5 cm and 25 cm. Three soil samples were collected at each sampling site and aggregated into one sample. The abundant grass species were collected from each location.

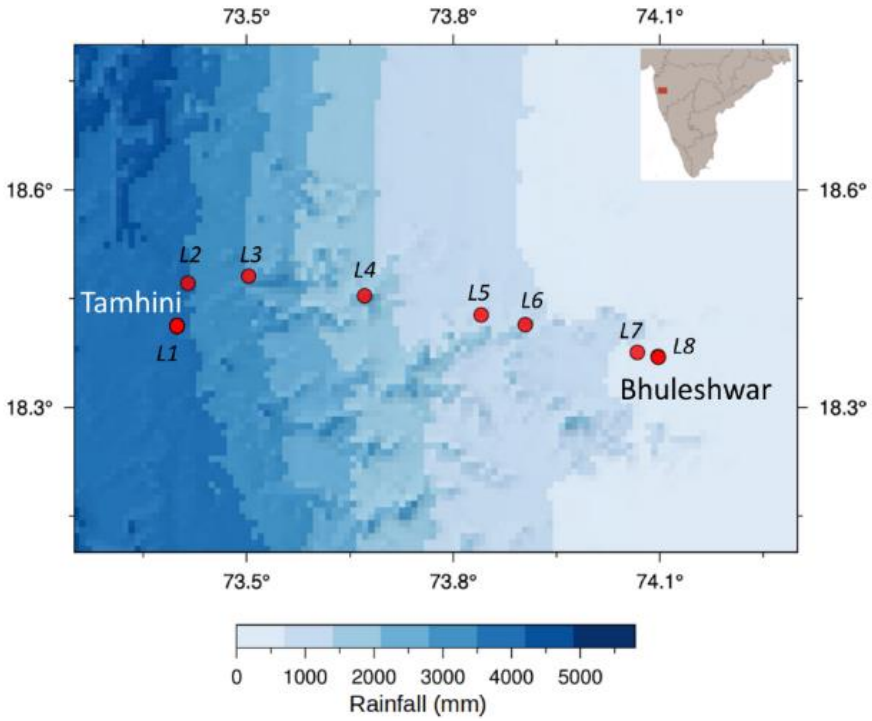

Fig. 2.7. Selected sampling sites along precipitation gradient.

Fig. 2.8. Field photograph of the sampling locations. The locations of L-1, L-3 and L-8 are given in Fig. 2.7.

2.3 Extraction, identification and characterization of leaf wax compounds

The detailed procedure for extraction of leaf wax *n*-alkanes and *n*-alkanoic acids from plant leaves, *n*-alkanes from soil samples; their identification, and quantification are discussed here. The *n*-alkanes and *n*-alkanoic acids investigations were carried out in the Stable Isotope Laboratory of the Indian Institute of Science Education and Research Kolkata (SILIKA).

2.3.1 Extraction of leaf wax n-alkanes and n-alkanoic acids from plant leaves and soil samples

The total lipid fractions of the plant leaf samples were obtained by powdering the dried leaves and using the ultrasonication technique of McInerney et al., (2011). Samples were mixed with a solvent (dichloromethane/methanol), 93:7 v/v (HPLC grade) and sonicated for 20 minutes at room temperature (25-30 °C). Total lipids from soil samples were extracted in an accelerated solvent extractor (Dionex ASE-350, Thermo Fisher Scientific) using a mixture of dichloromethane and methanol (93:7) at a temperature of 100°C and pressure of 1600 psi.

After obtaining the total lipid fractions, a rotavapor (R-210; Buchi Labortechnik AG, Flawil, Switzerland) was used to concentrate the extracted lipids. The *n*-alkanes were separated from the total lipid fraction by short-column silica gel chromatography. A pre-ashed pipette with activated silica gel (100–200 mesh) was used to prepare the column and the non-polar fraction (containing the *n*-alkanes) was eluted with hexane. Thereafter, a mixture of dichloromethane and methanol (2:1) was used to elute the silica gel columns to obtain the acid fractions. Saponification of acid fractions was carried out with 1 M KOH in methanol at 70 °C for 2 h. After incubation, the vials were allowed to cool and then 5 % NaCl solution in DCM-extracted HPLC-grade water was added to each vial. Later, the pH of the mixture was lowered (<2) using HCl and the "acids" fractions were extracted using hexane. For *n*-alkanoic acid analysis, the obtained acid fractions were methylated using BF_3-methanol and converted to the corresponding methyl esters. The obtained methyl esters were dried by passing through a Na_2SO_4 (anhydrous) column.

2.3.2 Identification and quantification of n-alkanes and n-alkanoic acids

The *n*-alkanes and *n*-alkanoic acids were analyzed by gas chromatography (7890A GC System; Agilent Technologies, Santa Clara, CA, USA) equipped with a split/splitless injector, non-polar capillary column (HP5-MS; 30 m × 250 µm × 0.25 µm), and flame ionization detector

(FID). The concentrated samples were injected in 1:1 split mode with an inlet temperature at 320 °C. The oven temperature was increased from 60 to 320 °C at 8 °C minute^{-1} with a holding time of 12 minutes. Individual *n*-alkanes were identified using the characteristic retention times (RT) obtained from the calibration standards SUPELCO C_8–C_{40} alkane and Fluka alkane mixture (C_{10}–C_{40}). The standards were also used to calculate the relative concentrations of the individual *n*-alkanes in the samples. For calibration purposes, during the analysis of the samples, the SUPELCO C_8–C_{40} *n*-alkane standard and Fluka alkane mixture standard (C_{10}–C_{40}) were measured at different dilutions (1.0 ng, 1.5 ng, and 2.0 ng μL^{-1}). The peak areas of individual *n*-alkanes (C_8–C_{40} and C_{10}–C_{40}) were then calculated. For the respective *n*-alkane homologues (C_8–C_{40} and C_{10}–C_{40}), calibration graphs of peak areas versus injected concentrations were obtained. The relative concentration of *n*-alkanes in the samples was calculated from the calibration equations (for respective homologues) obtained from the regression analysis. Likewise, individual *n*-alkanoic acids were identified using five Sigma-Aldrich standards Palmitic-C_{16}, Oleic-C_{18}, Behenic-C_{22}, Montanic-C_{28}, and Melissic-C_{30} acids with known concentrations. During the analysis of *n*-alkanoic acids, the SUPELCO C_8–C_{40} *n*-alkane standard and Fluka *n*-alkane mixture standard (C_{10}–C_{40}) were analyzed. The equations for individual *n*-alkanoic acid homologues were obtained using *n*-alkanoic acid and *n*-alkane standards. The relative concentration of *n*-alkanoic acids in the samples was calculated using the calibrated equations (for respective homologues). The repeat measurements of *n*-alkanoic acid and *n*-alkane standards were associated with an uncertainty of ±2%.

2.3.3 Characterization of leaf wax n-alkanes and n-alkanoic acids

The *n*-alkanes and *n*-alkanoic acids were characterized using average chain length (ACL) of long-chain lengths i.e., *n*-C_{25} to *n*-C_{35} (ACL_{alk}) (Poynter and Eglinton, 1990) and *n*-C_{26} to *n*-C_{36} (ACL_{acid}) (Galy et al., 2011), respectively. The ACL_{alk} and ACL_{acid} reported for tropical angiosperm trees (in Chapter 3) were calculated using the following equations:

$$ACL_{alk} = \frac{(25\times C_{25}) + (27\times C_{27}) + (29\times C_{29}) + (31\times C_{31}) + (33\times C_{33}) + (35\times C_{35})}{(C_{25} + C_{27} + C_{29} + C_{31} + C_{33} + C_{35})} \quad (2.1)$$

$$ACL_{acid} = \frac{(26\times C_{26}) + (28\times C_{28}) + (30\times C_{30}) + (32\times C_{32}) + (34\times C_{34}) + (36\times C_{36})}{(C_{26} + C_{28} + C_{30} + C_{32} + C_{34} + C_{36})} \quad (2.2)$$

where, C is the concentration of individual chain length (as in subscript) of *n*-alkane and *n*-alkanoic acid.

2.4 Isotopic measurements

2.4.1 δD measurements of leaf wax n-alkanes and n-alkanoic acids

The δD values of individual *n*-alkanes and *n*-alkanoic acids were measured using Trace GC Ultra (Thermo Fisher Scientific, Strada Rivoltana 20090 Rodano, Milan, Italy) coupled with a MAT-253 IRMS linked via GC Isolink (pyrolysis interface) and Thermo Fisher Scientific Conflo IV interface. The Trace GC Ultra equipped with a non-polar capillary column HP5-MS was used for analyzing the samples. The samples were injected in splitless mode with an inlet temperature of 280 °C and helium as a carrier gas (flow rate maintained at 1 mL minute^{-1}). The GC oven temperature was programmed to increase with a ramp of 10 °C minute^{-1} from 40 °C to 320 °C and then held isothermally for 12 minutes. To measure the δD values, the hydrogen atoms in samples were converted to H_2 through a reduction interface in a pyrolysis furnace (at 1420 °C). H_2 reference gas was introduced into MAT-253 in a series of pulses at the beginning and end of each analysis to standardize the hydrogen isotope values. The H_2 reference gas was calibrated against international standard mixtures A7 (C_{16}–C_{30}) before the isotope analyses. Instrument performance was routinely checked using a Fluka alkane mixture (C_{10}–C_{40}) at different dilutions. During the analysis of the samples, the reproducibility in the A7 (C_{16}–C_{30}) and Fluka alkane mixture were found to be ±2‰ (1-σ). Before the measurement of hydrogen isotope, the H^{3+} factor was calculated using ISODAT NT 3.0. The H^{3+} factor ranged between 7 and 10 ppm nA^{-1}, indicating a contribution of <0.07–0.1% H^{3+} to HD^+. The samples were analyzed in duplicates or triplicates for the determination of the δD values. Pre-concentration and dilution procedures were carried out for the chain lengths of excessively low and high concentrations, respectively.

Isotope fractionation associated with the addition of BF_3-methanol during *n*-alkanoic acid extraction was corrected using a mass balance equation:

$$\delta D_{acid} = \frac{[(2C_n + 2) * \delta D_{FAME}] - [3 * \delta D_{Me}]}{(2C_n - 1)}$$

where, δD_{acid} values are the corrected values for target *n*-alkanoic acid, C_n is the number of C-atom for each alkanoic acid chain length, δD_{FAME} values are uncorrected values measured from

fatty acid methyl esters, and δD_{Me} is δD value of the methanol in BF_3-methanol used to methylate the samples. The δD values of *n*-alkanes and *n*-alkanoic acids are reported with respect to Vienna Standard Mean Ocean Water (VSMOW). The measurements were carried out in the Stable Isotope Laboratory of the Indian Institute of Science Education and Research Kolkata (SILIKA).

2.4.2 $\delta^{13}C$ measurements of leaf wax n-alkanes

The $\delta^{13}C$ measurements of leaf wax *n*-alkanes extracted from soil samples were carried out using Trace GC Ultra (Thermo Fisher Scientific, Strada Rivoltana 20090 Rodano, Milan, Italy) in conjunction with a MAT-253 IRMS linked via GC Isolink and Thermo Fisher Scientific Conflo IV interface. The samples were examined using the Trace GC Ultra with a non-polar capillary column HP5-MS and split/splitless injector. The *n*-alkane samples were injected in splitless mode with an inlet temperature of 280°C and helium as carrier gas (at a flow rate of 1 ml minutes $^{-1}$). The temperature of the GC oven had been set to rise with a ramp of 10 °C per minute from 40 to 320 °C and to be maintained isothermally for 12 minutes. Individual compounds of the samples were burned in GC Isolink over nickel, copper, and platinum wire at 950 °C with oxygen and helium (1% v/v). The CO_2 produced during combustion was introduced into the MAT-253. A series of reference gas (CO_2) pulses were introduced into the MAT- 253 at the beginning and end of each analysis to standardize the carbon isotope values. Before the isotope measurements, the CO_2 reference gas was calibrated using international standard mixtures A5 (C16-C30). Fluka alkane mixtures (C10-C40) at various dilutions (0.5 to 15.0 ng ml^{-1}) with known $\delta^{13}C$ values were used to routinely check the instrument performance. The reproducibility of the A5 and Fluka alkane mixture was found to be ±1.0‰ and ±0.4‰, respectively. The $\delta^{13}C$ values of *n*-alkanes are reported with respect to Vienna Pee-Dee Belemnite. The measurements were carried out in the Stable Isotope Laboratory of the Indian Institute of Science Education and Research Kolkata (SILIKA).

2.4.3 δD measurements of water and vapor samples

The tap/tracer water and atmospheric vapor samples were analyzed for δD values using the laser-based water isotope analyzer (ABB-LGR IWA-45P). The analyzer follows off-axis integrated cavity output spectroscopy (OA-ICOS) method for measurements of isotopic compositions (Baer et al., 2002). The method introduces laser photons of the known line strength

in an optical cavity filled with sample water in vapor form, the measured absorption spectra are recorded and processed by post-analysis software to estimate the isotopic composition. Three standards supplied by ABB-LGR having different δD compositions (std-1: −154 ± 0.5‰, std-2: −51.60 ± 0.5‰, std-3: −9.20 ± 0.5‰) were used in sequence after each batch of 4 water samples during measurements. A protocol 'Standard Natural range optimized for high precision spline type' of measurement was followed. This required taking 1ml volume of each sample in standard glass bottles. Using 1 μL syringe, samples from these bottles were extracted by an auto-injector system that passed it into a miniature chamber heated at 85°C converting the liquid water fully into vapor form before introducing it in the water isotope analyzer. The δD values are reported with respect to Vienna Standard Mean Ocean Water (VSMOW). The δD measurements of water and atmospheric vapor samples were conducted at the Physical Research Laboratory (PRL), India.

2.4.4 $\delta^{13}C$ measurements of bulk soil organic matter and grass samples

For the bulk $\delta^{13}C$ measurements, approximately 15mg of powdered soil samples and 1mg of powdered grass leaves were packed in tin capsules. Before the $\delta^{13}C$ measurements were carried out, roots and gravels were removed from the soil samples. They were acidified in 6N HCl for the removal of carbonates, rinsed in deionized H_2O and dried. The grass samples were dried before powdering. The continuous flow IRMS (Isoprime 100; Isoprime, Elementar) attached to Vario Pyro cube elemental analyser (Elementar) was used for $\delta^{13}C$ measurements. The repeatability and accuracy were assessed by analyzing laboratory standards: Merck and Fluka sucrose of $\delta^{13}C$ values as −12.1‰ and −26.7‰, respectively, and sulfanilamide with $\delta^{13}C$ = −27.8‰. The precision of repeated measurements of laboratory standard was 0.15 ‰. The $\delta^{13}C$ values are reported relative to Vienna Pee-Dee Belemnite. The measurements were carried out at the Indian Institute of Science Education and Research Pune.

Chapter 3

Apparent fractionation factor for *n*-alkanes and *n*-alkanoic acids of tropical angiosperm trees

3.1 Introduction

The hydrogen isotopic composition (δD) of leaf wax *n*-alkanes and *n*-alkanoic acids reflect the δD values of precipitation (δD_{precip}) (Sachse et al., 2012; Tipple and Pagani, 2013) which in turn carry information about precipitation amount or atmospheric circulation (Managave et al., 2023). They have also been recognized as a proxy for reconstructing past precipitation variability (Feakins et al., 2014; Collins et al., 2013; Aichner et al., 2015; Niedermeyer et al., 2016). Quantifying the hydrogen isotope fractionation between leaf wax compounds and source water (ε_{app}) is a prerequisite for δD based paleo-hydrological studies. However, as highlighted in Chapter 1, the characterization of the ε_{app} values have been mostly done in field-based studies and were predominantly carried out in northern mid-latitude regions as compared to that in the tropics. Further, the ε_{app} values estimated in field-based studies are often associated with inherent uncertainties which could stem from (i) incorrect source water δD values, (ii) species-effect, and (iii) varying climatic conditions (as in transect studies).

This chapter deals with the results of an outdoor controlled experiment aimed at characterizing δD and ε_{app} values of tropical species. The experiment was conducted at the nursery in the Indian Institute of Science Education and Research, Pune. The rationale behind the outdoor experiment is given in Chapter 2. The laboratory procedure adopted to quantify the abundance and isotopic composition of different homologues of *n*-alkane and *n*-alkanoic acids is also given in Chapter 2. To characterize the ε_{app} values of leaf wax *n*-alkanes and *n*-alkanoic acids in plant species from monsoonal climate, three deciduous and four evergreen angiosperm trees were grown with water of known δD value under similar climatic conditions. The leaves of these plants were analyzed for the concentration and δD values of *n*-alkanes and *n*-alkanoic acids of different chain lengths. This chapter reports (i) chain length distributions of *n*-alkanes and *n*-alkanoic acids of tropical angiosperm trees, (ii) δD and ε_{app} values for *n*-alkanes and *n*-alkanoic acids of species from a monsoonal region, (iii) intra-species, inter-species and inter-taxa variability in δD and thus ε_{app} values, and (iv) apparent fractionation between (*n*-1) alkanes and *n*-alkanoic acids pairs (e.g., $\varepsilon_{31/32}$). The implications of the results are discussed at the end.

3.2 Results

3.2.1 Characterization of leaf wax compounds

n-alkanes

The mean *n*-alkane ($\sum_{C23-C35}$) concentration of the studied species was 118 ± 115 μg/g dry leaf (n = 13). No significant difference was observed in the mean amount of waxes of *n*-alkanes in deciduous and evergreen species (p = 0.950, two-tailed *t*-test). Evergreen and deciduous species produced 31 to 410 μg/g and 31 to 292 μg/g dry leaf *n*-alkanes, respectively.

In mature leaves, a typical odd over even predominance was observed in the long chain *n*-alkanes (C_{29-35}) (Fig. 3.1). The chain length distribution of *n*-alkanes varied with species (Fig. 3.1). *Haldina cordifolia*, *Sterculia urens*, *Syzigium cumini*, *Callophylum inophyllum* and *Memecylon umbellatum* produced *n*-C_{31} as the most abundant *n*-alkane, whereas in *Tectona grandis* and *Diospyrus malabarica*, *n*-C_{33} was the dominant homologue (Fig. 3.1). In addition, *Tectona grandis* also produced a significant amount of *n*-C_{35}. No systematic difference between the most abundant chain lengths of the *n*-alkanes of deciduous and evergreen species was observed. The ACL_{alk} of all species was 31 ± 1 (n = 13). Deciduous ACL_{alk} (31.7 ± 1.1; range: 31.1-33) was higher than that of evergreen species (30.6 ± 0.6; range: 30-31.7). Although a higher ACL_{alk} value in deciduous species was observed, it was mainly attributable to one species i.e., *Tectona grandis*.

n-alkanoic acids

The mean *n*-alkanoic acid ($\sum_{C24-C36}$) concentration of all species was 128 ± 99 μg/g dry leaf (n = 14). The *n*-alkanoic acid concentrations of deciduous species were not significantly different from those of evergreen (p = 0.101, two-tailed *t*-test). Evergreen species and deciduous species produced 13 to 233 μg/g and 71 to 322 μg/g dry leaf *n*-alkanoic acids, respectively.

An even over odd predominance was observed in the higher chain *n*-alkanoic acids (C_{28-36}) of mature leaves (Fig. 3.1). As with *n*-alkanes, the distribution of *n*-alkanoic acid chain lengths was species-specific (Fig. 3.1). *Memecylon umbellatum* produced equal amounts of *n*-C_{30} and *n*-C_{32}, *Haldina cordifolia*, *Callophylum inophyllum*, *Syzigium cumini* produced high amounts of *n*-C_{32}, whereas in *Tectona grandis* and *Diospyrus malabarica*, *n*-C_{34} was the most dominant *n*-

alkanoic acid chain length. The ACL_{acid} of all species was 30.4 ± 1.1 (n = 14). ACL_{acid} was not significantly different for evergreen and deciduous species (p = 0.332, two-tailed *t*-test). ACL_{acid} observed in deciduous species was 30.7 ± 1.1 (range: 29-31.9, n = 6) and in evergreen species was 30.1 ± 1 (range: 28.5-31.4, n = 8).

3.2.2 δD values of n-alkane and n-alkanoic acids

n-alkanes

Mean δD values of *n*-C_{29}, *n*-C_{31} and *n*-C_{33} of the studied species were −121 ± 19‰ (n = 12), −121 ± 22‰ (n = 14) and −122 ± 21‰ (n = 11), respectively. There were no significant differences between deciduous and evergreen δD_{alk} values (p = 0.175, two-tailed *t*-test). The δD_{alk} value of deciduous species *n*-C_{29}, *n*-C_{31} and *n*-C_{33} were −124 ± 33‰ (n = 4), −120 ± 30‰ (n = 6) and −123 ± 27‰ (n = 6), respectively and they were −120 ±10‰ (n = 8), −121 ± 17‰ (n = 8) and −122 ± 13‰ (n= 8), respectively, for evergreen species. The δD_{alk} values of different species and their replicates are given in Fig. 3.2. δD_{alk} values did not show any systematic variation (i.e. no consistent increase or decrease) with the chain length (Fig. 3.2).

n-alkanoic acids

Mean δD values of *n*-C_{28}, *n*-C_{30} and *n*-C_{32} acids of the studied species were −131 ± 17‰ (n = 8), −128 ± 27‰ (n = 12) and −126 ± 26‰ (n = 10), respectively. There were no significant differences between deciduous and evergreen δD_{acid} (p = 0.473, two-tailed *t*-test). Deciduous species δD_{acid} values of *n*-C_{28}, *n*-C_{30} and *n*-C_{32} were −136 ± 18‰ (n = 5), −133 ± 25‰ (n = 5) and −121 ± 24‰ (n = 4), whereas for evergreen species they were −123 ± 14‰ (n = 3), −124 ± 30‰ (n = 7) and −130 ± 28‰ (n = 6), respectively. Except for *Memecylon umbellatum and Tectona grandis*, δD_{acid} did not change systematically with the chain-length (Fig. 3.2).

3.2.3 Apparent fractionation (ε_{app})

ε_{app} of *n*-alkanes ($\varepsilon_{app-alk}$) and *n*-alkanoic acids ($\varepsilon_{app-acid}$) were calculated as

$$\varepsilon_{app} = 1000 \left[\left(\frac{\delta D_{wax} + 1000}{\delta D_{water} + 1000}\right) - 1\right] \quad (3.1)$$

where, δD_{wax} and δD_{water} are δD values of either *n*-alkanes or *n*-alkanoic acids and source water, respectively.

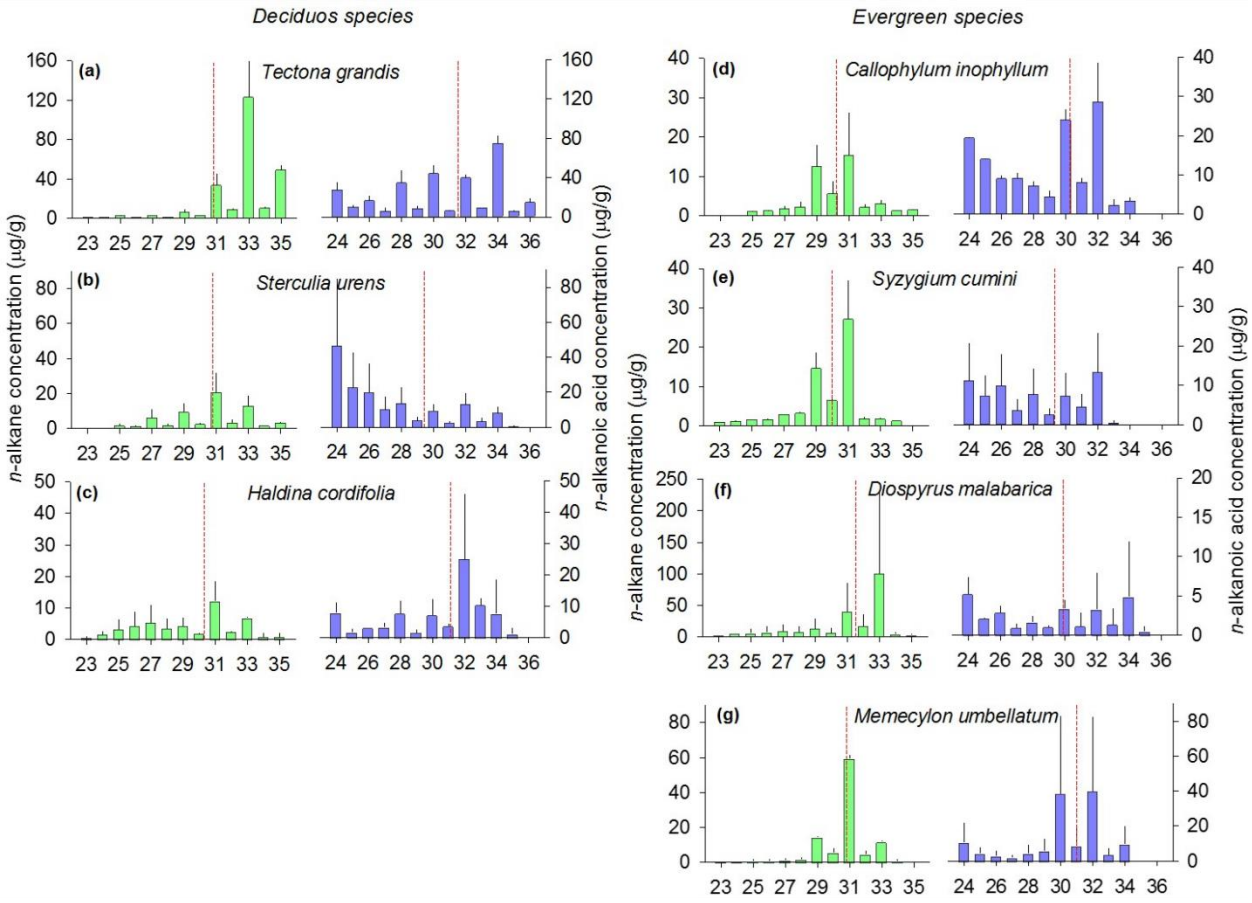

Fig. 3.1. The *n*-alkanes (green bars) and *n*-alkanoic acids (blue bars) chain length concentration distributions and Average Chain Lengths (dotted red line) of deciduous (a, b and c) and evergreen (d, e, f and g) species. For every species, duplicates were analyzed. The black bars represent the standard deviation (1-σ) of the chain length abundances in two individuals of the same species.

Fig. 3.3 and Table 3.1 show the $\varepsilon_{app-alk}$ and $\varepsilon_{app-acid}$ values of different chain lengths of individual plants of each species, different species and taxa. The $\varepsilon_{app-alk}$ values for *n*-C_{29}, *n*-C_{31} and *n*-C_{33} of the individuals of the studied species were −120 ± 19‰ (n = 12), −119 ± 23‰ (n = 14) and −121 ± 21‰ (n = 11), whereas $\varepsilon_{app-acid}$ values for *n*-C_{28}, *n*-C_{30} and *n*-C_{32} were −130 ± 17‰ (n = 8), −126 ± 27‰ (n = 12) and −125 ± 26‰ (n = 10), respectively (Fig. 3.3; Table 3.1).

There was no significant difference in the average $\varepsilon_{app-alk}$ (and $\varepsilon_{app-acid}$) values of deciduous and evergreen taxa (p>0.05, two-tailed *t*-test) (Fig. 3.3). The $\varepsilon_{app-alk}$ for deciduous *n*-C_{29}, *n*-C_{31} and *n*-C_{33} were −122 ± 33‰, −119 ± 30‰ and −121 ± 27‰, whereas for evergreen species they were −119 ± 10‰, −120 ± 17‰ and −120 ± 13‰, respectively. $\varepsilon_{app-acid}$ for deciduous *n*-C_{28}, *n*-C_{30} and *n*-C_{32} were −134 ± 18‰, −132 ± 25‰ and −119 ± 25‰, whereas for evergreen species they were −122 ± 14‰, −122 ± 30‰ and −128 ± 28‰.

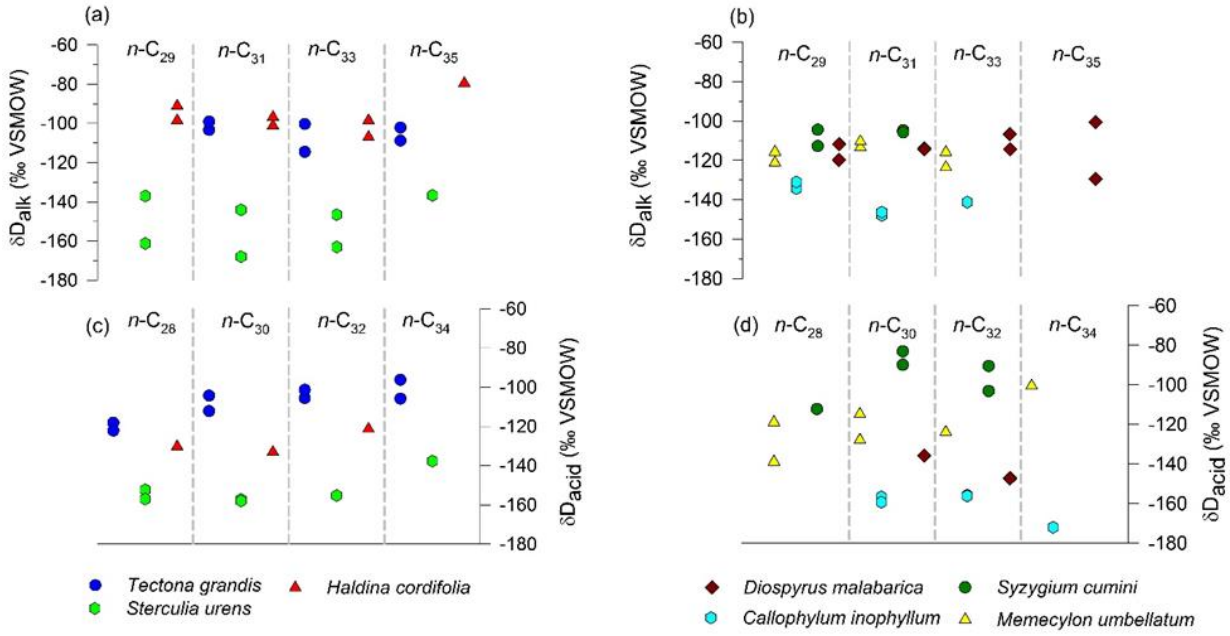

Fig. 3.2. The δD values of different homologues of *n*-alkanes (a, b) and *n*-alkanoic acids (c, d) of deciduous (left panels) and evergreen (right panels) species. Two symbols of the same color represent individuals of a species.

A large variation in ε_{app} values among species was observed (Table 3.1). The $\varepsilon_{app-alk}$ of *n*-C_{29}, *n*-C_{31} and *n*-C_{33} varied from −91‰ to −161‰ , −97‰ to −168‰ and −97‰ to −163‰, respectively. $\varepsilon_{app-acid}$ of *n*-C_{28}, *n*-C_{30} and *n*-C_{32} varied from −111‰ to −156‰, −82‰ to −158‰ and −82‰ to −155‰, respectively. Overall, a spread varying from 45 to 70‰ among species ε_{app} values was observed in our study.

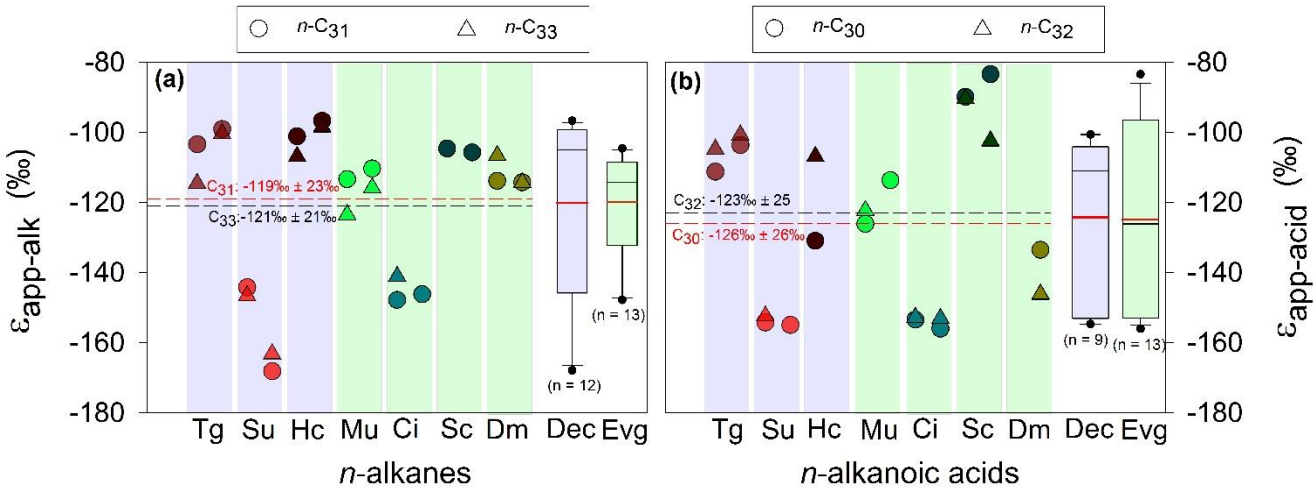

Fig.3.3. ε_{app} for (a) *n*-alkanes ($\varepsilon_{app-alk}$) and (b) *n*-alkanoic acids ($\varepsilon_{app-acid}$) for the abundant chain lengths of individual plants of each species and taxa. Symbols of the same color represent ε_{app} values of individuals of a species. Species abbreviations: Tg - *Tectona grandis*, Su - *Sterculia urens*, Hc - *Haldina cordifolia*, Mu - *Memecylon umbellatum*, Ci - *Callophylum inophyllum*, Sc - *Syzygium cumini*, Dm - *Diospyros malabarica*. Dec: deciduous species and Evg: evergreen species. Mean and median values of ε_{app} for deciduous and evergreen species are shown by red and black lines, respectively, in the box and whisker plots in (a) and (b). The horizontal dotted lines show the mean ε_{app} of all plants for different chain lengths.

3.3. Discussion

3.3.1 Predominance of longer chain n-alkanes in tropical angiosperm trees

An increasing number of region-specific modern vegetation studies have been conducted to understand the abundance of chain lengths of leaf wax compounds (Diefendorf et al., 2011; Bush et al., 2013; Feakins et al., 2016a; Cerda-Peña et al., 2022; Dasgupta et al., 2022). It has been observed that in *n*-alkanes of tropical trees there is a predominance of chain lengths *n*-C_{29} and *n*-C_{31} (Feakins et al., 2016a) whereas in temperate angiosperms chain lengths *n*-C_{27} and *n*-C_{29} are dominant (Cerda-Peña et al., 2022). The taxa-specific distinction in chain length abundance of temperate angiosperm trees has been reported by Diefendorf et al., (2011), where evergreen and deciduous species show a dominance of chain lengths *n*-C_{31} and *n*-C_{29}, respectively. However, a predominance of chain lengths *n*-C_{31} and *n*-C_{33} was observed in the investigated tropical deciduous

and evergreen angiosperm trees. A significant production of *n*-C_{35} in *Tectona grandis* was also noticed (Fig. 3.1a). Sarkar et al., (2014) also observed a similar abundance for *Tectona grandis* in a dry deciduous mixed forest in the Lonar catchment area, central India. It thus appears that the C_3 angiosperm trees in a semi-arid monsoonal region are characterized by the dominance of longer chain-length *n*-alkanes (Fig. 3.1).

	Plants	$\varepsilon_{app-alk}$ (‰)			$\varepsilon_{app-acid}$ (‰)			$\varepsilon_{alk/acid}$ (‰)	
		C_{29}	C_{31}	C_{33}	C_{28}	C_{30}	C_{32}	$\varepsilon_{29/30}$	$\varepsilon_{31/32}$
Deciduous	*Su1*	−137	−144	−147	−151	−156	−154	20	10
	Su2	−161	−168	−163	−156	−156	–	−8	–
	Tg1	–	−103	−114	−117	−111	−104	–	−1
	Tg2	–	−99	−100	−121	−103	−100	–	−1
	Hc1	−91	−101	−105	−129	−133	−120	47	19
	Hc2	−99	−97	−97	–	–	–	–	–
Evergreen	*Mu1*	−121	−113	−124	−137	−126	−122	4	8
	Mu2	−116	−110	−116	−117	−113	–	−5	–
	Ci1	−134	−148	−141	–	−155	−154	23	6
	Ci2	−131	−146	–	–	−158	−155	30	8
	Sc1	−104	−105	–	−111	−88	−89	−19	−19
	Sc2	−113	−106	–	–	−82	−102	−36	−6
	Dm1	−120	−114	−113	–	−134	−146	15	35
	Dm2	−112	−114	−107	–	–	–	–	–

Table 3.1 Apparent fractionation ($\varepsilon_{app-alk}$ and $\varepsilon_{app-acid}$) of individual chain lengths of different species and their fractionation between *n*-alkanoic acid and *n*-alkanes ($\varepsilon_{29/30}$ and $\varepsilon_{31/32}$).

3.3.2 $\varepsilon_{app-alk}$ and $\varepsilon_{app-acid}$ estimates

3.3.2.1 Chain-length dependence of ε_{app}

Paleo precipitation δD reconstructions are often based on one of the chain lengths of *n*-alkanes and *n*-alkanoic acids, for example, *n*-C_{29} (Liu et al., 2017; Ghosh et al., 2020) and *n*-C_{26} (Thomas et al., 2012). However, while comparing the reconstructed δD values of such studies with studies that have reported δD values of a different chain length, for example, *n*-C_{29} and *n*-C_{31} (Jambrina-Enríquez et al., 2022), or *n*-C_{28} and *n*-C_{30} (Curtin et al., 2019), a need for correction might exist. It has been reported in some studies that δD values increase with increasing chain lengths, implying systematic changes in $\varepsilon_{app-alk}$ (Chikaraishi et al., 2004; Feakins et al., 2016;

Corcoran et al., 2022) and $\varepsilon_{app-acid}$ (Chikaraishi et al., 2004; Feakins et al., 2016) with chain-length. In our study, $\varepsilon_{app-alk}$ did not exhibit a chain length-dependent increase (Table 3.1). Except for *Memecylon umbellatum* and *Tectona grandis*, other species did not show a systematic increase in δD_{acid} values (Fig. 3.2) and consequently $\varepsilon_{app-acid}$ values with increasing chain lengths. Nevertheless, this increase was much lower than inter-species variability in ε_{app} values. When individuals of the species studied were considered, the $\varepsilon_{app-alk}$ for *n*-C_{29}, *n*-C_{31} and *n*-C_{33} of all plants were −120 ± 19‰, −119 ± 23‰ and −121 ± 21‰, respectively (Fig. 3.3). The $\varepsilon_{app-acid}$ for *n*-C_{30} and *n*-C_{32} were −126 ± 27‰ and −125 ± 26‰ respectively, whereas for *n*-C_{28} the values were lower (−131 ± 17‰) but not significantly lower (at p = 0.80, one way ANOVA test). The similarity of the average inter-species ε_{app} of different chain lengths in *n*-alkanes (and in *n*-alkanoic acids) implies no correction is required while estimating ε_{app} values of one chain length from the other, when the catchment area is dominated by angiosperm trees in a semi-arid monsoonal region.

3.3.2.2 Deciduous and evergreen taxa distinction

Typically, vegetation change can introduce variability in a region's ε_{app} values and impact interpretation of paleo-precipitation δD values (Hou et al., 2007; Feakins and Sessions., 2010; Liu et al., 2016). In monsoonal climate past vegetation shifts from evergreen to deciduous taxa have been reported (Kumaran et al., 2013; Prasad et al., 2014). This study gives an opportunity to assess the effect of change in vegetation between tropical deciduous and evergreen taxa on the ε_{app} values. For chain length *n*-C_{31}, ε_{app} values of −119 ± 30‰ (n = 6) and −120 ± 17‰ (n = 8) were observed for deciduous and evergreen species, respectively; for chain length *n*-C_{30}, they were −132 ± 25‰ (n = 5) and −122 ± 30‰ (n = 7), respectively. No significant differences (p > 0.22, two-tailed *t*-test) in the ε_{app} values of *n*-alkanes (and *n*-alkanoic acids) between the studied deciduous and evergreen species suggest that shifts between deciduous and evergreen taxa would have little effect on the reconstruction of δD_{precip} in the monsoonal region.

3.3.2.3 Inter-species ε_{app} variation

The ε_{app} values are influenced by the δD value of the leaf water, which is controlled by the δD value of the source water, leaf morphology and environmental conditions (Smith and Freeman, 2006; Feakins and Sessions, 2010; McInerney et al., 2011; Kahmen et al., 2013). In our study, as all the plants were grown in similar climatic conditions and were irrigated with water of the same δD value, the range in their ε_{app} values reflected the combined effect of ε_{bio} and the evaporative enrichment of the leaf water resulting from varying leaf morphology.

The ε_{bio} values of plants can be affected by multiple factors such as different biosynthetic pathways (Sachse et al., 2012), differential contributions from distinct NADPH sources to hydrogen in leaf wax compounds (Kahmen et al., 2013), enzymatic isotope effects during secondary hydrogen exchange reactions such as decarboxylation of *n*-alkanoic acids to *n*-alkanes (Chikaraishi and Naraoka, 2007). These factors can lead to a high variability in ε_{bio} among species. For example, a species-specific ε_{bio} variation of 65‰ was observed in a growth chamber study conducted by Kahmen et al., (2013). In deciduous angiosperm trees of temperate region, the species mean ε_{bio} values varied from -129 ± 10‰ to -147 ± 14‰ for *n*-alkanes and -106 ± 23‰ to -119 ± 15‰ for *n*-alkanoic acids has been reported by Freimuth et al., (2017). In a tropical transect study conducted by Feakins et al., (2016) ε_{bio} values could not be estimated due to a weaker correlation between δD values of leaf water (sampled during the afternoon of dry season) and leaf wax compounds. Therefore, expected species-specific ε_{bio} within tropical angiosperm trees is poorly constrained.

Studies evaluating the effect of leaf morphology on evaporative enrichment of the leaf water are rare. Different dicot species (*Phaseolus vulgaris, Helianthus annuus, Populus balsamifera*) when grown under similar conditions in a growth chamber have revealed a minor control (typically less than 5‰; a maximum of 16‰) of leaf morphology of different species on δD value of the leaf water (Kahmen et al., 2013). Assuming a similar control in the species investigated in this study, a spread from 45 to 70‰ in ε_{app} among species observed in this study can not be fully explained by differences in leaf water evaporative enrichment resulting from variations in the leaf morphology. Therefore, the spread in ε_{app} of the studied species was likely primarily controlled by variation in species-specific ε_{bio}.

The observed uncertainties in $\varepsilon_{app-alk}$ and $\varepsilon_{app-acid}$ for *n*-C_{31} and *n*-C_{30} as 23‰ and 27‰, respectively. The uncertainties in inter-species ε_{app} values observed in our study are similar to those in the transect and field studies (with probable uncertainties in source water δD value and external climatic conditions) conducted across different latitudes (Fig. 3.4). The observed 1σ uncertainties in ε_{app} from community-averaged studies are typically 20‰ for *n*-alkanes and 31‰ for *n*-alkanoic acids (Feakins et al., 2016; Berke et al., 2019; Corcoran et al., 2022). Similar values of inter-species variability in the ε_{app} values (1σ = 21‰) were also reported by Feakins and Sessions (2010). As discussed, the main source of variability in ε_{app} in the studied species assemblage stem from species-effect. The comparable variability in ε_{app} observed in this study and that reported in the field and transect studies further indicated that the species-effect exerts a major control on community-scale ε_{app} variability.

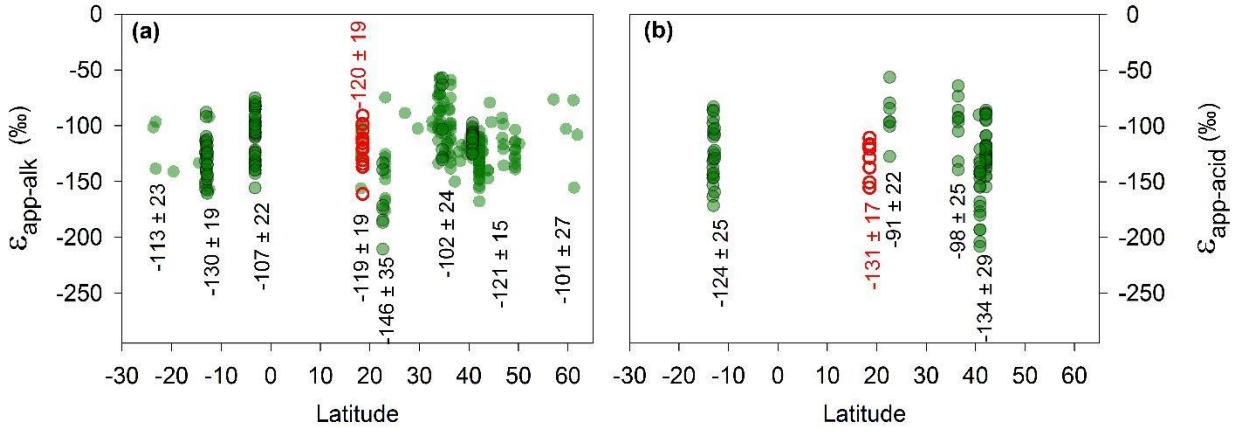

Fig. 3.4. Global compilation of $\varepsilon_{app-alk}$ for *n*-C_{29} alkanes (a) and $\varepsilon_{app-acid}$ for *n*-C_{28} acids (b) in C3 tree species. Red circles represent values from this study. Data sources: Sachse et al., (2012); Yang et al., (2021); Duan et al., (2014); Feakins et al., (2016); Friemuth et al., (2017); Griepentorg et al., (2019); Liu and An, (2019); Roy and Sanyal., (2022).

3.3.2.4 Comparison with the $\varepsilon_{app-alk}$ and $\varepsilon_{app-acid}$ of other regions

Fig. 3.4 shows latitudinal variation in $\varepsilon_{app-alk}$ and $\varepsilon_{app-acid}$ of C_3 plants along with the values reported in our study for chain lengths *n*-C_{29} and *n*-C_{28}. The $\varepsilon_{app-alk}$ and $\varepsilon_{app-acid}$ of C_3 plants revealed higher values in mid-latitudes as compared to the low-latitudes (30 °S to 30 °N)

and high-latitudes (40 °N to 70 °N), mainly because of transpirational enrichment of the leaf water in deuterium (Chikaraishi and Naraoka, 2003; Feakins and Sessions, 2010).

The $\varepsilon_{app-alk}$ (−120 ± 19‰) for *n*-C_{29} and $\varepsilon_{app-acid}$ (−131 ± 17‰) for *n*-C_{28} values reported here are similar to that of tropical C_3 plants (Fig. 3.4), further strengthening the observed coherence of ε_{app} values in the tropics (Feakins et al., 2016). However, one study (Roy and Sanyal, 2022) carried out in a humid tropical climate (Gangetic floodplains) reported different $\varepsilon_{app-alk}$ (−171 ± 27‰) and $\varepsilon_{app-acid}$ (−91 ± 22‰) values, highlighting potential regional-climate-induced heterogeneity in the ε_{app}values in the tropical region as well.

3.3.3 Paired $\varepsilon_{alk/acid}$ fractionation

In modern vegetation studies, *n*-alkanes have been the focus of the majority of ε_{app} estimations (Bi et al., 2005; Douglas et al., 2012; Berke et al., 2019). Due to the paucity of *n*-alkanoic acid studies often the ε_{app} values of *n*-alkanes and an offset between *n*-alkanes and coexisting *n*-alkanoic acids are used to estimate ε_{app} for *n*-alkanoic acids (Konecky et al., 2016; Sachse et al., 2012). To understand the relationship between ε_{app} of *n*-alkanes and *n*-alkanoic acids from the monsoonal region, a comparison of $\varepsilon_{app-alk}$ and $\varepsilon_{app-acid}$ were done (Table 3.1, Fig. 3.3).

The relationship between ε_{app} of *n*-alkanes and *n*-alkanoic acids is also expressed in terms of the hydrogen isotope fractionation between *n*-alkanes and *n*-alkanoic acids ($\varepsilon_{alk-acid}$). The $\varepsilon_{alk-acid}$ is calculated as:

$$\varepsilon_{alk-acid} = 1000 \left[\left(\frac{\delta D_{alk} + 1000}{\delta D_{acid} + 1000}\right) - 1\right] \qquad (3.2)$$

where δD_{alk} and δD_{acid} are the δD values of *n*-alkanes and *n*-alkanoic acids, respectively. $\varepsilon_{alk-acid}$ is also used to express hydrogen isotopic fractionation during decarboxylation wherein *n*-alkanoic acids produce long-chain (*n*−1) alkanes with a loss of one carbon.

The $\varepsilon_{alk/acid}$ values for chain lengths *n*-C_{29}/*n*-C_{30} ($\varepsilon_{29/30}$) and *n*-C_{31}/*n*-C_{32} ($\varepsilon_{31/32}$) estimated in this study showed the species effect (Table 3.1 and Fig. 3.5). The most positive and

negative $\varepsilon_{alk/acid}$ values were observed in *Haldina cardifolia* and *Syzygium cumini*, respectively (Fig. 3.5). However, the mean $\varepsilon_{29/30}$ and $\varepsilon_{31/32}$ of all plants revealed marginally higher δD values of the *n*-alkanes than that of the corresponding acids; $\varepsilon_{29/30}$ and $\varepsilon_{31/32}$ values were 7 ± 25‰ and 6 ± 15‰, respectively (Fig. 3.5). Further no significant difference between $\varepsilon_{alk-acid}$ of deciduous and evergreen species, were observed (p = 0.905 for $\varepsilon_{31/32}$ and p = 0.316 for $\varepsilon_{29/30}$, two-tailed *t*-test).

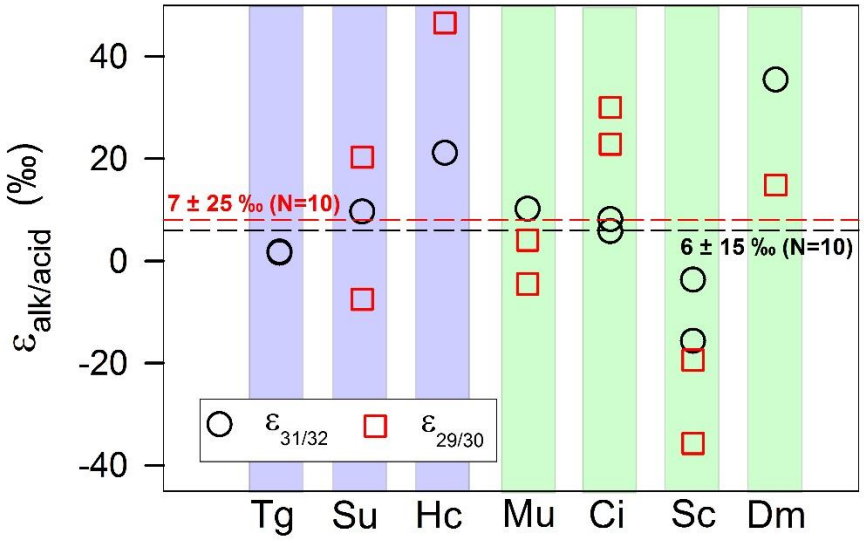

Fig. 3.5. Paired $\varepsilon_{alk/acid}$ of individuals of different species observed in this study. Purple and green bars mark deciduous and evergreen species, respectively. Within a bar, two similar symbol represent individuals of a species. The red and black line shows the mean $\varepsilon_{C29/30}$ and $\varepsilon_{C31/C32}$, respectively. Species abbreviations: Tg - *Tectona grandis*, Su - *Sterculia urens*, Hc - *Haldina cordifolia*, Mu - *Memecylon umbellatum*, Ci - *Callophylum inophyllum*, Sc - *Syzygium cumini*, Dm - *Diospyros malabarica*.

A compilation of $\varepsilon_{alk/acid}$ from various climate zones by Yang et al., (2021) showed significant differences in $\varepsilon_{alk/acid}$ values of tropical and temperate regions. Values of $\varepsilon_{29/30}$ in temperate and tropical zones were 25 ± 32‰ and 0 ± 20‰, respectively (Yang et al., 2021). Feakins et al., (2016) reported an average of −3 ± 17‰ for $\varepsilon_{29/30}$ in tropical Andes plants, even

though for some species it was as high as 30‰. Similarity of $\varepsilon_{alk/acid}$ reported here and those reported for the tropical region (Fig. 3.6) (Feakins et al., 2016; Yang et al., 2021) indicate minimal hydrogen isotopic fractionation during decarboxylation in tropical angiosperm trees.

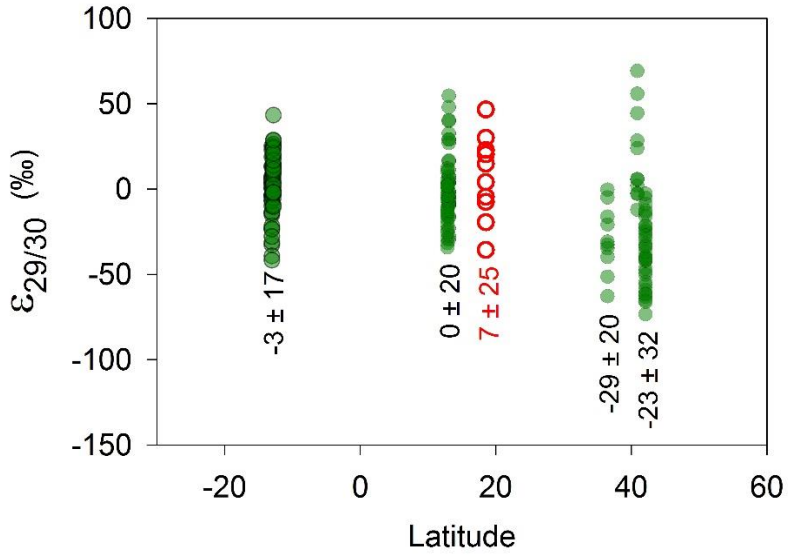

Fig. 3.6. Global variability in $\varepsilon_{alk/acid}$ for chain lengths *n*-C_{29} alkanes and *n*-C_{30} alkanoic acids. Red circles represent values from this study. Data source: Yang et al., (2021).

3.3.4 Implications for paleo-precipitation δD reconstruction

The results of the present experiment have the following implications for the lipid biomarker-based paleoclimatic investigations.

- The ε_{app} values for different chain lengths of *n*-alkanes (and *n*-alkanoic acids) were similar. In the tropical catchments dominated by angiosperm trees, a single ε_{app} value could be considered for different chain-lengths of *n*-alkanes (and *n*-alkanoic acids) while reconstructing δD_{precip} values.

- For angiosperm trees in semi-arid monsoonal region, −119 ± 23‰ and −126 ± 27‰ can be used as the community-averaged $\varepsilon_{app-alk}$ and $\varepsilon_{app-acid}$ values, respectively.

- A similar community-averaged ε_{app} value for *n*-alkanes and corresponding *n*-alkanoic acids suggested ε_{app} values of *n*-alkanes can be used to reconstruct δD_{precip} values from the δD values of *n*-alkanoic acids in the region dominated by angiosperm trees.

- Lack of taxa-specific distinction in ε_{app} values observed in this study suggests that the reconstructed δD_{precip} values may not be sensitive to the relative proportion of deciduous and evergreen taxa in the catchment area.

3.4. Conclusions

Field and transect-based studies, mainly used to estimate ε_{app} at a community level, had difficulties in assessing the relative effects of the δD value of the source water, species composition and environmental conditions on ε_{app} variability. The number of species investigated in this study was modest in comparison to that considered in the field-based investigations. Further, the grasses and shrubs could not be studied. Nevertheless, the experiment dealt with representative deciduous (n = 3) and evergreen (n = 4) species. Our study with a known source water δD value revealed the species effect as the primary controller of inter-species ε_{app} variability ($1\sigma \approx 23‰$ for *n*-alkanes and ≈ 27‰ for *n*-alkanoic acids). The interspecies scatter in ε_{app} observed here are similar to that in transect studies, indicating the species-effect reflecting variation in ε_{bio} has a dominant control on community-averaged ε_{app}. However, no systematic difference was observed between ε_{app} values of deciduous and evergreen plants. This probably indicates that a shift in vegetation from deciduous to evergreen may not lead to a significant shift in community-scale ε_{app} in reconstructed δD_{precip} values in monsoonal regions.

Chapter 4

Seasonality in *n*-alkane and *n*-alkanoic acid δD records from tropical angiosperm trees

4.1. Introduction

Finding seasonality in the paleoclimate records i.e. climate of which season the record represents is crucial for understanding its utility in terms of testing the reliability of the climate models. As discussed in Chapter 1 (Section 1.1), finding bias toward the climate of a specific season is straightforward in the case of proxies such as tree-rings. This is done by calibrating annual responses of tree-rings (say ring-width or oxygen isotopic composition) against monthly climate parameters such as temperature. The reconstructions are biased towards the months which yield statistically significant correlations (and explain higher variance) with annual response.

The climatic parameters controlling the hydrogen isotope composition (δD) of leaf-wax *n*-alkanes and *n*-alkanoic acids, used widely in paleohydrologic research, are fairly known. However, the climatic parameters of exactly which period (i.e. early or entire period of the leaf's lifespan) these biomarkers represent is unclear. As the δD records of *n*-alkanes and *n*-alkanoic acids in lacustrine or marine archives have much lower resolution (typically representing centennial-scale variability), an approach of calibrating them against monthly/seasonal climate parameters is not possible.

The findings (discussed in detail in Section 1.2.3) on the seasonality in the δD records of *n*-alkanes and *n*-alkanoic acids are ambiguous. The leaf wax δD values of field-grown barley (Sachse et al., 2010), a temperate tree (Tipple et al., 2013) reflected the δD of environmental conditions at the early stages of leaf formation whereas temperate deciduous trees (Sachse et al., 2009), semi-desert angiosperm (Pedentchouk et al, 2008) and sub-tropical deciduous trees (Huang et al., 2018) suggested that the δD records integrate the climate conditions of the entire growing season. The observations that the δD records of *n*-alkanes are biased toward the early growing season whereas, that of *n*-alkanoic acids are not biased towards any particular season further adds to the ambiguity. It should be stressed that the seasonality study from the tropics is conspicuously missing. Additionally, the effect of carryover of photosynthates from a growing season to the next growing season in tropical deciduous species on seasonality in the δD records of leaf wax compounds is not known. Further, whether vegetation type (i.e. deciduous vs evergreen) and climatic regime (i.e. temperate vs tropical) influence the seasonality in the δD records of *n*-alkanes and *n*-alkanoic acids is unclear.

The success of finding the seasonality in the δD records of the leaf wax compounds (Section 1.2.3 in Chapter 1) hinges on finding whether *n*-alkanes and *n*-alkanoic acids are periodically or continuously produced in the leaves. The limitations of periodically measuring the abundance of leaf wax compounds and the efficacy of using tracer water in deciphering the seasonality are discussed in Chapter 1 (Section 1.2.3).

This chapter elaborates on the results of an experiment carried out to decipher seasonality in the δD values in *n*-alkanes and *n*-alkanoic acids of tropical trees. The experiment involved growing tropical evergreen and deciduous species with normal water (δD = −2‰) for 88 days and then with isotopically-labeled tracer water (δD = 1000‰) for 110 days. The mature leaves of all the plants were periodically sampled, both before and after the application of the tracer water, and their δD values were measured. The details regarding the experimental setup and isotopic measurements are given in sections 2.1 and 2.4 in chapter 2.

The expected δD values of *n*-alkanes and *n*-alkanoic acids, if the new wax is synthesized using tracer water, were modeled using a plant physiological model. The measured and expected δD values of *n*-alkane and *n*-alkanoic acids were used to assess seasonality in them. The δD values of new leaves that sprouted during the next growing season were used to evaluate the effect of carryover of photosynthates on seasonality. This chapter discusses the results of this experiment and discusses their implications.

4.2 Results

4.2.1 Measured δD values of n-alkanes and n-alkanoic acids

The measured δD values of *n*-alkanes and *n*-alkanoic acids in mature leaves during the growing season of 2019 are provided in Table 4.1. The new leaves δD values of *n*-alkanes and *n*-alkanoic acids collected during the next growing season are given in Table 4.2.

	Plants	*n*-alkanes				*n*-alkanoic acids			
		δD_{alk}^{Aug}	δD_{alk}^{Sept}	δD_{alk}^{Oct}	δD_{alk}^{Nov}	δD_{acid}^{Aug}	δD_{acid}^{Sept}	δD_{acid}^{Oct}	δD_{acid}^{Nov}
Deciduous	*Tg1*	−105	−117	−101	−121	−106	−110	−89	−125
	Tg2	−101	−102	−119	−122	−101	−100	-	−92
	Hc1	−93	−95	−110	−64	−133	-	−86	−35
	Hc2	−100	−114	−121	−70	-	−120	−114	−54
	Su1	−139	−120	−111	-	−157	−152	−122	-
	Su2	−163	−109	−81	−73	−158	−149	−115	−92
Evergreen	*Mu1*	−115	−99	−92	−14	−124	−134	−113	−56
	Mu2	−112	−116	−111	−107	-	−117	−109	−89
	Sc1	−106	−115	−81	−61	−91	−88	−76	−92
	Sc2	−107	−109	−113	−115	−103	−103	−108	-
	Ci1	−149	−161	−176	−145	−156	−147	-189	-152
	Ci2	−148	−186	−180	−166	−156	−182	-	−161
	Dm1	−121	−126	−126	6	−136	−134	−159	25
	Dm2	−113	−118	−120	−109	-	−122	−144	−139

Table 4.1. Measured hydrogen isotopic compositions of *n*-alkanes and *n*-alkanoic acids in mature leaves of each plant for August, September, October and November.

4.2.2 Modeled monthly δD values of n-alkanes and n-alkanoic acids when synthesized using the tracer water alone

The δD values of *n*-alkanes and *n*-alkanoic acids expected, if they are completely utilizing the tracer water for their synthesis were calculated. A conservative estimate of δD values of the leaf wax compounds synthesized using tracer water alone during September, October and November were calculated by (i) modeling δD values of the leaf water during various months, (ii) estimating biosynthetic fractionations for August for *n*-alkane and *n*-alkanoic acid for various plants, and (iii) calculating the expected monthly δD values of leaf wax compounds synthesized using the tracer water alone from the modeled leaf water δD values and biosynthetic fractionations. Table 4.3 gives the details of the notations used.

Plants	*n*-alkanes						*n*-alkanoic acids					
	δD_{alk}^{Apr}			δD_{alk}^{May}		δD_{alk}^{June}	δD_{acid}^{Apr}			δD_{acid}^{May}		δD_{acid}^{June}
	1st	4th	26th	19th	22nd	15th	1st	4th	26th	19th	22nd	15th
Tg1	-	−42	-	−59	-	-	-	−51	-	−52	-	-
Tg2	-	−66	-	−64	-	-	-	−68	-	−68	-	-
Hc1	1	-	−108	-	-	-	−19	-	−37	-	-	-
Hc2	-	-	−63	-	-	−86	-	-	-	-	-	−72
Su1	−50	-	−107	-	−132	-	−64	-	−113	-	−138	-
Su 2	-	-	-	-	−73	−112	-	-	-	-	−88	−97

Table 4.2. Measured hydrogen isotopic compositions of *n*-alkanes and *n*-alkanoic acids in the young leaves of each plant during April, May and June.

Sections	Description	Notations	
4.2.2.1	The modeled δD values of the leaf water for various months	δD_{LW}^{Aug*}, δD_{LW}^{Sept*}, δD_{LW}^{Oct*}, δD_{LW}^{Nov*} (Equation 4.1)	
		n-alkane	*n*-alkanoic acid
4.2.2.2	The δD values of leaf wax compounds measured during various months	δD_{alk}^{Aug}, δD_{alk}^{Sept}, δD_{alk}^{Oct}, δD_{alk}^{Nov}	δD_{acid}^{Aug}, δD_{acid}^{Sept}, δD_{acid}^{Oct}, δD_{acid}^{Nov}
	The biosynthetic fractionation between δD_{LW}^{Aug*} and δD_{alk}^{Aug} (and δD_{acid}^{Aug})	$\varepsilon_{bio}^{alk\_Aug}$ (Equation 4.2)	$\varepsilon_{bio}^{acid\_Aug}$ (Equation 4.3)
4.2.2.3	The expected monthly δD values of leaf wax compounds synthesized using the tracer water alone	δD_{alk}^{Sept*}, δD_{alk}^{Oct*}, δD_{alk}^{Nov*} (Equation 4.4)	δD_{acid}^{Sept*}, δD_{acid}^{Oct*}, δD_{acid}^{Nov*} (Equation 4.5)
4.2.3	Measured difference between the δD values of leaf wax compounds after (September, October and November) and before (August) applying the tracer water.	$\Delta\delta D_{alk}^{Sept-Aug}$, $\Delta\delta D_{alk}^{Oct-Aug}$, $\Delta\delta D_{alk}^{Nov-Aug}$ (Equation 4.6)	$\Delta\delta D_{acid}^{Sept-Aug}$, $\Delta\delta D_{acid}^{Oct-Aug}$, $\Delta\delta D_{acid}^{Nov-Aug}$ (Equation 4.7)
	Expected difference between the δD values of leaf wax compounds after (September, October and November) and before (August) applying the tracer water if the leaf wax compounds post application of the tracer water were synthesized using the tracer water alone.	$\Delta\delta D_{alk}^{Sept*-Aug}$, $\Delta\delta D_{alk}^{Oct*-Aug}$, $\Delta\delta D_{alk}^{Nov*-Aug}$ (Equation 4.8)	$\Delta\delta D_{acid}^{Sept*-Aug}$, $\Delta\delta D_{acid}^{Oct*-Aug}$, $\Delta\delta D_{acid}^{Nov*-Aug}$ (Equation 4.9)

Table 4.3. The steps and associated notations used to estimate the increase in the δD values of leaf wax compounds if synthesized using the tracer water alone. Aug, Sept, Oct and Nov represent August, September, October and November, respectively.

4.2.2.1 Modeling δD values of the leaf water during various months

The Craig-Gordon model, modified by Flanagan and Ehleringer (1991), was used to determine the isotopic enrichment of the leaf water. The following equation was used

$$R_{LW} = \alpha^* \left[\alpha_k R_{XW} \left(\frac{e_i - e_s}{e_i}\right) + \alpha_{kb} R_{XW} \left(\frac{e_s - e_a}{e_i}\right) + R_a \left(\frac{e_a}{e_i}\right)\right]. \quad (4.1)$$

In equation (4.1), R is the molar ratio of heavy to light isotope and the subscripts a, LW and XW refer to bulk air, leaf water, and xylem water, respectively. α* refers to the liquid-vapour fractionation factor, α_k refers to the kinetic fractionation factor associated with diffusion in air and α_{kb} is the kinetic fractionation factor associated with diffusion at the boundary layer. The default values of α_k and α_{kb} in the model were 1.0164 and 1.011, respectively (Roden et al., 1999). α* varies with leaf temperature (Majoube, 1971). e_a, e_s and e_i are the partial pressure of water vapor in bulk air, leaf surface and leaf intercellular air space, respectively. The e_s is the only term that is controlled by the leaf's physiological characteristics. It was calculated using an equation developed by Ball et al., (1987). The values of e_i were estimated from the leaf temperature. Boundary layer conductance was considered as 1 mol m^{-2} s^{-1} (Roden et al., 1999; Managave, 2014). Tipple et al., (2015) showed the utility of the Craig-Gordon model in modeling δD values of *n*-alkanes. Due to a lack of leaf parameters such as effective path length, a sophisticated model involving the Péclet effect (Cernusak et al., 2016) was not used. The details of the environmental and plant parameters utilized for the calculation are provided in chapter 2 (Section 2.1.5.2).

4.2.2.2 Estimation of biosynthetic fractionations of n-alkanes and n-alkanoic acids for August for various plants

The $\varepsilon_{bio}^{alk\_Aug}$ and $\varepsilon_{bio}^{acid\_Aug}$ values for studied plants were estimated as follows

$$\varepsilon_{bio}^{alk\_Aug} = 1000 \times \left[\left(\frac{\delta D_{alk}^{Aug} + 1000}{\delta D_{LW}^{Aug*} + 1000}\right) - 1\right] \quad (4.2)$$

$$\varepsilon_{bio}^{acid\_Aug} = 1000 \times \left[\left(\frac{\delta D_{acid}^{Aug} + 1000}{\delta D_{LW}^{Aug*} + 1000}\right) - 1\right] \quad (4.3)$$

where, δD_{alk}^{Aug} and δD_{acid}^{Aug} are measured δD values of leaf wax *n*-alkanes and *n*-alkanoic acids before the application of tracer water (i.e. in August), respectively.

4.2.2.3 Expected monthly δD values of leaf wax compounds synthesized using the tracer water alone

The expected monthly δD values of *n*-alkanes (for example, for September, δD_{alk}^{Sept*}) and *n*-alkanoic acids (for example, for September, δD_{acid}^{Sept*}) if the leaf wax compounds were produced using the tracer water alone were estimated as follows

$$\delta D_{alk}^{Sept*} = \delta D_{LW}^{Sept*} + \varepsilon_{bio}^{alk\_Aug} \quad (4.4)$$

$$\delta D_{acid}^{Sept*} = \delta D_{LW}^{Sept*} + \varepsilon_{bio}^{acid\_Aug} \quad (4.5)$$

The expected monthly δD values of *n*-alkanes and *n*-alkanoic acids were calculated for October and November as well. The results are provided in Table 4.4.

4.2.3 Increase in δD values of leaf wax compounds after applying the tracer water

The observed and expected increase in δD values of leaf wax compounds after applying the tracer water were calculated. To quantify the observed increase in δD values of *n*-alkanes and *n*-alkanoic acids after the application of tracer water, the measured δD values of *n*-alkanes and *n*-alkanoic acids in August (the month during which the plants received regular water) were subtracted from the measured δD values of *n*-alkanes and *n*-alkanoic acids of the months during which the plants received tracer water (i.e. September, October and November). For example, for September, the measured increase in the δD values of *n*-alkanes ($\Delta\delta D_{alk}^{Sept-Aug}$) and *n*-alkanoic acids ($\Delta\delta D_{acid}^{Sept-Aug}$) was calculated as follows:

$$\Delta\delta D_{alk}^{Sept-Aug} = \delta D_{alk}^{Sept} - \delta D_{alk}^{Aug} \quad (4.6)$$

$$\Delta\delta D_{acid}^{Sept-Aug} = \delta D_{acid}^{Sept} - \delta D_{acid}^{Aug} \quad (4.7)$$

To quantify the expected increase in δD values of *n*-alkanes and *n*-alkanoic acids after the application of tracer water, the measured δD values of *n*-alkanes and *n*-alkanoic acids in August (the month during which the plants received regular water) were subtracted from the modelled δD values of *n*-alkanes and *n*-alkanoic acids of the months during which the plants received tracer water (i.e. September, October and November). For example, for September, the expected increase in the δD values of *n*-alkanes ($\Delta\delta D_{alk}^{Sept*-Aug}$) and *n*-alkanoic acids ($\Delta\delta D_{acid}^{Sept*-Aug}$) was calculated as follows:

$$\Delta\delta D_{alk}^{Sept*-Aug} = \delta D_{alk}^{Sept*} - \delta D_{alk}^{Aug} \quad (4.8)$$

$$\Delta\delta D_{acid}^{Sept*-Aug} = \delta D_{acid}^{Sept*} - \delta D_{acid}^{Aug} \quad (4.9)$$

The results of the measured and expected differences of leaf wax compounds for all months are given in Table 4.5 and Table 4.6, respectively.

	Plants	*n*-alkanes						*n*-alkanoic acids					
		δD_{alk}^{Sept*}	Er	δD_{alk}^{Oct*}	Er	δD_{alk}^{Nov*}	Er	δD_{acid}^{Sept*}	Er	δD_{acid}^{Oct*}	Er	δD_{acid}^{Nov*}	Er
Deciduous	*Tg1*	241	124	441	133	434	101	240	124	441	133	433	101
	Tg2	241	124	446	127	441	102	241	124	446	127	441	102
	Hc1	207	118	386	133	398	105	168	118	347	133	359	105
	Hc2	194	120	378	129	396	103	162	120	345	129	364	103
	Su1	169	114	337	129	363	103	152	114	319	129	345	103
	Su2	144	111	314	131	339	107	149	111	319	131	344	107
Evergreen	*Mu1*	157	118	332	135	358	111	148	118	323	135	349	111
	Mu2	160	115	337	138	356	105	148	115	325	138	345	105
	Sc1	189	113	352	132	392	102	204	113	367	132	407	102
	Sc2	185	114	362	132	390	103	189	114	366	132	394	103
	Ci1	146	117	322	127	342	107	139	117	316	127	335	107
	Ci2	146	114	313	127	334	111	138	114	305	127	326	111
	Dm1	175	117	363	135	372	104	155	115	338	137	354	104
	Dm2	187	115	348	134	383	107	152	114	338	132	349	108

Table 4.4. Modeled hydrogen isotopic compositions of *n*-alkanes and *n*-alkanoic acids in mature leaves of each plant, if there occurs new leaf wax synthesis using tracer water only during September, October and November. Er refers to the error associated with each modeled value.

	Plants	*n*-alkanes			*n*-alkanoic acids		
		$\Delta\delta D_{alk}^{Sept-Aug}$	$\Delta\delta D_{alk}^{Oct-Aug}$	$\Delta\delta D_{alk}^{Nov-Aug}$	$\Delta\delta D_{acid}^{Sept-Aug}$	$\Delta\delta D_{acid}^{Oct-Aug}$	$\Delta\delta D_{acid}^{Nov-Aug}$
Deciduous	*Tg1*	−12	4	−16	−4	17	−19
	Tg2	−1	−18	−21	1	-	9
	Hc1	−2	−17	29	-	47	98
	Hc2	−14	−21	30	-	-	-
	Su1	19	28	-	5	35	-
	Su2	54	82	90	9	43	66
Evergreen	*Mu1*	16	23	101	−10	11	68
	Mu2	−4	1	5	-	-	-
	Sc1	−9	25	45	3	15	−1
	Sc2	−2	−6	−8	0	−5	-
	Ci1	−12	−27	4	9	−33	4
	Ci2	−38	−32	−18	−26	-	−5
	Dm1	−5	−5	127	2	−23	161
	Dm2	−5	−7	4	-	-	-

Table 4.5. The measured increases in δD values of *n*-alkanes and *n*-alkanoic acids of mature leaves during September, October and November, compared to August δD values.

4.2.4 Estimation of newly synthesized n-alkanes and n-alkanoic acids: a mass balance approach

The fraction of newly synthesized leaf wax compounds was estimated using a mass balance approach. Here, the calculation is shown for November. The mass balance approach considered the δD_{alk}^{Aug} (and δD_{acid}^{Aug}) and δD_{alk}^{Nov*} (and δD_{acid}^{Nov*}) as two end-members, and δD_{alk}^{Nov} (and δD_{acid}^{Nov}) as the mixture, to estimate the newly synthesized *n*-alkanes (f_{new_alk}) and *n*-alkanoic acids (f_{new_acid}) amounts for November. The following mass balance equation was used:

$$f_{new\_alk} = \frac{\delta D_{alk}^{Nov} - \delta D_{alk}^{Aug}}{\delta D_{alk}^{Nov*} - \delta D_{alk}^{Aug}} \quad (4.10)$$

$$f_{new\_acid} = \frac{\delta D_{acid}^{Nov} - \delta D_{acid}^{Aug}}{\delta D_{acid}^{Nov*} - \delta D_{acid}^{Aug}} \quad (4.11)$$

The f_{new_alk} and f_{new_acid} values were also calculated for September and October. The results are provided in Table 4.7.

In general, δD_{alk}^{Nov} and δD_{acid}^{Nov} showed the maximum enrichment. The maximum replacement of 26 ± 5% and 33 ± 7% of *n*-alkanes and *n*-alkanoic acids, respectively was observed in only one of the two plants of *Diospyros malabarica*. *Sterculia urens* was the only species that showed ~13% replacement in both plants (Table 4.7).

4.2.5 Uncertainty estimation associated with the estimations

Uncertainty associated with the parameters used in Equations 4.1 to 4.11 was estimated employing Monte Carlo simulation. These parameters and associated 1-σ uncertainty were derived from 1000 model runs with simultaneous and random 1-σ perturbations with the normal distribution of the input parameters given in chapter 2 (Tables 2.1 and 2.2). The runs with the negative vapor pressure deficit (i.e. when the leaf inside water vapor pressure was lower than that of the atmosphere) values were ignored. 10% uncertainty was considered for boundary layer conductance, barometric pressure and δD values of atmospheric water vapor. Uncertainty in the leaf temperature was the standard error of estimation in the regression of air and leaf temperatures which ranged from 0.5 to 0.9 °C.

4.2.6 Variation in the δD values of leaf wax n-alkanes and n-alkanoic acids during the growing season

Fig. 4.1 and Fig. 4.2 show temporal changes in δD values of *n*-alkanes and *n*-alkanoic acids in the periodically collected leaves of various species. Except for *Sterculia urens* (Fig. 4.1c), variations in the δD values of *n*-alkanes and *n*-alkanoic acids after the application of tracer water did not show a systematic increasing trend. Further, two individuals of the same species did not always show a coherent evolution of δD values of the *n*-alkanes (and *n*-alkanoic acids) (e.g. Fig. 4.2a, 4.2d). The δD values of *n*-alkanes and *n*-alkanoic acids of the leaves collected in August

(δD_{alk}^{Aug}, δD_{acid}^{Aug}), September (δD_{alk}^{Sept}, δD_{acid}^{Sept}) and October (δD_{alk}^{Oct}, δD_{acid}^{Oct}) were, in general, lower than for those collected in November (δD_{alk}^{Nov}, δD_{acid}^{Nov}) (Fig. 4.1, 4.2).

The expected δD values of *n*-alkanes and *n*-alkanoic acids if synthesized using the tracer water alone in September (δD_{alk}^{Sept*}, δD_{acid}^{Sept*}), October (δD_{alk}^{Oct*}, δD_{acid}^{Oct*}) and November (δD_{alk}^{Nov*}, δD_{acid}^{Nov*}) are also shown in Fig. 4.1 and 4.2.

4.2.7 Variation in δD values of leaf wax n-alkanes and n-alkanoic acids in the next growing season

Two/three sets of young leaves were collected from deciduous species at the beginning of the next growing season (i.e. 2020). The leaves in the first set were not fully expanded; the rest were fully expanded. The δD values of *n*-alkanes and *n*-alkanoic acids of the first set of leaves (collected in April 2020) were either equal to or more (by the maximum of 79‰) than δD_{alk}^{Nov} and δD_{acid}^{Nov} (Fig. 4.1). Higher δD values of *n*-alkanes than *n*-alkanoic acids in the first set of leaves compared to the second set of leaves were observed. The differences between δD values of *n*-alkanes and *n*-alkanoic acids were 12 ± 7‰ and -16 ± 28‰ in the first and second set of leaves, respectively, the two values being statistically different at $p < 0.05$.

4.2.8 Correlation between δD values of leaf wax n-alkanes and n-alkanoic acids

Throughout the experiment, covariation in the temporal evolution of δD values of *n*-alkanes and *n*-alkanoic acids was observed (Fig. 4.1, 4.2). Overall, the δD values of *n*-alkanes and *n*-alkanoic acids showed a positive correlation ($r^2 = 0.7$, $p < 0.05$, $n = 60$) (Fig. 4.3).

4.3 Discussion

4.3.1 Replacement of n-alkanes and n-alkanoic acids in a growing season

During the experiment, the plants were initially watered with normal tap water (δD = −2‰) from the 19th of May to the 15th of August and later from the 17th of August to the 5th of December, with deuterium-labeled tracer water (δD = 1000‰). In the set of leaves that were collected after tracer water application (i.e. in September, October and November), synthesis of new *n*-alkanes and *n*-alkanoic acids would have resulted in higher δD values.

Plants		*n*-alkanes						*n*-alkanoic acids					
		$\Delta\delta D_{alk}^{Sept*-Aug}$	Er	$\Delta\delta D_{alk}^{Oct*-Aug}$	Er	$\Delta\delta D_{alk}^{Nov*-Aug}$	Er	$\Delta\delta D_{acid}^{Sept*-Aug}$	Er	$\Delta\delta D_{acid}^{Oct*-Aug}$	Er	$\Delta\delta D_{acid}^{Nov*-Aug}$	Er
Deciduous	*Tg1*	346	124	546	133	539	101	346	124	547	133	539	101
	Tg2	342	124	547	127	542	102	342	124	547	127	542	102
	Hc1	300	118	479	133	491	105	301	118	480	133	492	105
	Hc2	294	120	478	129	496	103	-	-	-	-	-	-
	Su1	308	114	476	129	502	103	309	114	476	129	502	103
	Su2	307	111	477	131	502	107	307	111	477	131	502	107
Evergreen	*Mu1*	272	118	447	135	473	111	272	118	447	135	473	111
	Mu2	272	115	449	138	468	106	-	-	-	-	-	-
	Sc1	295	113	458	132	498	102	295	113	458	132	498	102
	Sc2	292	114	469	132	497	103	292	114	469	132	497	103
	Ci1	295	117	471	127	491	107	295	117	472	127	491	107
	Ci2	294	114	461	127	482	111	294	114	461	127	482	111
	Dm1	296	117	484	135	493	104	291	115	474	137	490	104
	Dm2	300	115	461	134	496	107	-	-	-	-	-	-

Table 4.6. The expected increases in δD values of *n*-alkanes and *n*-alkanoic acids of mature leaves during September, October and November, compared to measured August δD values. Er refers to errors associated with the expected difference values.

	Plants	f_{new_alk} (%)						f_{new_acid} (%)					
		Sept	Er	Oct	Er	Nov	Er	Sept	Er	Oct	Er	Nov	Er
Deciduous	*Tg1*	−3	1	1	1	−3	1	−1	1	3	1	−4	1
	Tg2	0	1	−3	1	−4	1	0	1	2	1	2	1
	Hc1	−1	1	−4	1	6	1	4	2	10	3	20	4
	Hc2	−5	2	−4	1	6	1	4	2	4	1	16	3
	Su1	6	2	6	2	13	3	2	1	7	2	13	3
	Su2	18	6	17	5	18	4	3	1	9	3	13	3
Evergreen	*Mu1*	6	3	5	2	21	5	−4	2	2	1	14	3
	Mu2	−1	1	0	1	1	1	3	2	3	1	7	2
	Sc1	−3	2	5	2	9	2	1	1	3	1	0	1
	Sc2	−1	1	−1	1	−2	1	0	-	−1	1	2	1
	Ci1	−4	2	−6	2	1	1	3	2	−7	2	1	1
	Ci2	−13	5	−7	2	−4	1	−9	4	−7	2	−1	1
	Dm1	−2	1	−1	1	26	5	1	1	−5	2	33	7
	Dm2	−2	1	−2	1	1	1	5	2	−2	1	−1	1

Table 4.7. The estimated fraction of newly synthesized *n*-alkanes (f_{new_alk}) and *n*-alkanoic acids (f_{new_acid}) for September, October and November.

However, only a few plants showed higher δD values (Fig. 4.1 and 4.2). In some species (Fig. 4.1a, 4.1b) a decrease (mostly < 20‰; maximum of 36 ‰) in δD values of *n*-alkanes and *n*-alkanoic acids was observed. The decrease in δD values of *n*-alkanes and *n*-alkanoic acids observed in mature leaves of a plant could reflect the inter-leaf δD variability (i.e. δD variations among different leaves that flushed together) established before application of the tracer water which may vary up to 38‰ (Hou et al., 2007). A decrease in the δD values of *n*-alkanes was also observed after the application of tracer water in the mature leaves of a deciduous species (Figure 5 in Kahmen et al., 2011).

The difference between δD_{alk}^{Nov} and δD_{alk}^{Aug} ($\Delta\delta D_{alk}^{Nov-Aug}$) for studied plants ranged from −21‰ to 127‰ (mean 29 ± 49‰, 1-σ) which was higher than the corresponding differences for September ($\Delta\delta D_{alk}^{Sept-Aug}$) and October ($\Delta\delta D_{alk}^{Oct-Aug}$) which ranged from −38‰ to 54‰ (mean −1 ± 21‰, 1-σ) and −32‰ to 82‰ (mean 2 ± 30‰, 1-σ), respectively (Table 4.5). A similar sense of difference was also observed for *n*-alkanoic acids: $\Delta\delta D_{acid}^{Sept-Aug}$ varied from −26‰ to 9‰ (mean −1 ± 10‰, 1-σ); $\Delta\delta D_{acid}^{Oct-Aug}$, from −33‰ to 47‰ (mean 12 ± 28‰, 1-σ); and $\Delta\delta D_{acid}^{Nov-Aug}$, from −19‰ to 161‰ (mean 42 ± 60‰, 1-σ) (Table 4.5). Here, the negative differences are likely caused by inter-leaf δD variabilities established before the application of the tracer water.

The expected increase in δD values of *n*-alkanes if the earlier formed leaf wax (synthesized using the normal water) was completely replaced by new wax (synthesized using the tracer water) for September ($\Delta\delta D_{alk}^{Sept*-Aug}$), October ($\Delta\delta D_{alk}^{Oct*-Aug}$) and November ($\Delta\delta D_{alk}^{Nov*-Aug}$) ranged from 272 ± 118‰ to 346 ± 124‰, 447 ± 135‰ to 547 ± 127‰, and 468 ± 106‰ to 542 ± 102‰, respectively (Table 4.6). The corresponding values for *n*-alkanoic acids for September ($\Delta\delta D_{acid}^{Sept*-Aug}$), October ($\Delta\delta D_{acid}^{Oct*-Aug}$) and November ($\Delta\delta D_{acid}^{Nov*-Aug}$) varied from 272 ± 118‰ to 346 ± 124‰, 447 ± 135‰ to 547 ± 133‰, and 473 ± 111‰ to 542 ± 102‰, respectively (Table 4.6). The source water δD value during the second irrigation regime was 1002‰ higher than that during the first regime. However, because of the isotopic exchange of the leaf water with the deuterium-depleted ambient water vapor (Kahmen et al., 2011), a concomitant increase in δD values of the modeled leaf wax compounds was not observed (Fig. 4.1 and 4.2).

The observed increase in δD values of *n*-alkanes and *n*-alkanoic acids in various months were much less than the expected values if the leaf wax pool is completely replaced (Fig. 4.4) which indicated that the leaf wax compounds in the plants were (i) not replaced in September and October in the majority of the individuals and (ii) either not or partially replaced in November. The photosynthates formed using the tracer water were likely used to form structural components (such as the latewood) of plants and/or stored for utilization in the next growing season. The utilization of photosynthates formed during the mid- and late-growing seasons to form the latewood of the current year and the earlywood of the next year has been demonstrated (Kagawa et al., 2006).

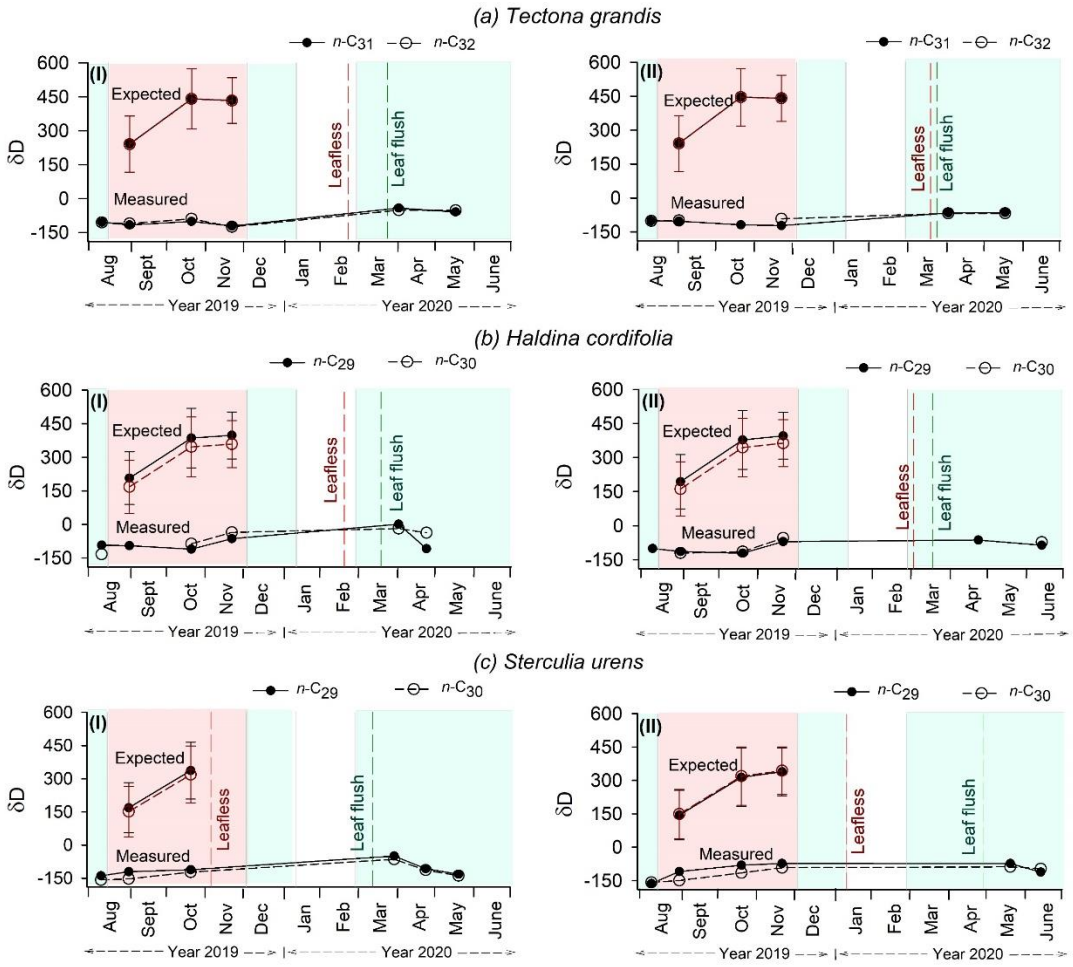

Fig. 4.1. The measured and expected δD_{alk} (solid lines) and δD_{acid} (dashed lines) values of deciduous species when irrigated with normal (δD = −2‰) water (green region) and isotopically-labeled (δD = 1000‰) water (pink region). The period when the plants were not irrigated is shown by white color. The symbols with error bars represent expected δD values if the biomarkers were synthesized using the isotopically-labeled water alone. Two panels for each species present δD variability of two individuals.

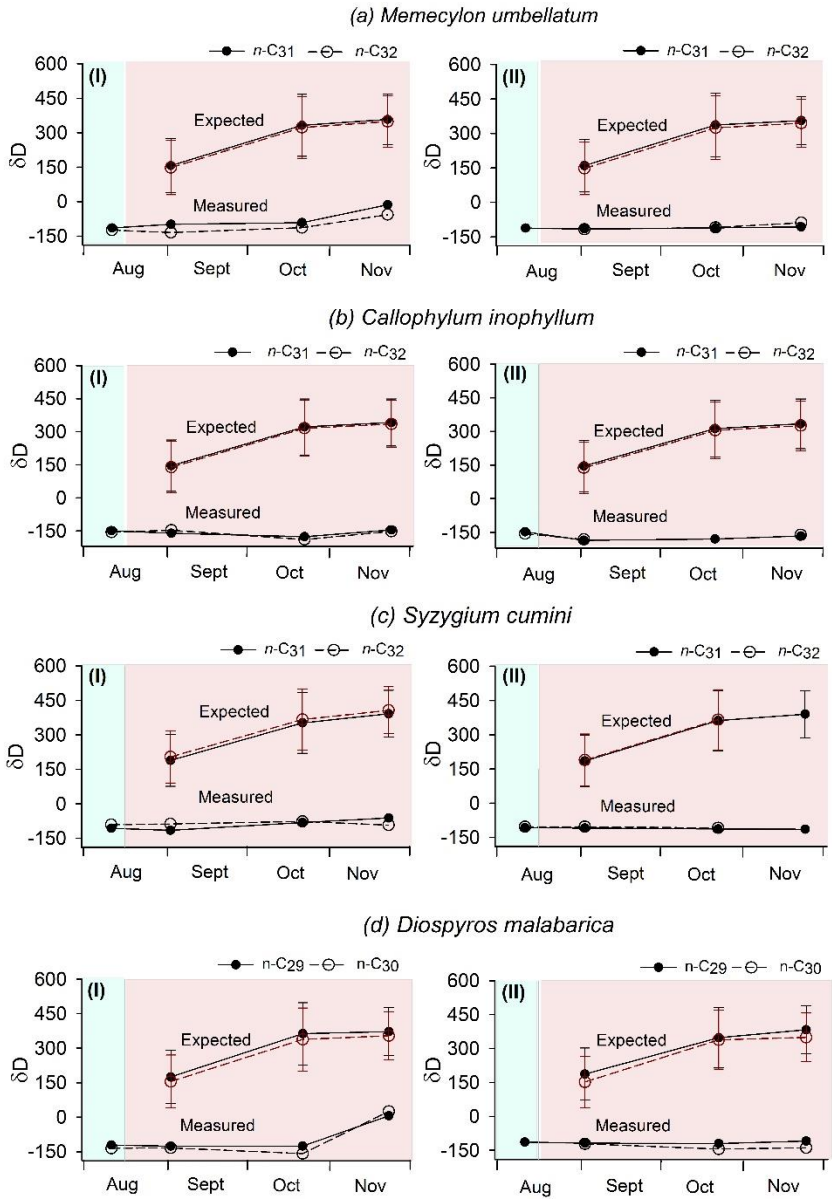

Fig. 4.2. The measured and expected δD_{alk} (solid lines) and δD_{acid} (dashed lines) values of evergreen species when irrigated with normal (δD = −2‰) water (green region) and isotopically-labeled (δD = 1000‰) water (pink region). The symbols with error bars represent expected δD values if the biomarkers were synthesized using the isotopically-labeled water alone. The months are of the year 2019. Two panels for each species present δD variability of two individuals.

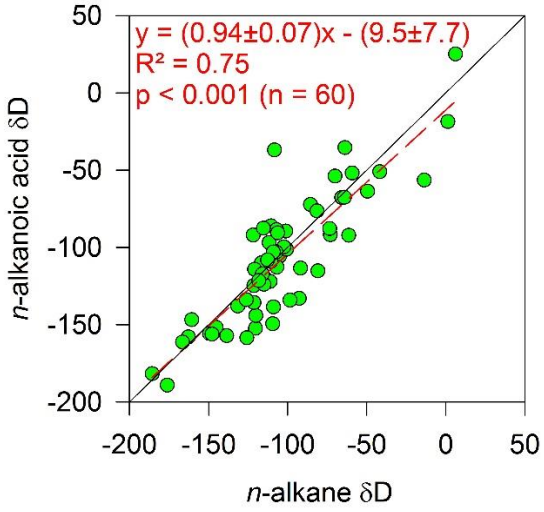

Fig. 4.3. Correlation between observed δD values of *n*-alkanes and *n*-alkanoic acids. The black and red lines are 1:1 and linear best-fit lines, respectively.

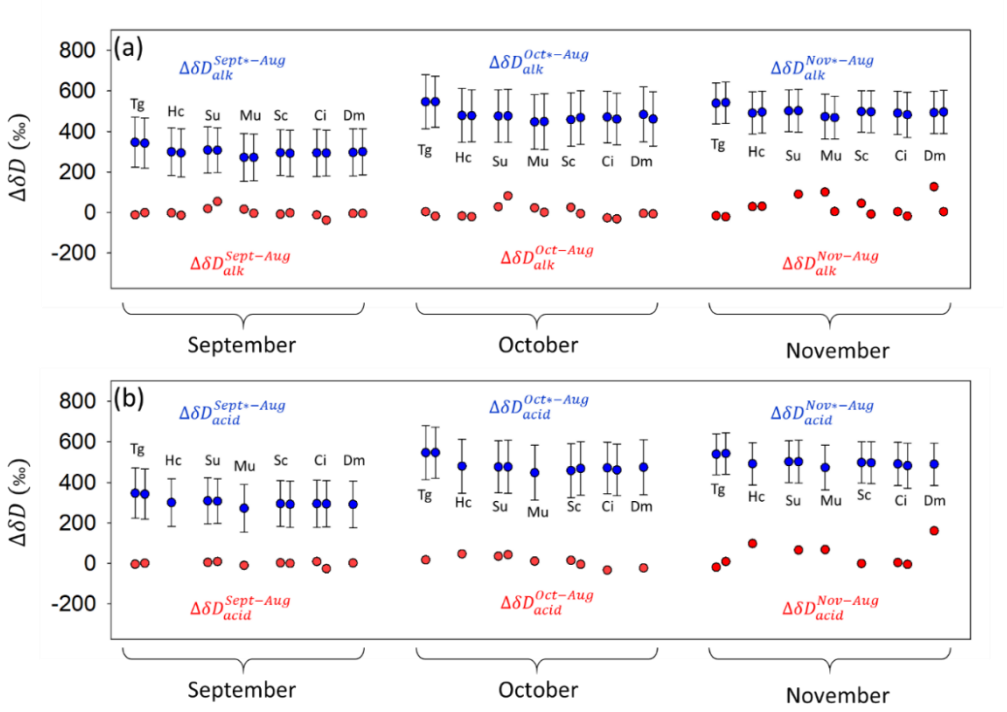

Fig. 4.4. The observed and expected increase in δD values of (a) *n*-alkanes and (b) *n*-alkanoic acids for various months. See Table 4.3 for an explanation of the abbreviations. Tg: *Tectona grandis*, Hc: *Haldina cordifolia*, Su: *Sterculia urens*, Mu: *Memecylon umbellatum*, Sc: *Syzygium cumini*, Ci: *Callophylum inophyllum*, Dm: *Diospyros malabarica*.

4.3.1.1 Extent of replenishment of leaf wax compounds during a growing season

In general, δD_{alk}^{Nov} and δD_{acid}^{Nov} showed the maximum enrichment. The results of the estimation of newly synthesized leaf wax compounds using a mass balance approach indicated no or minor replacement (typically ≤ 2 %) by newly formed wax compounds (Table 4.7). The negative f_{new} values indicate cases where δD values of leaf wax compounds of the subsequent months were lower as compared to the δD values in August. This is likely due to the inter-leaf δD variability (see discussion in section 1.2.3, Chapter 1). If the negative values of replacement (resulting due to the lower δD values in November than in August) were considered as no replacement, the average replacement of *n*-alkanes and *n*-alkanoic acids were 7% (s.e.m. = 2%) and 9% (s.e.m. = 3%), respectively. This implies that the bulk of the *n*-alkanes and *n*-alkanoic acids are synthesized during the early stages of the leaf's development in tropical angiosperm trees.

4.3.2 Timing of n-alkane and n-alkanoic acid synthesis

The field-based investigations of temperate (Freimuth et al., 2017) and sub-tropical (Yang et al., 2021) angiosperms revealed that in deciduous species, *n*-alkanes are synthesized during the early growing season whereas *n*-alkanoic acids are produced throughout the growing season. This implies that *n*-alkanes and *n*-alkanoic acids record climatic conditions during the early and entire growing season, respectively. Had this been held for tropical species, the *n*-alkanoic acids alone would have reflected the δD values of the tracer water in this study. However, covariation in the temporal evolution of δD values of *n*-alkanes and *n*-alkanoic acids was observed (Fig. 4.3) (r^2 = 0.7, $p < 0.05$, n = 60). Contrary to extra-tropical studies (Freimuth et al., 2017, Yang et al., 2021), our results suggested synchronous production of *n*-alkanes and *n*-alkanoic acids, and bias towards climatic conditions during the early stages of the leaf's growth. Our results find no difference in the behavior of tropical evergreen and deciduous species in terms of replenishment of *n*-alkanes and *n*-alkanoic acids. This is in contrast to the suggestion of continuous production of *n*-alkanes only in evergreen species in sub-tropics (Yang et al., 2021).

4.3.3 Effect of the transfer of photosynthates from a growing season to the next on seasonality

It has been suggested that in deciduous species, stored carbohydrate reserves (formed during the previous year's late growing season) are utilized for the synthesis of leaf wax *n*-alkanes

and *n*-alkanoic acids in new leaves of the current growing season (Tipple et al. 2013; Freimuth et al. 2017). The carryover of bud waxes produced in winter to the next growing season has also been indicated (Freimuth et al. 2017). Our experiment allowed us to verify the effect of carryover of photoassimilate on the seasonality in δD records of *n*-alkanes and *n*-alkanoic acids.

The metabolic shift from heterotrophic (i.e. derived from the photosynthates formed in the previous growing season) to autotrophic (i.e. formed by photosynthesis using ambient water) synthesis occurs when the leaf is expanded to 30 to 60% of its maximum size (Turgeon, 1989). As the size of the leaves from the first set falls within this range, the δD values of their *n*-alkanes and *n*-alkanoic acids likely reflect the mixing of the current and previous year's photosynthates. Had they been synthesized using the stored photosynthates (likely synthesized using the tracer water) alone they would have shown much higher δD values, similar to δD_{alk}^{Nov*} and δD_{acid}^{Nov*}.

The δD values of *n*-alkanes and *n*-alkanoic acids of the first set of new leaves (collected in April 2020) were either equal to or more than δD_{alk}^{Nov} and δD_{acid}^{Nov} (Fig. 4.1). This could have been resulted either from the transfer of photosynthates to the next growing season and/or from a higher transpirational enrichment of deuterium (~24-29 ‰) in the leaf water of expanding leaves before the development of cuticles (Freimuth et al., 2017). The lowering of δD values in the second and third set of leaves suggested a higher contribution from the autotrophic leaf wax synthesis as observed by Gamarra and Kahmen (2015) and Freimuth et al., (2017). The higher δD values of *n*-alkanes than *n*-alkanoic acids in the first set of leaves (the difference of 12 ± 7‰) and the converse in the second set (the difference of -16 ± 28‰) further support this conclusion as indicated by Freimuth et al., (2017). In some plants, the lowered δD values of the second/third set of leaves values were comparable to δD values of August, September and October of 2019 (Fig. 4.1). This suggests that by the time the leaf matures, the contribution of the previous year's photosynthates to the leaf wax pool of the current year is minimal; hence does not significantly lessen the early growing season bias in the leaf wax δD records of deciduous species.

4.3.4 Implication for the leaf wax δD-based reconstruction from the tropics

The majority of the deciduous and evergreen mature leaves did not synthesize leaf wax *n*-alkanes and *n*-alkanoic acids for ~ 4 months (i.e. during the application of tracer water for 110 days) in a growing season. As this period is significant compared to the range of the length of

rainy season observed in tropical biomes (~60 to ~240 days, Bombardi et al., 2019), our results have a bearing on interpreting leaf wax δD-based paleoclimate reconstructions from the tropics.

In tropical deciduous forests, the leaf emergence and fall are associated with the start and end of the rainy season, respectively (Van Schaik et al., 1993; Mediavilla and Escudero, 2003). The leaf wax-based δD records from dry tropical forests, which constitute about 42% of tropical forests (Van Bloem et al., 2004), are likely to be biased towards climatic conditions during the early growing season.

Tropical rain forest covers about 25% of tropical ecological zone (FRA, 2000). Deciphering the seasonality in the leaf wax δD records from evergreen biomes may not be straightforward due to varying leaf production patterns. While the sunlight dominantly controls pantropical leaf phenology (Van Schaik et al., 1993; Tang et al., 2017; Li et al., 2021), the effect of vapor pressure deficit and soil moisture stress has also been observed (Li et al., 2021). The leaf phenology in many evergreen species varies from twice a year (bimodal production) with peaks occurring during April-March and September-October at the equator (3°S to 3°N) whereas unimodal production occurs during July-August at latitudes beyond 5°S and 5°N (Li et al., 2021). Thus, the leaf wax δD records in evergreen catchments at the equator likely integrate climate conditions of months associated with bimodal leaf production whereas those at relatively higher latitudes will reflect the climate conditions during the single episode of leaf flushing. Further, region-specific leaf flushing patterns have also been observed. For example, in monsoonal climates the major leaf flushing in evergreen plants occurs immediately after the rainy season i.e. during the early dry season, but much before the flushing in deciduous species (Chakrabarty et al., 2021). This demonstrates the need to consider the leaf phenological pattern in the catchment while interpreting the δD-based leaf wax records from the tropical evergreen biomes.

The influence of the summer monsoonal rainfall on the Indian economy is well established (Mooley and Parthasarathy, 1983; Gadgil, 2003). The paleoclimate investigators (e.g. Sinha et al., 2007; Prasad et al., 2014; Sarkar et al. 2015; McGrath et al. 2021) and climate modelers (Sharmila et al., 2015; Vittal et al., 2020) often consider the core monsoon zone (CMZ) as a region of interest because its inter-annual precipitation variability correlates well with the All Indian Summer Monsoon Rainfall (Gadgil, 2003). Long-term hydroclimate reconstruction from CMZ could

provide a crucial 'target' dataset for testing the utility of the global and regional circulation models in predicting monsoonal precipitation during different mean states of climate. The current (Champion and Seth, 1968) and past (Ali et al., 2019) vegetation of the CMZ is dominated by tropical dry and moist deciduous forests. The tree species from these regions show a clear seasonality in leaf production (Kushwaha and Singh, 2005). Extending the inferences of this work, it is essential to consider the early growing season bias in leaf wax δD records from CMZ.

An interesting implication of vegetation-specific seasonality is that, on an orbital time scale, when the dominant vegetation at a location shifts between evergreen (usually existed during the wetter periods such as Holocene Climate Optima, HCO) and deciduous (observed during the drier periods such as the late Holocene), the seasonality in the leaf wax δD records might not be stationary with drier phases exhibiting a stronger bias towards climatic conditions of the early growing season.

4.3.5 Implication for leaf wax δD records from regions with seasonally varying moisture sources

Many regions in the tropics exhibit seasonally varying moisture sources each having distinct isotopic characteristics during a growing season (Araguás-Araguás et al., 1998; Yadava et al., 2007; Levin et al., 2009; Sánchez-Murillo et al., 2016). For example, the southern part of India receives the southwest (from June to September) and the northeast (from October to December) monsoons each having a distinct isotopic signature (e.g. Yadava et al., 2007). The regions near the transition between tropic and temperate zones often experience isotopically distinct tropical and extra-tropical air masses during summer and winter, respectively (Araguás-Araguás et al., 1998). Even though the seasonal vegetation from such regions receives both moisture sources, due to its production mainly during the early stages of leaf growth, *n*-alkanes and *n*-alkanoic acids might not record the isotopic signature of the moisture received during the latter part of the leaf growth. Therefore, the seasonality issue in leaf wax δD-based records is likely to be critical in regions that receive two or more moisture sources during the growing season.

4.4 Conclusions

Our seasonality study from the tropics, in conjunction with those from temperate (Tipple et al., 2013; Freimuth et al., 2017) and subtropical (Yang et al., 2021) regions, indicate that the *n*-

alkane δD records are biased towards the climatic conditions prevailing during the early stages of the leaf's growth. This study indicates δD records of *n*-alkanoic acids from the tropics are also biased towards the same. The climatic conditions that control the δD values of the source and leaf water during the early stages of the leaf's growth are preserved in the leaf wax δD records and should be considered while testing the predictive skills of the climate models. In the case of catchments dominated by deciduous species, this period coincides with the early growing season. A critical examination of community-scale leaf production patterns is required to decipher the seasonality in δD records from the evergreen biomes. Therefore, the inclusion of an ecosystem-level assessment of the leaf maturation period is recommended while carrying out leaf wax δD-based paleoclimatic investigations.

Chapter 5

Calibration of plant-derived isotope proxies against precipitation along a precipitation gradient in western peninsular India

5.1 Introduction

Precipitation plays a crucial role in controlling the carbon isotopic compositions ($\delta^{13}C$) of plants. Precipitation can modulate relative humidity which in turn affects the stomatal conductance and ultimately the $\delta^{13}C$ of plants (Farquahar, 1983; Diefendorf et al., 2010). It also controls the relative proportion of trees and grasses, which have distinct $\delta^{13}C$ values, at a given location. The $\delta^{13}C$ of plant-derived materials are incorporated into the soil, thereby influencing the $\delta^{13}C$ of soil organic matter ($\delta^{13}C_{SOM}$). Thus, $\delta^{13}C_{SOM}$ can be used for past precipitation and vegetation reconstructions.

For quantitative reconstructions of past vegetation and precipitation conditions, calibrations of the $\delta^{13}C_{SOM}$ and $\delta^{13}C$ of modern plants against precipitation amount are used. For calibration, the modern plants and soil samples are collected from locations experiencing different precipitation, preferably a precipitation gradient, and their $\delta^{13}C$ values are measured. The measured $\delta^{13}C$ values of modern plants and $\delta^{13}C_{SOM}$ are then correlated with the precipitation amount and a calibration equation is established (Stevenson et al., 2005; Lee et al., 2005; Feng et al., 2008; Murphy and Bowman, 2009; Kohn, 2010; Ma et al., 2012). India has several regions with a large rainfall gradient which provides an excellent opportunity to carry out such calibration exercise. However, only a few studies (Basu et al., 2015; Kirkels et al., 2022) have attempted to calibrate the plant-derived isotope proxies with precipitation amounts in India.

To understand the variation of plant-derived proxies with precipitation amount in western peninsular India, a field study along a precipitation gradient of ~500 to 3700mm/yr was conducted (see Fig. 2.7 in Chapter 2). The ecosystems along the transect ranged from tropical forests to shrub/grasslands. The detailed locations of the field have been provided in chapter 2 (Section 2.2). This chapter deals with the results and implication of the variability of (i) the types of C_4 grass species, (ii) $\delta^{13}C$ values of C_4 grasses, (iii) $\delta^{13}C$ of *n*-alkanes ($\delta^{13}C_{alk}$) values in grasses, (iv) $\delta^{13}C_{SOM}$ values, (v) $\delta^{13}C_{alk}$ values in soil, and (vi) δD of *n*-alkanes (δD_{alk}) values in soil, with precipitation amount.

5.2 Results

5.2.1 Grasses: speciation and their $\delta^{13}C$

Grasses were one of the main vegetation types, especially in the low and intermediate precipitation locations. There were occurrences of both C_3 and C_4 grasses in the region; the former was found only in the shaded areas in the higher precipitation regions (rainfall >2500 mm/yr) while the latter was found everywhere. The C_4 grasses were a minor component of the vegetation in high precipitation regions and mainly occupied open patches in thick vegetation. In intermediate precipitation regions (~1000 mm/yr), the proportion of grass was more than that in higher precipitation regions whereas in low precipitation areas (~500 to 600 mm/yr) the grasses constitute the dominant vegetation. As the C_3 grasses were absent in low precipitation regions, they were not considered for calibration against precipitation in this study. Henceforth in this chapter and thesis, the term grass refers to C_4 grasses only.

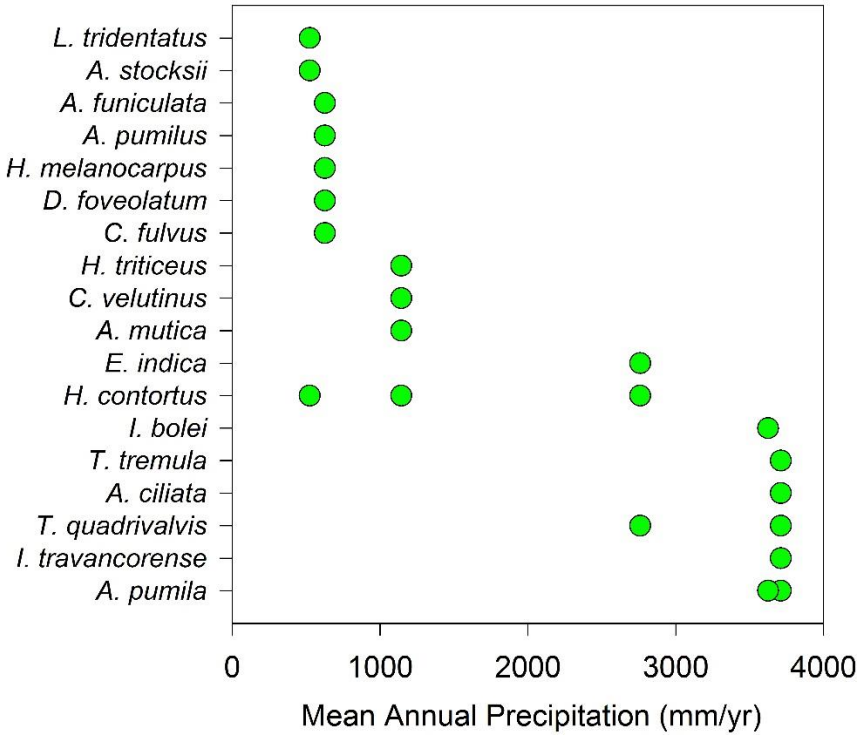

Fig. 5.1. Different grass species identified along the precipitation gradient.

Various grass species were present along the precipitation gradient. We observed clear speciation in C_4 grasses along the precipitation gradient (Fig. 5.1). Species such as *Chrysopogon fulvus*, *Dichanthium foveolatum*, *Heteropogon melanocarpus*, *Andropogon pumilus*, *Aristida funiculata*, *Heteropogon contortus*, *Aristida stocksii*, and *Lophopogon tridentatus* were found in low precipitation (~500-600 mm/yr) regions. *Arundinella pumila*, *Ischaemum travancorense*, *Themeda quadrivalvis*, *Arundinella ciliata*, *Themeda tremula*, *Ischaemum bolei*, *Heteropogon contortus*, *Eleusine indica* were found in high precipitation (>2500 mm/yr) regions. *Heteropogon contortus*, *Apluda mutica*, *Chrysopogon velutinus*, *Heteropogon triticeus* were found inintermediate precipitation (~1000 mm/yr) regions. *Heteropogon contortus* occurred at low, intermediate and high rainfall locations.

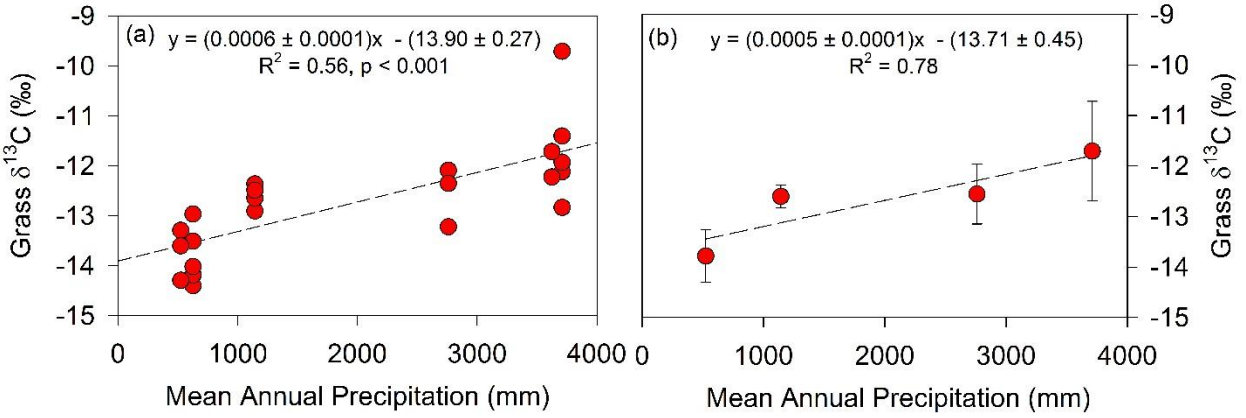

Fig. 5.2. Variations in $\delta^{13}C$ values of grass leaves with precipitation amount. (a) $\delta^{13}C$ values of individual samples, and (b) site-averaged $\delta^{13}C$ values of grasses.

Fig. 5.2 shows variation in the $\delta^{13}C$ values of bulk grass leaves with the precipitation amount. The $\delta^{13}C$ values of grasses along the precipitation gradient varied by 4.7‰ (i.e. from −14.4‰ to −9.7‰) (Fig. 5.2a), with an average value of −12.7 ± 1.1‰ (n = 22, 1σ). The $\delta^{13}C$ values of various grass species at a location was as high as 0.9 ‰ (1σ). When the average $\delta^{13}C$ values in the given rainfall regime were considered, the $\delta^{13}C$ values of grasses varied by 2.1 ± 1.0 ‰ (i.e. from −13.8 ± 0.5‰ to −11.7 ± 0.9‰) (Fig. 5.2b). A positive correlation was observed between $\delta^{13}C$ values of grasses and precipitation amount along the transect. The $\delta^{13}C$ values varied from −13.8 ± 0.5‰ to −11.7 ± 0.9‰ with an increase in precipitation from ~500 to 3700 mm/yr with a regression slope of 0.06‰/ 100mm (Fig. 5.2a).

The $\delta^{13}C_{alk}$ of grasses varied from −26.6‰ to −19.1‰. The *n*-C_{29}, *n*-C_{31} and *n*-C_{33} varied from −26.6‰ to −21.2‰, −26.1‰ to −20.5‰ and −25.5‰ to −19.1‰, respectively. As compared to the variation in $\delta^{13}C$ of bulk leaves, a higher variation in the $\delta^{13}C_{alk}$ values was observed. Due to this large variation, the $\delta^{13}C$ of all homologues of *n*-alkanes did not show a systematic variation with precipitation amounts (Fig. 5.3).

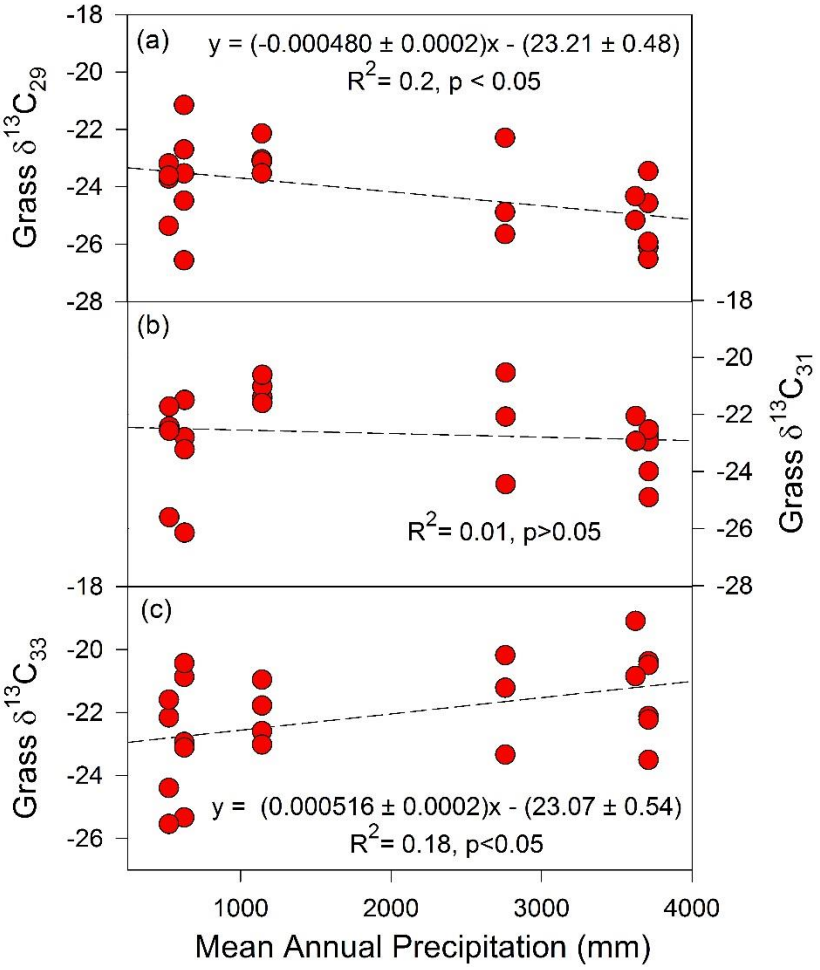

Fig. 5.3. Variations of $\delta^{13}C$ of (a) *n*-C_{29}, (b) *n*-C_{31}, and (c) *n*-C_{33} alkanes of the grasses with precipitation amounts.

5.2.2 Soil Organic Matter (SOM)

The $\delta^{13}C_{SOM}$ values varied by 13.2‰ (i.e. from −27.5‰ to −14.3‰) along the precipitation gradient. The $\delta^{13}C_{SOM}$ values at high, intermediate and low rainfall locations were −24.9 ± 2.1‰,

−16 ± 0.3‰, and −15.6 ± 1.2‰, respectively. We observed a significant ($p < 0.001$) negative correlation between $\delta^{13}C_{SOM}$ values with precipitation amount with a regression slope of −0.34‰/ 100 mm (Fig. 5.4).

The $\delta^{13}C_{alk}$ of different homologues in soil varied between −36.6‰ to −23.1‰. The *n*-C_{29}, *n*-C_{31} and *n*-C_{33} varied from −33.3‰ to −25.4‰, −36.2‰ to −25.7‰, and −36.6‰ to −23.1‰, respectively. All the homologues showed negative correlation with precipitation amounts (Fig. 5.5). From high precipitation (>2500 mm/yr) to low precipitation (~500-600 mm/yr) regions, the $\delta^{13}C$ values of *n*-C_{29}, *n*-C_{31} and *n*-C_{33} alkanes varied between −32 ± 0.9‰ to −27.6 ± 1.6‰, −34.2 ± 1.4‰ to −27.7 ± 1.4‰, −34 ± 1.9‰ to −26.1 ± 2.3‰, respectively.

The δD_{alk} values in soil varied between −150‰ to −100‰. The *n*-C_{29}, *n*-C_{31} and *n*-C_{33} varied from −140‰ to −100‰, −144‰ to −119‰, and −150‰ to −121‰, respectively. Homologues *n*-C_{31} and *n*-C_{33} showed a positive correlation with precipitation amounts whereas the *n*-C_{29} did not show any correlation (Fig. 5.6).

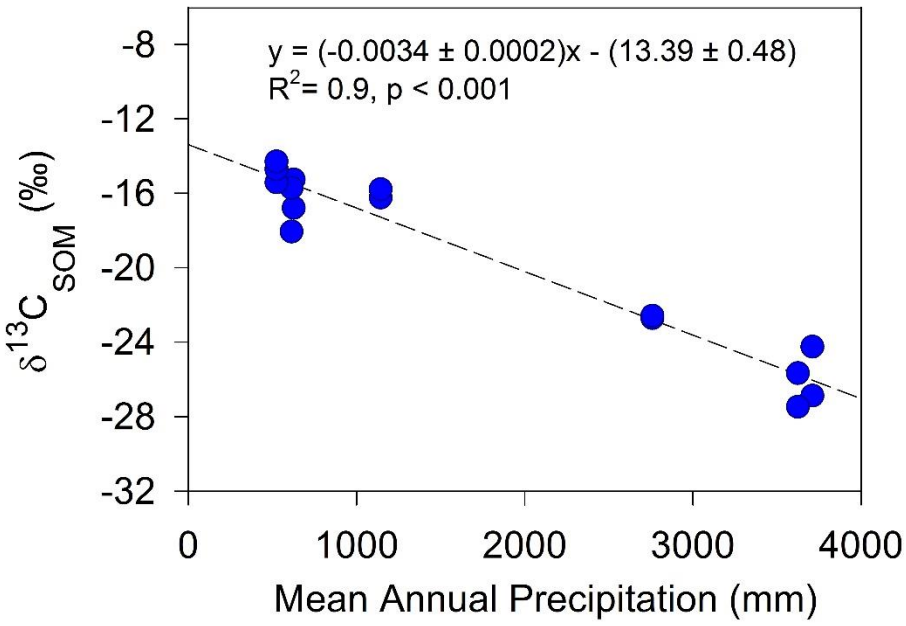

Fig. 5.4. Variation of the bulk $\delta^{13}C_{SOM}$ with precipitation amount.

5.3 Discussion

5.3.1 Variation of $\delta^{13}C$ values of grasses with precipitation

In the studied transect, we observed a positive correlation between grass $\delta^{13}C$ values with precipitation amount (Fig. 5.2). In India, only a few studies (Basu et al., 2015; Kirkels et al., 2022) have correlated $\delta^{13}C$ values of C_4 grasses and precipitation. In the Gangetic plains of India, the $\delta^{13}C$ values of C_4 plants showed a positive correlation with precipitation (Basu et al., 2015), whereas in the Godavari basin region, no correlation was observed (Kirkels et al., 2022). Globally, the correlation between $\delta^{13}C$ values of C_4 grasses with precipitation amounts has been observed to be positive in Australia (Murphy and Bowman, 2009), negative in northern (Ma et al., 2012) and northeastern China (Weiguo et al., 2005) and zero in south Africa (Swap et al., 2004) and eastern Mediterranean region (Hartman and Danin, 2010).

The observed positive correlation between $\delta^{13}C$ of grasses with precipitation is at odds with the expected negative correlation between $\delta^{13}C$ of vegetation and precipitation. The negative correlation is expected through the influence of precipitation on stomatal conductance. A higher precipitation often leads to higher relative humidity and hence higher stomatal conductance. This in turn results in a higher concentration of intercellular carbon dioxide (CO_2) which leads to higher isotopic fractionation i.e. relatively more ^{12}C is favored. The converse is true when the precipitation at a given location is lower (and lower stomatal conductance; lower concentration of intercellular CO_2). Therefore, a negative correlation is expected between the $\delta^{13}C$ of grasses and precipitation.

The isotope fractionation in plants starts with the diffusion of CO_2 through the stomatal apertures. The CO_2 then dissolves and gets converted to HCO_3^- and further fixed by phosphoenolpyruvate (PEP) carboxylase into oxaloacetate. In C_4 plants, after multiple transformations, the CO_2 is released in the bundle sheath cells and re-fixed by RuP_2 carboxylase. However, some CO_2 may leak out of bundle sheath cells into the mesophyll cells, where it might combine with CO_2 that diffuses through stomata (Farquahar, 1983).

For $\delta^{13}C$ values of C_4 plants, the following equation was established by Farquahar, (1983): $\delta^{13}C_{plant} = \delta^{13}C_{env} - a - (b_4+b_3\varphi-a)\, p_i/p_a$, where, $\delta^{13}C_{plant}$ and $\delta^{13}C_{env}$ are $\delta^{13}C$ of the C_4 plant and atmosphere, respectively; 'a' is the isotopic fractionation (4.4‰) during diffusion of CO_2 through

the stomata; 'b_4' is the fractionation by phosphoenolpyruvate (~ −5.7‰ at 25 °C) and 'b_3' is the fractionation by ribulose bisphosphate (~27‰); 'p_i' is the concentration of intercellular CO_2 and 'p_a' is the concentration of ambient atmospheric CO_2. 'φ', also known as leakiness, refers to the proportion of carbon that leaks back into the mesophyll cells.

The φ of the C_4 plants determines whether the association between precipitation amount and $\delta^{13}C$ is positive (Murphy and Bowman, 2009; Basu et al., 2015), negative (Weiguo et al., 2005; Ma et al., 2012) or zero (Swap et al., 2004; Kirkel et al., 2022). When φ is below 3.7, a positive correlation may be observed between the $\delta^{13}C$ of C_4 vegetation and precipitation amount (Murphy and Bowman, 2009; Basu et al., 2015). The positive correlation between the $\delta^{13}C$ of C_4 grasses and the precipitation amount observed in this study suggests that the φ values of the C_4 grasses in the regions are likely to be low (< 3.7).

5.3.2 Correlation between $\delta^{13}C$ values of grass and precipitation: Implication for paleo-vegetation reconstruction

Quantitative reconstruction of past vegetation using an isotope mass balance equation requires fixing $\delta^{13}C$ values of the end members of vegetation (i.e. C_3 and C_4 plants). Typically, $\delta^{13}C$ values of modern plants are used for this. However, if the precipitation amount controls $\delta^{13}C$ values of C_3 and C_4 end members, $\delta^{13}C$ values of the modern plants may be different from the ancient plants that were the source of organic matter in paleosols or sediments, as the ancient plants might have thrived in a different climate setting compared to the present. Thus, there is a need to account for the effect of past climate conditions on $\delta^{13}C$ values of plant end members (Zhang et al., 2003; Yang et al., 2015; Sarangi et al., 2021).

To know the effect of precipitation on $\delta^{13}C$ values of the end-members, often calibrations of $\delta^{13}C$ values of modern vegetation against precipitation are utilized (Zhang et al., 2003; Vidic and Montanez, 2004; Weiguo et al., 2005). This calibration could then be used to fix the end member $\delta^{13}C$ values if the precipitation during that period is independently known (for example, from δD studies).

In the studied region, the $\delta^{13}C$ values of C_4 grasses increased from −13.8 ± 0.5‰ to −11.7 ± 0.9‰ with an increase in precipitation from ~500 to 3700 mm/yr which translates to 0.07 ± 0.03

‰ per 100 mm of precipitation. The actual fit yielded an equation: $\delta^{13}C_{C4\ grass} = (0.0006 \pm 0.0001) * \text{Rainfall} - (13.9 \pm 0.27)$ (Fig. 5.2a). This suggests low sensitivity of the end member $\delta^{13}C$ of grasses for precipitation variability in the study area. This implies that minor fluctuations in precipitation amounts in the study region would not exert a substantial influence on the $\delta^{13}C$ values of C_4 grasses. Therefore, when the past precipitation changes are of lower magnitude, use of modern end member $\delta^{13}C$ values of grasses in isotopic mass balance equations might not introduce significant error in the reconstructed vegetation composition in this region.

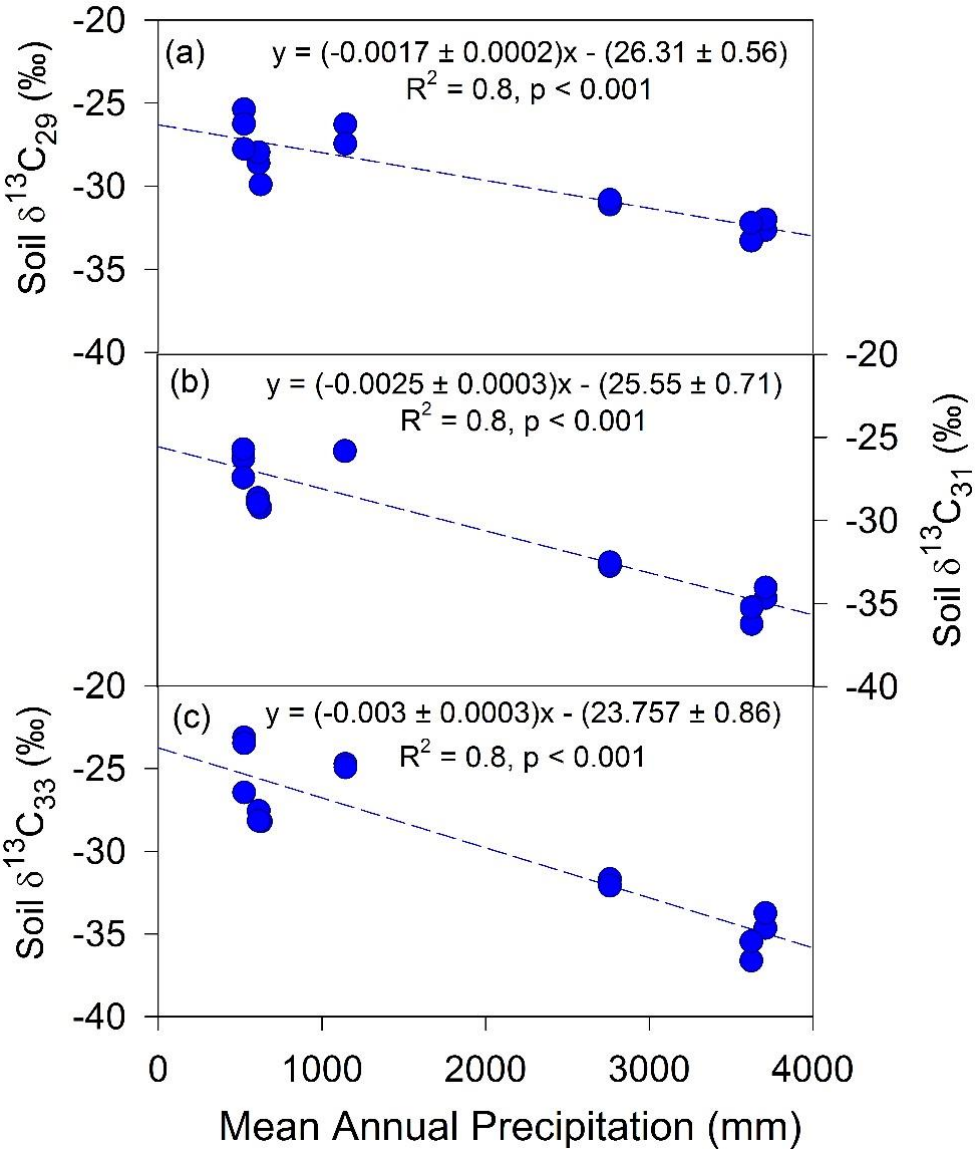

Fig. 5.5. Variations of $\delta^{13}C_{alk}$ of (a) *n*-C_{29}, (b) *n*-C_{31}, and (c) *n*-C_{33} in soil with precipitation amount.

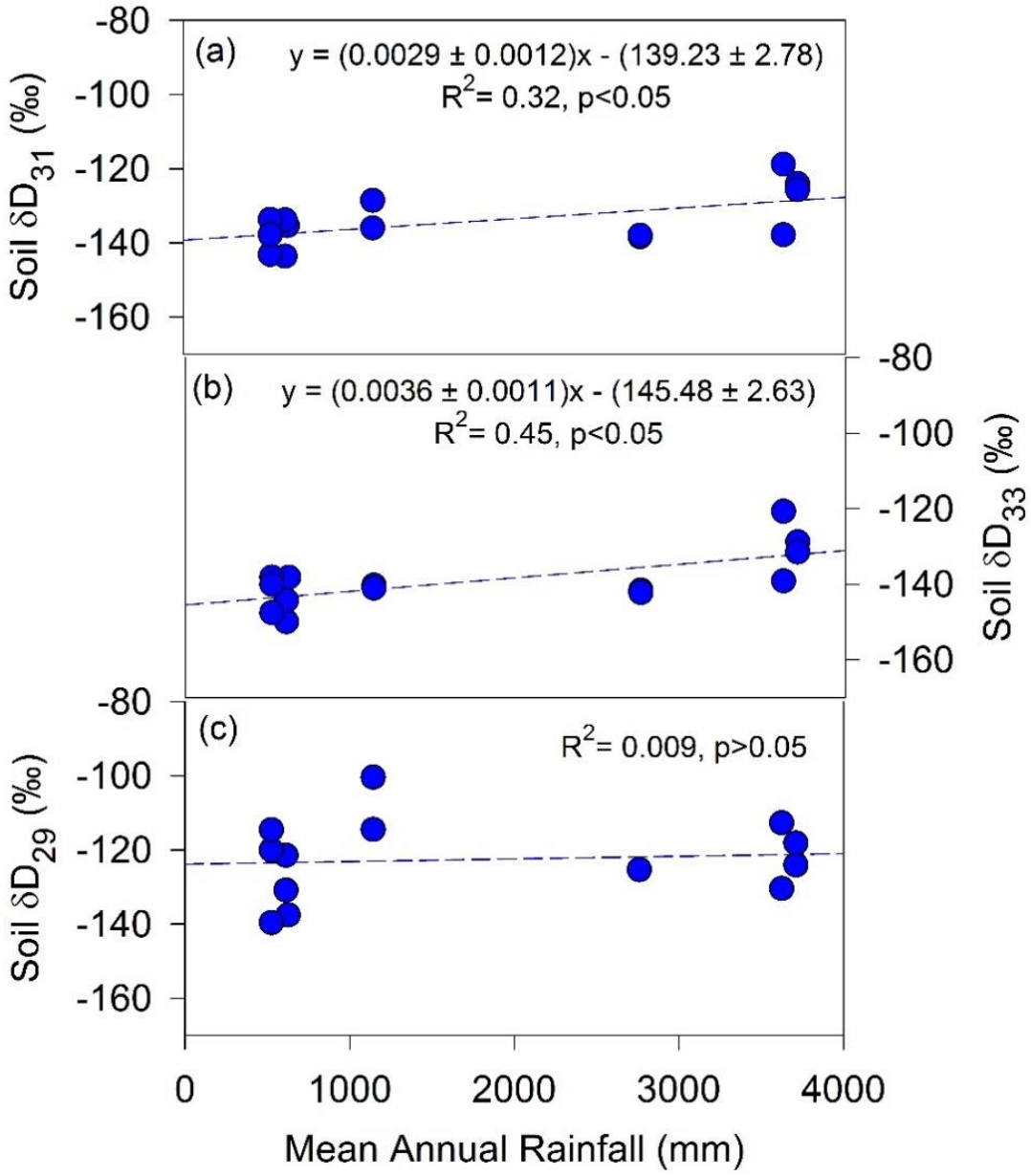

Fig. 5.6. Variations of δD_{alk} of chain lengths (a) *n*-C_{31}, (b) *n*-C_{33} and (c) *n*-C_{29} in soil with precipitation amount.

5.3.3 Variation in $\delta^{13}C_{SOM}$ values with precipitation

In the study, a decrease in $\delta^{13}C_{SOM}$ values with increasing precipitation was observed (Fig. 5.4). Decrease in $\delta^{13}C_{SOM}$ values with precipitation has also been observed in arid and semi-arid

central East Asia (Lee et al., 2005), Northern China (Ma et al., 2012), multiple bio-climatic zones of central east Asia (Feng et al., 2008) and Palouse region of USA (Stevenson et al., 2005).

The inverse relationship between $\delta^{13}C_{SOM}$ values and precipitation observed in this study was likely a result of contribution from local vegetation. The proportion of C_3/C_4 vegetation in a region is influenced by a range of climate factors, including rainfall intensity and seasonality, temperature, atmospheric CO_2 concentration (pCO_2), and humidity (Singh et al., 2016; Amir et al., 2018). However, it's noted that the expansion of C_3 or C_4 vegetation in different ecosystems may respond differently to these climate factor (Amir et al., 2024). For example, proportion of C_4 vegetation increases with precipitation in North-West Indo-Gangetic Plain (Amir et al., 2024), whereas, in other regions of Ganga Plain (Agrawal et al., 2012), expansion of C_3 vegetation was favored during high precipitation conditions. In the studied transect, trees were dominant in higher precipitation regions whereas in lower precipitation regions there was a predominance of grasses along with few scattered trees (Fig. 2.8 in chapter 2). The majority of tropical trees use C_3 photosynthetic pathway (Cernusak et al., 2007) whereas tropical grasses use C_4 photosynthetic pathway (Cerling et al., 2011). The C_3 and C_4 vegetation use different photosynthetic pathways, and they fractionate carbon isotopes to a different extent which is reflected in their $\delta^{13}C$ values; ~ −20‰ to −37‰ for C_3 plants (Kohn, 2010) and ~ −9‰ to −16‰ for C_4 plants (Wynn and Bird, 2008). In the studied transect, the C_4 grasses have $\delta^{13}C$ values of -12.7 ± 1.1‰ ($n = 22$, 1σ). Thus, the observed $\delta^{13}C_{SOM}$ value of -24.9 ± 2.1‰ suggests a significant contribution from C_3 plants. Overall, the observed $\delta^{13}C_{SOM}$ values in low (-15.6 ± 1.2‰) and high (-24.9 ± 2.1‰) precipitation regions indicated a dominant contribution from C_4 and C_3 vegetation, respectively.

5.3.4 Correlation between $\delta^{13}C_{SOM}$ values with precipitation: Implication for past precipitation reconstruction

The calibration equation obtained from the correlation between modern $\delta^{13}C_{SOM}$ values and precipitation amount was as follows: Rainfall = $-$ (276.460 ± 18.133) ∗ $\delta^{13}C_{SOM}$ – (3605.487 ± 357.629), the standard error of estimate being 340 mm. This equation can be utilized to reconstruct past precipitation conditions from $\delta^{13}C_{SOM}$ values of paleosols in western peninsular India.

To understand the modern $\delta^{13}C_{SOM}$ variation with precipitation amount in India, we have combined our results with the available data from the core monsoon zone (Kirkels et al., 2022),

lower Gangetic floodplains (Roy and Sanyal, 2022) and peninsular India (S.M. Devi, personal communication) (Fig. 5.7). The study by Kirkels et al., (2022) include $\delta^{13}C_{SOM}$ from the grasslands (C_4 flora), dry deciduous forests, thorny shrublands, moist and evergreen deciduous forests of the core monsoon zone (Kirkels et al., 2022). The soil organic carbon from mixed moist deciduous and evergreen trees, shrubs and grasses of lower Gangetic floodplains was sampled by Roy and Sanyal (2022). The present study and the one done by S.M. Devi included semi-evergreen forests, mixed forests and shrub/grasslands of western peninsular India.

Plotting $\delta^{13}C_{SOM}$ data from various geographical regions of India revealed a negative logarithmic association between $\delta^{13}C_{SOM}$ and precipitation amount (Fig. 5.7). The data exhibits a relatively narrow spread in $\delta^{13}C_{SOM}$ values at both low and high precipitation regimes, indicating a relatively consistent response of plant-derived $\delta^{13}C$ values in these precipitation conditions. In contrast, a substantial spread observed in $\delta^{13}C_{SOM}$ values at the intermediate precipitation regime indicated an increased variability in $\delta^{13}C$ values of plant-derived materials in the soil.

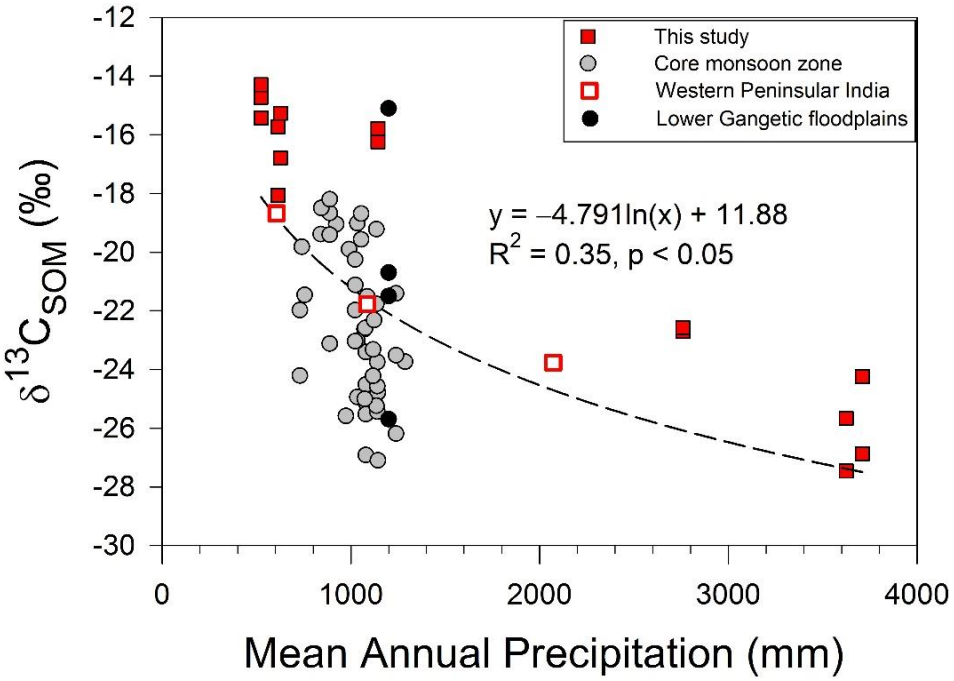

Fig. 5.7. Variations in $\delta^{13}C_{SOM}$ and precipitation amount in modern soils of India. (Data source: the core monsoon zone from Kirkels et al., 2022; Lower Gangetic floodplain from Roy and Sanyal, 2022; Western Peninsular India from personal communication with S. M. Devi).

In Fig. 5.7, only the present study covers regions with high precipitation. Nevertheless, the plot (Fig. 5.7) indicated a saturation of $\delta^{13}C_{SOM}$ values in locations experiencing precipitation more than 2000 mm/yr which is dominated by the C_3 flora. The dominance of C_3 flora at higher precipitation regimes provides a plausible explanation for the observed logarithmic relationship between $\delta^{13}C_{SOM}$ and precipitation amount. Additionally, in a global compilation, Stein et al., (2021) showed saturation of $\delta^{13}C_{SOM}$ values within C_3-dominated ecosystems around precipitation of ~1500-2000 mm/yr indicating plant physiological response of C_3 flora themselves becomes less sensitive to increase in precipitation around ~2000mm of precipitation.

The substantial variation in $\delta^{13}C_{SOM}$ values observed in regions experiencing precipitation between ~500 to ~1500 mm/yr (Fig. 5.7) can be attributed to the influence of mixed C_3-C_4 vegetation rather than precipitation amount. The presence of mixed C_3-C_4 vegetation could be attributed to the influence of topography-mediated local hydrological conditions on the vegetation composition in a region.

5.3.5 Correlation between $\delta^{13}C_{alk}$ in soil and precipitation

In the studied transect, the $\delta^{13}C_{alk}$ in soils decreased with increasing mean annual precipitation (Fig. 5.5). In high precipitation regions, the $\delta^{13}C$ values of *n*-C_{29}, *n*-C_{31} and *n*-C_{33} were −32 ± 0.9‰, −34.2 ± 1.4‰ and −34 ± 1.9‰, respectively. In low precipitation regions, the $\delta^{13}C$ values of *n*-C_{29}, *n*-C_{31} and *n*-C_{33} were −27.6 ± 1.6‰, −27.7 ± 1.5‰ and −26.2 ± 2.3‰, respectively.

As with the $\delta^{13}C_{SOM}$ variations along the precipitation gradient, the negative correlation between $\delta^{13}C_{SOM}$ values and precipitation amount may be the result of contribution from local vegetation. The $\delta^{13}C$ values of *n*-alkanes of C_4 grasses in the studied transect varied from −26.6‰ to −19.1‰. In Western India, the $\delta^{13}C$ values of *n*-alkanes of C_3 and C_4 plants ranged from −37.4‰ to −30.1‰ and −25.8‰ to −21‰, respectively (Basu et al., 2019). Considering the reported $\delta^{13}C$ values of vegetation (Basu et al., 2019 and this study), the $\delta^{13}C_{alk}$ values observed in the studied transect represent the dominant contribution from C_3 and C_4 vegetation at high and low precipitation locations.

5.3.6 Correlation between $\delta^{13}C_{alk}$ in soil and $\delta^{13}C_{SOM}$ values

In this study, both $\delta^{13}C_{SOM}$ and $\delta^{13}C_{alk}$ in soil showed a negative correlation with precipitation amount. When different homologues of $\delta^{13}C_{alk}$ in soil and $\delta^{13}C_{SOM}$ values were compared, strong positive correlations were observed between them (Fig. 5.8) (Table 5.1). This suggests that $\delta^{13}C_{alk}$ in soil and $\delta^{13}C_{SOM}$ values provide consistent information regarding precipitation amount. Thus, $\delta^{13}C_{SOM}$ investigations, which are analytically easy to carry out, would be adequate for past precipitation reconstruction in western peninsular India.

5.3.7 Correlation between δD_{alk} in soil and mean annual precipitation

In the tropics, the δD values of precipitation decrease with increase in precipitation amount (Dansgaard, 1964). Since the plants' δD_{alk} values reflect the δD values of precipitation, an inverse relationship of δD_{alk} with precipitation amount is expected. Contrary to this, in the studied transect δD_{alk} values in soil showed a positive correlation (Fig. 5.6).

The positive correlation observed here indicated the effect of vegetation on δD_{alk} values in soil. Several studies have reported higher δD_{alk} values in trees compared to grasses (Krull et al., 2006; Hou et al., 2007; Basu et al., 2019) owing to the differences in apparent fractionation factors (ε_{app}) among trees and grasses (Chikaraishi and Naraoka, 2003; Sachse et al., 2012). For example, in the Banni grassland of western India, Basu et al., (2019) reported δD values *n*-C_{29} alkane of C_3 trees and C_4 grasses as −133 ± 25.1‰ and −176 ± 28.9‰, respectively and their corresponding ε_{app} values were −113 ± 25.1‰ and −156 ± 28.9‰, respectively. In the present study, we could not analyze the δD values of local vegetation. Nevertheless, the positive correlation observed in this study indicates the influence of local vegetation composition (i.e. C_4 and C_3 vegetation domination at low and high precipitation regions, respectively) on the measured δD_{alk} values in soil. This suggests that the measured δD values of the leaf wax derived compounds should be corrected for the vegetation composition before reconstructing the δD values of precipitation.

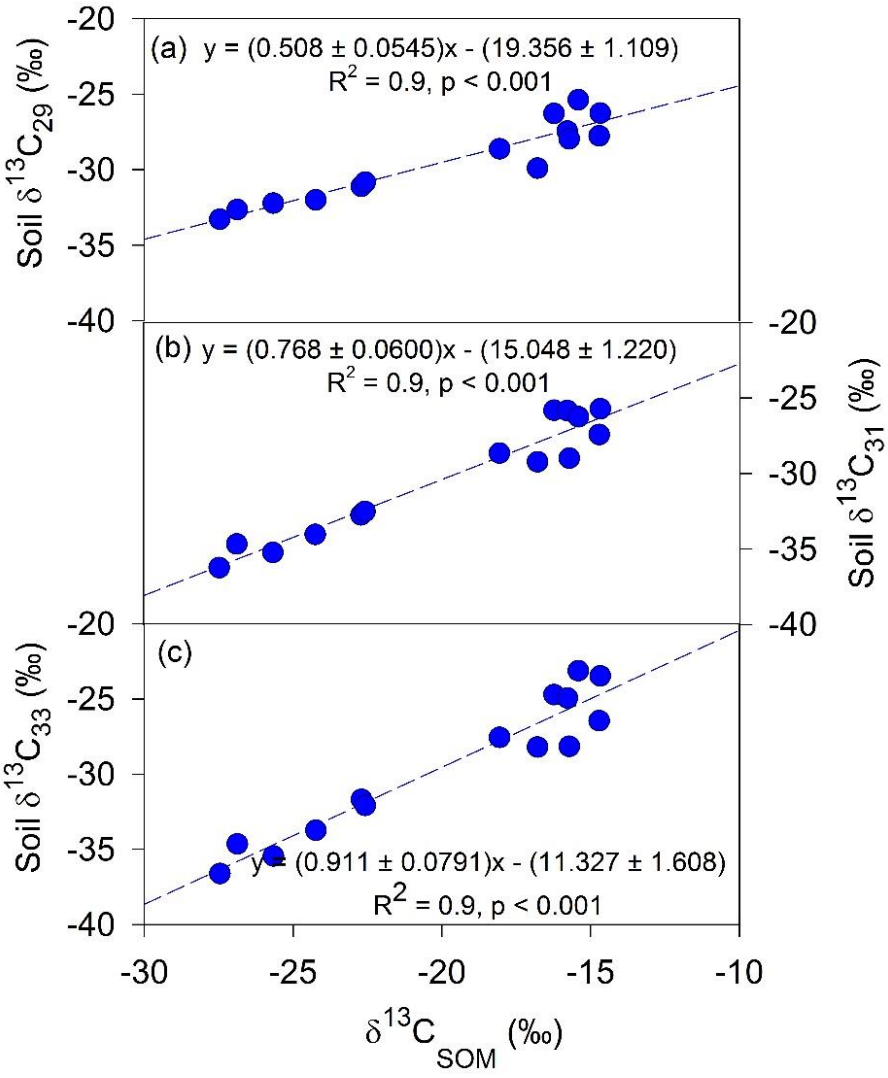

Fig. 5.8. Correlations of $\delta^{13}C_{alk}$ of (a) *n*-C_{29}, (b) *n*-C_{31}, and (c) *n*-C_{33} in soil with $\delta^{13}C_{SOM}$ values.

	$\delta^{13}C_{29}$	$\delta^{13}C_{31}$	$\delta^{13}C_{33}$	$\delta^{13}C_{SOM}$
$\delta^{13}C_{29}$	1			
$\delta^{13}C_{31}$	0.97	1		
$\delta^{13}C_{33}$	0.98	0.99	1	
$\delta^{13}C_{SOM}$	0.93	0.96	0.95	1

Table 5.1. Correlations (r-values) between $\delta^{13}C_{alk}$ of different homologues and $\delta^{13}C_{SOM}$.

5.4 Conclusion

Precipitation is an integral factor in shaping the relative abundance of C_3-C_4 plants in a region and their $\delta^{13}C$ values. The precipitation along the studied transect in western peninsular India varied from ~500 to 3700 mm/yr. The regions experiencing low precipitation (~500-600 mm/yr) had a predominance of grasses along with few scattered trees whereas high precipitation (>2500 mm/yr) regions dominated trees. To calibrate the variations of plant-derived isotope proxies along the precipitation gradient, we investigated the bulk $\delta^{13}C$ as well as $\delta^{13}C_{alk}$ values of C_4 grasses; $\delta^{13}C_{SOM}$, $\delta^{13}C_{alk}$ and δD_{alk} values in soil along the transect.

Along the precipitation gradient, differential speciation of C_4 grasses was observed. The $\delta^{13}C$ of modern grasses showed a positive correlation with precipitation amount. For quantitative paleo-vegetation reconstructions at glacial/interglacial timescales, the calibration equation obtained in this study [$\delta^{13}C_{C4\ grass} = (0.0006 \pm 0.0001) * \text{Rainfall} - (13.9 \pm 0.27)$] can be used to fix the C_4 grass end member. However, given the low sensitivity of $\delta^{13}C_{C4\ grass}$ for precipitation changes in the equation, such correction may not be necessary when the precipitation variability is low.

The $\delta^{13}C_{SOM}$ showed a negative correlation with precipitation amount. Based on the correlation observed in this study, a calibration equation has been suggested for past precipitation reconstruction from $\delta^{13}C_{SOM}$ values in western peninsular India [$\text{Rainfall} = -(276.460 \pm 18.133) * \delta^{13}C_{SOM} - (3605.487 \pm 357.629)$]; standard error of estimate being 340 mm. A positive correlation was observed between the $\delta^{13}C_{SOM}$ and $\delta^{13}C_{alk}$ in soil, suggesting that the analysis of $\delta^{13}C_{SOM}$ is sufficient for precipitation reconstruction.

Contrary to the expected negative correlation between soil δD_{alk} values and precipitation amount, a positive correlation was observed between them in the studied transect. It appears that the positive correlation between the soil δD_{alk} values and precipitation could be a result of the differences in the apparent fractionation factors (between the δD values of *n*-alkane and the source water) of trees and grasses in the studied region. This issue should be considered before reconstructing past precipitation changes using δD_{alk} values.

Chapter 6
Conclusion

6.1 Conclusions

A variety of climate proxies are used for precipitation reconstruction. However, in most of the cases, the reconstructions are qualitative, limiting their utility. For quantitative precipitation reconstructions, characterization of the climate proxies is needed. This work aims at characterizing some of the plant-derived isotope proxies that are widely used in precipitation reconstructions. The proxies considered were (i) the hydrogen isotopic composition (δD) of leaf wax derived *n*-alkanes and *n*-alkanoic acids, (ii) carbon isotopic composition ($\delta^{13}C$) of soil organic matter, (iii) $\delta^{13}C$ and δD of *n*-alkanes in soil organic material, (iv) $\delta^{13}C$ of grass.

In this work, the δD and ε_{app} values of leaf wax *n*-alkanes and *n*-alkanoic acids in tropical angiosperm trees (two plants each of four evergreen and three deciduous species) were characterized by growing plants with water of known isotopic compositions. The seasonality in δD records on *n*-alkane and *n*-alkanoic acids were deciphered through an isotopic labelling experiment; whether or not the leaf wax compounds are synthesized in the mature leaves of tropical angiosperms was tested. In a field study, $\delta^{13}C$ and δD values of plant-derived proxies were calibrated against precipitation amounts along the precipitation gradient in western peninsular India. The following is the summary and conclusion of the present research work.

6.1.1 δD records of the leaf wax n-alkanes and n-alkanoic acids

6.1.1.1 Apparent fractionation factors (ε_{app})

The ε_{app}values in the studied species were −119 ± 23‰ (n = 14) for *n*-alkanes and −126 ± 27‰ (n = 12) for *n*-alkanoic acids of chain lengths C_{31} and C_{30}, respectively. These values can be used to reconstruct δD of the past precipitation from the measured δD of *n*-alkanes and *n*-alkanoic acids in the tropical records. The uncertainty on these values gets propagated to the uncertainty in δD of reconstructed precipitation and hence to the inferred precipitation amount or atmospheric circulation. This necessitates understanding factors that contribute to the uncertainty on the ε_{app} values. Despite all the species being grown with the water of the same δD value, variation in ε_{app} values were observed. This variability stems mainly from species effect i.e. variation in the ε_{app} values of different species. Further, the similarity of the ε_{app} values of different homologues of *n*-alkane (and *n*-alkanoic acids) suggested that in tropical catchments dominated by angiosperm trees, a single ε_{app} value could be considered while reconstructing

hydrogen isotope of precipitation (δD_{precip}) values. No systematic difference between the ε_{app} values of deciduous and evergreen plants was observed. This implies that a shift in vegetation from deciduous to evergreen might not lead to a significant shift in community-scale ε_{app} values.

6.1.1.2 Seasonality in tropical leaf wax records

Our long-term isotope-labelled experiment showed that *n*-alkanes and *n*-alkanoic acids are insignificantly produced in the mature leaves of tropical angiosperms; the bulk of them were produced during the early stages of the leaf's growth. As the δD of leaf wax compounds reflect the δD of the ambient precipitation, our results suggest that the δD records of *n*-alkanes and *n*-alkanoic acids from the tropics are biased towards the climate conditions existing during the early stages of the leaf's growth.

In the case of catchments dominated by deciduous species, the leaf emergence and fall closely follow the rainy season. Hence the δD records of *n*-alkanes and *n*-alkanoic acids from such locations reflect climatic conditions at the beginning of the rainy season. The leaf phenology in evergreen tropical locations is known to be affected by many factors such as sunlight variability, vapor pressure deficit between leaf interior and atmosphere, and soil moisture. The leaf production is reported to be bimodal near the equator and unimodal beyond 5°S and 5°N. This suggests that a critical examination of community-scale leaf production patterns is required to decipher the seasonality in δD records from the evergreen biomes.

In tropical deciduous species, stored carbohydrate reserves (formed during the previous growing season) are utilized for the synthesis of leaf wax *n*-alkanes and *n*-alkanoic acids in new leaves. In our experiment, the δD analysis of *n*-alkanes and *n*-alkanoic acids of new leaves indicated minor incorporation of the previous year's photosynthates. As the leave matures, the contribution of the previous year's photosynthates to the leaf wax pool of the current year is minimal. Hence, the early growing season bias in the leaf wax δD records of deciduous species is not affected by the transfer of previous year's photosynthates.

Quantitative paleo-precipitation data generated from leaf wax δD records are biased towards the precipitation conditions during the early stages of the leaf's growth. During validations

of the climate models, climate parameters during the early stages of the leaves should be considered as a 'target' dataset for replication.

6.1.2 Correlations of plant-derived isotope proxies with precipitation amount

This study reports the correlations of isotopes of soil organic matter and C_4 grasses with precipitation amount in western peninsular India. The $\delta^{13}C_{SOM}$ and $\delta^{13}C_{alk}$ in soil exhibited a negative correlation with the precipitation amount, whereas δD_{alk} in soil showed a positive correlation. The $\delta^{13}C$ values of C_4 grasses were positively correlated with precipitation amount.

6.1.2.1 $\delta^{13}C_{SOM}$ and $\delta^{13}C_{alk}$ in soil

Along the precipitation gradient, the $\delta^{13}C_{SOM}$ values increased from −24.9 ± 2‰ to −15.6 ± 1.2‰, corresponding to a decrease in precipitation from 3700 mm/yr to ~500mm/yr. The following equation was derived from the correlation: [Rainfall = −(276.460 ± 18.133) ∗ $\delta^{13}C_{SOM}$ – (3605.487 ± 357.629)]. This equation provides a means for past precipitation reconstruction from $\delta^{13}C_{SOM}$ values in paleosols in western peninsular India.

The $\delta^{13}C_{alk}$ in soil exhibited a negative correlation with precipitation amount. Across the gradient, from high (>2500 mm/yr) to low (~500-600 mm/yr) precipitation regions, the $\delta^{13}C$ values of *n*-C_{29}, *n*-C_{31} and *n*-C_{33} alkanes varied within the ranges of −32 ± 0.9‰ to −27.6 ± 1.6‰, −34.2 ± 1.4‰ to −27.7 ± 1.4‰, −34 ± 1.9‰ to −26.1 ± 2.3‰, respectively. This study presents calibration equations correlating various chain lengths $\delta^{13}C_{alk}$ values with precipitation.

Upon comparing the values of $\delta^{13}C_{alk}$ in soil and $\delta^{13}C_{SOM}$, strong positive correlations were identified between them. This implies that the $\delta^{13}C_{SOM}$ investigations, which are analytically easy to carry out, would suffice for past precipitation reconstructions in western peninsular India.

6.1.2.2 δD_{alk} in soil

In tropical regions, the δD values of precipitation typically decrease with an increase in the precipitation amount. Given that the plants' δD_{alk} values reflect the δD values of precipitation, one would expect an inverse correlation of δD_{alk} with precipitation amount. However, in the study area, δD_{alk} values in soil showed a positive correlation with precipitation amount. This discrepancy suggests the influence of local vegetation composition (in terms of C_3 and C_4 end member contributions) on the measured δD_{alk} values in soil. Therefore, it is recommended to

correct the measured δD_{alk} values for vegetation composition before reconstructing the δD values of precipitation.

6.1.2.3 $\delta^{13}C$ of C_4 grasses

Along the precipitation gradient, differential speciation of C_4 grasses was observed. The $\delta^{13}C$ values showed a positive correlation with precipitation amount, increasing from −13.8 ± 0.5‰ to −11.7 ± 0.9‰ in tandem with the increase in precipitation from ~500 to 3700 mm/yr. The sensitivity of the $\delta^{13}C$ values of C_4 grasses to precipitation change was calculated as 0.07 ± 0.03 ‰ per 100 mm of precipitation. The low sensitivity implies that minor fluctuations in precipitation amount are unlikely to impact the end member $\delta^{13}C$ values of C_4 grasses significantly. Therefore, in cases of lower magnitude past precipitation changes, the use of modern $\delta^{13}C$ values of C_4 grass end-member may not introduce significant error in the vegetation reconstructions in western peninsular India.

6.2 Future directions

The following future work directions were recognized for reliable quantification of past precipitation in the tropics:

1. This study proposed community-scale ε_{app} values of deciduous and evergreen trees which would be beneficial in deciphering past precipitation variability in tree-dominated regions. The ε_{app} evaluation of grasses and shrubs needs to be considered for precipitation reconstruction if these growth forms occur in significant proportion in the catchments.

2. Along the precipitation gradient, the measured $\delta^{13}C_{SOM}$ values exhibited a negative correlation with precipitation amount, influenced by the relative contribution from local vegetation. To explore the variations of $\delta^{13}C_{SOM}$ with precipitation across India, the current data was compiled with available $\delta^{13}C_{SOM}$ data from other regions and a negative logarithmic correlation was derived. However, a substantial variability of ~14‰ in $\delta^{13}C_{SOM}$ values was observed within the precipitation range of ~500 - 1500 mm/yr, suggesting contributions from mixed C_3-C_4 vegetation. The considerable $\delta^{13}C_{SOM}$ variability at a specific precipitation regime restricts the direct applicability of

the obtained correlation. Towards this, it is important to understand how factors other than precipitation influence the relative abundance of C_3 and C_4 vegetation in a region receiving a given rainfall amount.

3. In this study, we have provided a calibration equation for $\delta^{13}C_{SOM}$ and precipitation, offering a tool for past precipitation reconstruction from paleosols. However, for reconstructing past precipitation conditions using $\delta^{13}C$ of organic matter from lacustrine or marine sediments the extent of isotopic alterations during transportation and deposition should be evaluated. In a catchment consisting of regions with distinct vegetation types (e.g. the precipitation gradient considered in the present study with evergreen forests in high rainfall region and grasslands in low rainfall region), it is important to evaluate (i) how their relative proportions vary as precipitation changes and (ii) in what proportions these regions contribute organic matter to the sedimentary archives such as lakes or marine sediments.

4. We calibrated the $\delta^{13}C$ values of C_4 grasses with precipitation amount along a precipitation gradient in western peninsular India. For broader applicability, similar calibration studies can be extended to C_3 growth forms.

Bibliography

Agrawal, S., Sanyal, P., Sarkar, A., Jaiswal, M.K. and Dutta, K., 2012. Variability of Indian monsoonal rainfall over the past 100 ka and its implication for C3–C4 vegetational change. Quaternary Research, 77(1), pp.159-170.

Aichner, B., Feakins, S.J., Lee, J.E., Herzschuh, U. and Liu, X., 2015. High-resolution leaf wax carbon and hydrogen isotopic record of the late Holocene paleoclimate in arid Central Asia. Climate of the Past, 11(4), pp.619-633.

Aichner, B., Rajabov, N., Shodmonov, M., Mętrak, M., Suska-Malawska, M., Strecker, M. and Sachse, D., 2021. Local effects on soil leaf wax hydrogen isotopes along a west to east transect through the Pamirs, Tajikistan. Organic Geochemistry, 160, p.104272.

Ali, S.N., Dubey, J., Shekhar, M. and Morthekai, P., 2019. Holocene Indian Summer Monsoon variability from the core monsoon zone of India, a pollen-based review. Grana, 58(5), pp.311-327.

Amir, M., Paul, D. and Chang, Y.P., 2024. Indian summer monsoon variability during the past~ 75 ka based on stable isotope records of sediments from NW India. Palaeogeography, Palaeoclimatology, Palaeoecology, 637, p.112016.

Amir, M., Paul, D., Singh, A., Gupta, S., Chabaux, F., Granet, M. and Balakrishnan, S., 2018. Link between climate and catchment erosion in the Himalaya during the late Quaternary. Chemical Geology, 501, pp.68-76.

Araguás-Araguás, L., Froehlich, K. and Rozanski, K., 1998. Stable isotope composition of precipitation over southeast Asia. Journal of Geophysical Research: Atmospheres, 103(D22), pp.28721-28742.

Armstrong, M.S., Kiem, A.S. and Vance, T.R., 2020. Comparing instrumental, palaeoclimate, and projected rainfall data: Implications for water resources management and hydrological modelling. Journal of Hydrology: Regional Studies, 31, p.100728.

Baczynski, A.A., McInerney, F.A., Wing, S.L., Kraus, M.J., Morse, P.E., Bloch, J.I., Chung, A.H. and Freeman, K.H., 2016. Distortion of carbon isotope excursion in bulk soil organic matter during the Paleocene-Eocene thermal maximum. GSA Bulletin, 128(9-10), pp.1352-1366.

Baer, D.S., Paul, J.B., Gupta, M. and O'keefe, A., 2002. Sensitive absorption measurements in the near-infrared region using off-axis integrated-cavity-output spectroscopy. Applied Physics B, 75, pp.261-265.

Ball, J.T., Woodrow, I.E. and Berry, J.A., 1987, October. A model predicting stomatal conductance and its contribution to the control of photosynthesis under different environmental conditions. In Progress in photosynthesis research: volume 4 proceedings of the VIIth international congress on photosynthesis providence, Rhode Island, USA, august 10–15, 1986 (pp. 221-224). Dordrecht: Springer Netherlands.

Banerji, U.S., Arulbalaji, P. and Padmalal, D., 2020. Holocene climate variability and Indian Summer Monsoon: an overview. The Holocene, 30(5), pp.744-773.

Basu, S., Agrawal, S., Sanyal, P., Mahato, P., Kumar, S. and Sarkar, A., 2015. Carbon isotopic ratios of modern C_3–C_4 plants from the Gangetic Plain, India and its implications to paleovegetational reconstruction. Palaeogeography, Palaeoclimatology, Palaeoecology, 440, pp.22-32.

Basu, S., Sanyal, P., Pillai, A.A. and Ambili, A., 2019. Response of grassland ecosystem to monsoonal precipitation variability during the Mid-Late Holocene: Inferences based on molecular isotopic records from Banni grassland, western India. PloS one, 14(4), p.e0212743.

Berke, M.A., Sierra, A.C., Bush, R., Cheah, D. and O'Connor, K., 2019. Controls on leaf wax fractionation and δ^2H values in tundra vascular plants from western Greenland. Geochimica et Cosmochimica Acta, 244, pp.565-583.

Bi, X., Sheng, G., Liu, X., Li, C. and Fu, J., 2005. Molecular and carbon and hydrogen isotopic composition of *n*-alkanes in plant leaf waxes. Organic geochemistry, 36(10), pp.1405-1417.

Bombardi, R.J., Kinter, J.L. and Frauenfeld, O.W., 2019. A global gridded dataset of the characteristics of the rainy and dry seasons. Bulletin of the American Meteorological Society, 100(7), pp.1315-1328.

Bonnefille, R. and Chalie, F., 2000. Pollen-inferred precipitation time-series from equatorial mountains, Africa, the last 40 kyr BP. Global and Planetary Change, 26(1-3), pp.25-50.

Bowen, G.J. and Revenaugh, J., 2003. Interpolating the isotopic composition of modern meteoric precipitation. Water resources research, 39(10).

Burton, K.W. and Vance, D., 2000. Glacial–interglacial variations in the neodymium isotope composition of seawater in the Bay of Bengal recorded by planktonic foraminifera. Earth and Planetary Science Letters, 176(3-4), pp.425-441.

Bush, R.T. and McInerney, F.A., 2013. Leaf wax *n*-alkane distributions in and across modern plants: Implications for paleoecology and chemotaxonomy. Geochimica et Cosmochimica Acta, 117, pp.161-179.

Cai, Y., Fung, I.Y., Edwards, R.L., An, Z., Cheng, H., Lee, J.E., Tan, L., Shen, C.C., Wang, X., Day, J.A. and Zhou, W., 2015. Variability of stalagmite-inferred Indian monsoon precipitation over the past 252,000 y. Proceedings of the National Academy of Sciences, 112(10), pp.2954-2959.

Cerda-Pena, C. and Contreras, S., 2022. Characterization and chemo-taxonomic evaluation of plant leaf waxes (long chain *n*-alkanoic acids, *n*-alkanes and *n*-alkanols) as a vegetation biomarker from species of the South American temperate forest (STF). Ecological Indicators, 136, p.108675.

Cerling, T.E., Harris, J.M., MacFadden, B.J., Leakey, M.G., Quade, J., Eisenmann, V. and Ehleringer, J.R., 1997. Global vegetation change through the Miocene/Pliocene boundary. Nature, 389(6647), pp.153-158.

Cerling, T.E., Wynn, J.G., Andanje, S.A., Bird, M.I., Korir, D.K., Levin, N.E., Mace, W., Macharia, A.N., Quade, J. and Remien, C.H., 2011. Woody cover and hominin environments in the past 6 million years. Nature, 476(7358), pp.51-56.

Cernusak, L.A., Aranda, J., Marshall, J.D. and Winter, K., 2007. Large variation in whole-plant water-use efficiency among tropical tree species. New Phytologist, 173(2), pp.294-305.

Cernusak, L.A., Barbour, M.M., Arndt, S.K., Cheesman, A.W., English, N.B., Feild, T.S., Helliker, B.R., Holloway-Phillips, M.M., Holtum, J.A., Kahmen, A. and McInerney, F.A., 2016. Stable isotopes in leaf water of terrestrial plants. Plant, Cell & Environment, 39(5), pp.1087-1102.

Chakrabarty, S., Sharma, S., Ganguly, S., Jezeera, A., Mohanbabu, N. and Barua, D., 2021. Quantitative estimates of deciduousness in woody species from a seasonally dry tropical forest are related to leaf functional traits and the timing of leaf flush. BioRxiv, pp.2021-03.

Champion, H. G., & Seth, S. K.,1968. A revised survey of the forest types of India. Government of India. Natraj Publisher, New Delhi.

Chevalier, M., Davis, B.A., Heiri, O., Seppä, H., Chase, B.M., Gajewski, K., Lacourse, T., Telford, R.J., Finsinger, W., Guiot, J. and Kühl, N., 2020. Pollen-based climate reconstruction techniques for late Quaternary studies. Earth-Science Reviews, 210, p.103384.

Chikaraishi, Y. and Naraoka, H., 2003. Compound-specific δD–δ^{13}C analyses of *n*-alkanes extracted from terrestrial and aquatic plants. Phytochemistry, 63(3), pp.361-371.

Chikaraishi, Y. and Naraoka, H., 2006. Carbon and hydrogen isotope variation of plant biomarkers in a plant–soil system. Chemical Geology, 231(3), pp.190-202.

Chikaraishi, Y. and Naraoka, H., 2007. δ^{13}C and δD relationships among three *n*-alkyl compound classes (*n*-alkanoic acid, *n*-alkane and *n*-alkanol) of terrestrial higher plants. Organic Geochemistry, 38(2), pp.198-215.

Chikaraishi, Y., Naraoka, H. and Poulson, S.R., 2004. Carbon and hydrogen isotopic fractionation during lipid biosynthesis in a higher plant (Cryptomeria japonica). Phytochemistry, 65(3), pp.323-330.

Codron, J., Lee-Thorp, J.A., Sponheimer, M. and Codron, D., 2013. Plant stable isotope composition across habitat gradients in a semi-arid savanna: implications for environmental reconstruction. Journal of Quaternary Science, 28(3), pp.301-310.

Collins, J.A., Schefuß, E., Mulitza, S., Prange, M., Werner, M., Tharammal, T., Paul, A. and Wefer, G., 2013. Estimating the hydrogen isotopic composition of past precipitation using leaf-waxes from western Africa. Quaternary Science Reviews, 65, pp.88-101.

Corcoran, M.C., Diefendorf, A.F., Lowell, T.V., Hall, B.L., Spoth, M.M., Schartman, A. and Brickle, P., 2022. Hydrogen and carbon isotope fractionation in modern plant wax *n*-alkanes from the Falkland Islands. Organic Geochemistry, 166, p.104404.

Curtin, L., D'Andrea, W.J., Balascio, N., Pugsley, G., de Wet, G. and Bradley, R., 2019. Holocene and Last Interglacial climate of the Faroe Islands from sedimentary plant wax hydrogen and carbon isotopes. Quaternary Science Reviews, 223, p.105930.

Daniels, W.C., Russell, J.M., Giblin, A.E., Welker, J.M., Klein, E.S. and Huang, Y., 2017. Hydrogen isotope fractionation in leaf waxes in the Alaskan Arctic tundra. Geochimica et Cosmochimica Acta, 213, pp.216-236.

Dansgaard, W., 1964. Stable isotopes in precipitation. tellus, 16(4), pp.436-468.

Dasgupta, B., Ajay, A., Prakash, P. and Sanyal, P., 2022. Understanding the disparity in *n*-alkane production among angiosperms and gymnosperms from the higher Himalayas: Inferences drawn from a Machine Learning approach. Organic Geochemistry, 171, p.104463.

Dayem, K.E., Molnar, P., Battisti, D.S. and Roe, G.H., 2010. Lessons learned from oxygen isotopes in modern precipitation applied to interpretation of speleothem records of paleoclimate from eastern Asia. Earth and Planetary Science Letters, 295(1-2), pp.219-230.

Dee, S., Noone, D., Buenning, N., Emile-Geay, J. and Zhou, Y., 2015. SPEEDY-IER: A fast atmospheric GCM with water isotope physics. Journal of Geophysical Research: Atmospheres, 120(1), pp.73-91.

Deshpande S., Sharma B.D., Nayar M.P., 1993. Flora adjoining areas of Mahabaleshwar 1. Botanical Survey of India.

Deshpande, R.D., Maurya, A.S., Kumar, B., Sarkar, A. and Gupta, S.K., 2013. Kinetic fractionation of water isotopes during liquid condensation under super-saturated condition. Geochimica et Cosmochimica Acta, 100, pp.60-72.

Diefendorf, A.F. and Freimuth, E.J., 2017. Extracting the most from terrestrial plant-derived *n*-alkyl lipids and their carbon isotopes from the sedimentary record: A review. Organic Geochemistry, 103, pp.1-21.

Diefendorf, A.F., Freeman, K.H., Wing, S.L. and Graham, H.V., 2011. Production of *n*-alkyl lipids in living plants and implications for the geologic past. Geochimica et Cosmochimica Acta, 75(23), pp.7472-7485.

Diefendorf, A.F., Mueller, K.E., Wing, S.L., Koch, P.L. and Freeman, K.H., 2010. Global patterns in leaf ^{13}C discrimination and implications for studies of past and future climate. Proceedings of the National Academy of Sciences, 107(13), pp.5738-5743.

Douglas, P.M., Pagani, M., Brenner, M., Hodell, D.A. and Curtis, J.H., 2012. Aridity and vegetation composition are important determinants of leaf-wax δD values in southeastern Mexico and Central America. Geochimica et Cosmochimica Acta, 97, pp.24-45.

Du, X., Hendy, I., Hinnov, L., Brown, E., Zhu, J. and Poulsen, C.J., 2021. High-resolution interannual precipitation reconstruction of Southern California: Implications for Holocene ENSO evolution. Earth and Planetary Science Letters, 554, p.116670.

Duan, Y. and Xu, L., 2012. Distributions of *n*-alkanes and their hydrogen isotopic composition in plants from Lake Qinghai (China) and the surrounding area. Applied geochemistry, 27(3), pp.806-814.

Duan, Y., Wu, Y., Cao, X., Zhao, Y. and Ma, L., 2014. Hydrogen isotope ratios of individual *n*-alkanes in plants from Gannan Gahai Lake (China) and surrounding area. Organic geochemistry, 77, pp.96-105.

FAO 2000. Global Forest Resources Assessment 2000 – main report. FAO Forestry Paper No. 140.Rome. www.fao.org/forestry/country/19971/en/ind/

Farquhar, G.D. and Lloyd, J., 1993. Carbon and oxygen isotope effects in the exchange of carbon dioxide between terrestrial plants and the atmosphere. In Stable isotopes and plant carbon-water relations (pp. 47-70). Academic Press.

Farquhar, G.D., 1983. On the nature of carbon isotope discrimination in C_4 species. Functional Plant Biology, 10(2), pp.205-226.

Feakins, S.J. and Sessions, A.L., 2010. Controls on the D/H ratios of plant leaf waxes in an arid ecosystem. Geochimica et Cosmochimica Acta, 74(7), pp.2128-2141.

Feakins, S.J. and Sessions, A.L., 2010. Controls on the D/H ratios of plant leaf waxes in an arid ecosystem. Geochimica et Cosmochimica Acta, 74(7), pp.2128-2141.

Feakins, S.J., Bentley, L.P., Salinas, N., Shenkin, A., Blonder, B., Goldsmith, G.R., Ponton, C., Arvin, L.J., Wu, M.S., Peters, T. and West, A.J., 2016. Plant leaf wax biomarkers capture gradients in hydrogen isotopes of precipitation from the Andes and Amazon. Geochimica et Cosmochimica Acta, 182, pp.155-172.

Feakins, S.J., Kirby, M.E., Cheetham, M.I., Ibarra, Y. and Zimmerman, S.R., 2014. Fluctuation in leaf wax D/H ratio from a southern California lake records significant variability in isotopes in precipitation during the late Holocene. Organic Geochemistry, 66, pp.48-59.

Feakins, S.J., Peters, T., Wu, M.S., Shenkin, A., Salinas, N., Girardin, C.A., Bentley, L.P., Blonder, B., Enquist, B.J., Martin, R.E. and Asner, G.P., 2016a. Production of leaf wax *n*-alkanes across a tropical forest elevation transect. Organic Geochemistry, 100, pp.89-100.

Feakins, S.J., Wu, M.S., Ponton, C. and Tierney, J.E., 2019. Biomarkers reveal abrupt switches in hydroclimate during the last glacial in southern California. Earth and Planetary Science Letters, 515, pp.164-172.

Feakins, S.J., Wu, M.S., Ponton, C. and Tierney, J.E., 2019. Biomarkers reveal abrupt switches in hydroclimate during the last glacial in southern California. Earth and Planetary Science Letters, 515, pp.164-172

Feng, Z.D., Wang, L.X., Ji, Y.H., Guo, L.L., Lee, X.Q. and Dworkin, S.I., 2008. Climatic dependency of soil organic carbon isotopic composition along the S–N Transect from 34 N to 52 N in central-east Asia. Palaeogeography, Palaeoclimatology, Palaeoecology, 257(3), pp.335-343.

Flanagan, L.B. and Ehleringer, J.R., 1991. Stable isotope composition of stem and leaf water: applications to the study of plant water use. Functional Ecology, pp.270-277.

Flato, G., J. Marotzke, B. Abiodun, P. Braconnot, S.C. Chou, W. Collins, P. Cox, F. Driouech, S. Emori, V. Eyring, C. Forest, P. Gleckler, E. Guilyardi, C. Jakob, V. Kattsov, C. Reason and M. Rummukainen, 2013: Evaluation of Climate Models. In: Climate Change 2013: The Physical Science Basis. Contribution of Working Group I to the Fifth Assessment Report of the Intergovernmental Panel on Climate Change [Stocker, T.F., D. Qin, G.-K. Plattner, M. Tignor, S.K. Allen, J. Boschung, A. Nauels, Y. Xia, V. Bex and P.M. Midgley (eds.)]. Cambridge University Press, Cambridge, United Kingdom and New York, NY, USA.

FRA 2000. Global Ecological Zoning for The Global Forest Resources Assessment 2000. Final report Rome, 2001. Forest Resources Assessment Programme, Working Paper 56, Rome 2001.

Freimuth, E.J., Diefendorf, A.F. and Lowell, T.V., 2017. Hydrogen isotopes of *n*-alkanes and *n*-alkanoic acids as tracers of precipitation in a temperate forest and implications for paleorecords. Geochimica et Cosmochimica Acta, 206, pp.166-183.

Fritts, H.C., Vaganov, E.A., Sviderskaya, I.V. and Shashkin, A.V., 1991. Climatic variation and tree-ring structure in conifers: empirical and mechanistic models of tree-ring width, number of cells, cell size, cell-wall thickness and wood density. Climate Research, pp.97-116.

Gadgil, S., 2003. The Indian monsoon and its variability. Annual Review of Earth and Planetary Sciences, 31(1), pp.429-467.

Galy, V., Eglinton, T., France-Lanord, C. and Sylva, S., 2011. The provenance of vegetation and environmental signatures encoded in vascular plant biomarkers carried by the Ganges–Brahmaputra rivers. Earth and Planetary Science Letters, 304(1-2), pp.1-12.

Galy, V., François, L., France-Lanord, C., Faure, P., Kudrass, H., Palhol, F. and Singh, S.K., 2008. C_4 plants decline in the Himalayan basin since the Last Glacial Maximum. Quaternary Science Reviews, 27(13-14), pp.1396-1409.

Gamarra, B. and Kahmen, A., 2015. Concentrations and δ^2H values of cuticular *n*-alkanes vary significantly among plant organs, species and habitats in grasses from an alpine and a temperate European grassland. Oecologia, 178, pp.981-998.

Gamarra, B., Sachse, D. and Kahmen, A., 2016. Effects of leaf water evaporative ^2H-enrichment and biosynthetic fractionation on leaf wax *n*-alkane δ^2H values in C_3 and C_4 grasses. Plant, cell & environment, 39(11), pp.2390-2403.

Gao, L., Burnier, A. and Huang, Y., 2012. Quantifying instantaneous regeneration rates of plant leaf waxes using stable hydrogen isotope labeling. Rapid Communications in Mass Spectrometry, 26(2), pp.115-122.

Gao, L., Edwards, E.J., Zeng, Y. and Huang, Y., 2014. Major evolutionary trends in hydrogen isotope fractionation of vascular plant leaf waxes. PloS one, 9(11), p.e112610.

Gao, L., Guimond, J., Thomas, E. and Huang, Y., 2015. Major trends in leaf wax abundance, δ^2H and $\delta^{13}C$ values along leaf venation in five species of C_3 plants: physiological and geochemical implications. Organic Geochemistry, 78, pp.144-152.

Garcin, Y., Schwab, V.F., Gleixner, G., Kahmen, A., Todou, G., Séné, O., Onana, J.M., Achoundong, G. and Sachse, D., 2012. Hydrogen isotope ratios of lacustrine sedimentary *n*-alkanes as proxies of tropical African hydrology: insights from a calibration transect across Cameroon. Geochimica et Cosmochimica Acta, 79, pp.106-126.

Garrigues, J.P., 1999. Action anthropique sur la dynamique des formations végétales au sud de l'Inde (Ghâts occidentaux, Etat du Karnataka, District de Shimoga). Unpublished PhD Thesis, Université Claude Bernard–Lyon I, Villeurbanne.

Ghosh, S., Sanyal, P., Roy, S., Bhushan, R., Sati, S.P., Philippe, A. and Juyal, N., 2020. Early Holocene Indian summer monsoon and its impact on vegetation in the Central Himalaya: Insight from δD and $\delta^{13}C$ values of leaf wax lipid. The Holocene, 30(7), pp.1063-1074.

Grice, K., Schouten, S., Wong, S.C., Stuart-Williams, H. and Farquhar, G., 2004. D/H isotopes of water, lipids and carbohydrates from modern plants grown under controlled conditions. Organic matter: Interfaces and interactions, p.66.

Griepentrog, M., De Wispelaere, L., Bauters, M., Bodé, S., Hemp, A., Verschuren, D. and Boeckx, P., 2019. Influence of plant growth form, habitat and season on leaf-wax *n*-alkane hydrogen-isotopic signatures in equatorial East Africa. Geochimica et Cosmochimica Acta, 263, pp.122-139.

Guiot, J., Harrison, S.P. and Prentice, I.C., 1993. Reconstruction of Holocene precipitation patterns in Europe using pollen and lake-level data. Quaternary Research, 40(2), pp.139-149.

Hartman, G. and Danin, A., 2010. Isotopic values of plants in relation to water availability in the Eastern Mediterranean region. Oecologia, 162, pp.837-852.

Haug, G.H., Hughen, K.A., Sigman, D.M., Peterson, L.C. and Rohl, U., 2001. Southward migration of the intertropical convergence zone through the Holocene. Science, 293(5533), pp.1304-1308.

Haywood, A.M., Valdes, P.J., Aze, T., Barlow, N., Burke, A., Dolan, A.M., Von Der Heydt, A.S., Hill, D.J., Jamieson, S.S., Otto-Bliesner, B.L. and Salzmann, U., 2019. What can palaeoclimate modelling do for you?. Earth Systems and Environment, 3, pp.1-18.

Hendy, I.L., Napier, T.J. and Schimmelmann, A., 2015. From extreme rainfall to drought: 250 years of annually resolved sediment deposition in Santa Barbara Basin, California. Quaternary International, 387, pp.3-12

Herrmann, N., Boom, A., Carr, A.S., Chase, B.M., West, A.G., Zabel, M. and Schefuß, E., 2017. Hydrogen isotope fractionation of leaf wax *n*-alkanes in southern African soils. Organic Geochemistry, 109, pp.1-13.

Hou, J., D'Andrea, W.J. and Huang, Y., 2008. Can sedimentary leaf waxes record D/H ratios of continental precipitation? Field, model, and experimental assessments. Geochimica et Cosmochimica Acta, 72(14), pp.3503-3517.

Hou, J., D'Andrea, W.J., MacDonald, D. and Huang, Y., 2007. Hydrogen isotopic variability in leaf waxes among terrestrial and aquatic plants around Blood Pond, Massachusetts (USA). Organic Geochemistry, 38(6), pp.977-984.

Hren, M.T., Pagani, M., Erwin, D.M. and Brandon, M., 2010. Biomarker reconstruction of the early Eocene paleotopography and paleoclimate of the northern Sierra Nevada. Geology, 38(1), pp.7-10.

Huang, X., Zhao, B., Wang, K., Hu, Y. and Meyers, P.A., 2018. Seasonal variations of leaf wax *n*-alkane molecular composition and δD values in two subtropical deciduous tree species: Results from a three-year monitoring program in central China. Organic Geochemistry, 118, pp.15-26.

Huang, Y., Shuman, B., Wang, Y. and Webb, T., 2004. Hydrogen isotope ratios of individual lipids in lake sediments as novel tracers of climatic and environmental change: a surface sediment test. Journal of Paleolimnology, 31, pp.363-375.

India Meteorological Department *Climatological Normals*: (1981 - 2010)

IPCC, 2023: Summary for Policymakers. In: Climate Change 2023: Synthesis Report.Contribution of Working Groups I, II and III to the Sixth Assessment Report of the Intergovernmental Panel on Climate Change [Core Writing Team, H. Lee and J. Romero (eds.)]. IPCC, Geneva, Switzerland, pp. 1-34, doi: 10.59327/IPCC/AR6-9789291691647.001

Jambrina-Enríquez, M., Mallol, C., Tostevin, G., Monnier, G., Pajović, G., Borovinić, N. and Baković, M., 2022. Hydroclimate reconstruction through MIS 3 in the Middle Paleolithic site of Crvena Stijena (Montenegro) based on hydrogen-isotopic composition of sedimentary *n*-alkanes. Quaternary Science Reviews, 295, p.107771.

Jetter, R., Kunst, L. and Samuels, A.L., 2006. Composition of plant cuticular waxes. Annual plant reviews volume 23: Biology of the plant cuticle, pp.145-181.

Jia, G., Wei, K. and Chen, F., 2008. Soil *n*-alkane δD vs. altitude gradients along Mount Gongga, China. Geochimica et Cosmochimica Acta, 72(21), pp.5165-5174.

Joshi, A.A., Ratnam, J. and Sankaran, M., 2020. Frost maintains forests and grasslands as alternate states in a montane tropical forest–grassland mosaic; but alien tree invasion and warming can disrupt this balance. Journal of Ecology, 108(1), pp.122-132.

Kagawa, A., Sugimoto, A. and Maximov, T.C., 2006. $^{13}CO_2$ pulse-labelling of photoassimilates reveals carbon allocation within and between tree rings. Plant, Cell & Environment, 29(8), pp.1571-1584.

Kahmen, A., Dawson, T.E., Vieth, A. and Sachse, D., 2011. Leaf wax *n*-alkane δD values are determined early in the ontogeny of Populus trichocarpa leaves when grown under controlled environmental conditions. Plant, Cell & Environment, 34(10), pp.1639-1651.

Kahmen, A., Schefuß, E. and Sachse, D., 2013. Leaf water deuterium enrichment shapes leaf wax *n*-alkane δD values of angiosperm plants I: Experimental evidence and mechanistic insights. Geochimica et Cosmochimica Acta, 111, pp.39-49.

Kirkels, F.M., De Boer, H.J., Concha Hernández, P., Martes, C.R., Van Der Meer, M.T., Basu, S., Usman, M.O. and Peterse, F., 2022. Carbon isotopic ratios of modern C_3 and C_4 vegetation on the Indian peninsula and changes along the plant–soil–river continuum–implications for vegetation reconstructions. Biogeosciences, 19(17), pp.4107-4127.

Knapp, S., Burls, N.J., Dee, S., Feng, R., Feakins, S.J. and Bhattacharya, T., 2022. A Pliocene Precipitation Isotope Proxy-Model Comparison Assessing the Hydrological Fingerprints of Sea Surface Temperature Gradients. Paleoceanography and Paleoclimatology, 37(12), p.e2021PA004401.Kohn, M.J., 2010. Carbon isotope compositions of terrestrial C_3 plants as indicators of (paleo) ecology and (paleo) climate. Proceedings of the National Academy of Sciences, 107(46), pp.19691-19695.

Konecky, B., Russell, J. and Bijaksana, S., 2016. Glacial aridity in central Indonesia coeval with intensified monsoon circulation. Earth and Planetary Science Letters, 437, pp.15-24.

Konecky, B.L., Russell, J.M., Johnson, T.C., Brown, E.T., Berke, M.A., Werne, J.P. and Huang, Y., 2011. Atmospheric circulation patterns during late Pleistocene climate changes at Lake Malawi, Africa. Earth and Planetary Science Letters, 312(3-4), pp.318-326.

Krull, E., Sachse, D., Mügler, I., Thiele, A. and Gleixner, G., 2006. Compound-specific $\delta^{13}C$ and $\delta^{2}H$ analyses of plant and soil organic matter: A preliminary assessment of the effects of vegetation change on ecosystem hydrology. Soil Biology and Biochemistry, 38(11), pp.3211-3221.

Kumaran, K.P.N., Limaye, R.B., Punekar, S.A., Rajaguru, S.N., Joshi, S.V. and Karlekar, S.N., 2013. Vegetation response to South Asian Monsoon variations in Konkan, western India during the Late Quaternary: Evidence from fluvio-lacustrine archives. Quaternary International, 286, pp.3-18.

Kushwaha, C.P. and Singh, K.P., 2005. Diversity of leaf phenology in a tropical deciduous forest in India. Journal of Tropical Ecology, 21(1), pp.47-56.

Ladd, S.N., Maloney, A.E., Nelson, D.B., Prebble, M., Camperio, G., Sear, D.A., Hassall, J.D., Langdon, P.G., Sachs, J.P. and Dubois, N., 2021. Leaf wax hydrogen isotopes as a hydroclimate proxy in the tropical Pacific. Journal of Geophysical Research: Biogeosciences, 126(3), p.e2020JG005891.

Lee, X., Feng, Z., Guo, L., Wang, L., Jin, L., Huang, Y., Chopping, M., Huang, D., Jiang, W., Jiang, Q. and Cheng, H., 2005. Carbon isotope of bulk organic matter: A proxy for precipitation in the arid and semiarid central East Asia. Global Biogeochemical Cycles, 19(4).

Levin, N.E., Zipser, E.J. and Cerling, T.E., 2009. Isotopic composition of waters from Ethiopia and Kenya: Insights into moisture sources for eastern Africa. Journal of Geophysical Research: Atmospheres, 114(D23).

Li, Q., Chen, X., Yuan, W., Lu, H., Shen, R., Wu, S., Gong, F., Dai, Y., Liu, L., Sun, Q. and Zhang, C., 2021. Remote sensing of seasonal climatic constraints on leaf phenology across pantropical evergreen forest biome. Earth's Future, 9(9), p.e2021EF002160.

Li, Y., Yang, S., Luo, P. and Xiong, S., 2019. Aridity-controlled hydrogen isotope fractionation between soil *n*-alkanes and precipitation in China. Organic Geochemistry, 133, pp.53-64.

Liu, J. and An, Z., 2019. Variations in hydrogen isotopic fractionation in higher plants and sediments across different latitudes: Implications for paleohydrological reconstruction. Science of the Total Environment, 650, pp.470-478.

Liu, J. and An, Z., 2019. Variations in hydrogen isotopic fractionation in higher plants and sediments across different latitudes: Implications for paleohydrological reconstruction. Science of the Total Environment, 650, pp.470-478.

Liu, J., An, Z., Wang, Z. and Wu, H., 2017. Using δD *n*-alkane as a proxy for paleo-environmental reconstruction: A good choice to sample at the site dominated by woods. Science of the total environment, 599, pp.554-559.

Liu, J., Liu, W., An, Z. and Yang, H., 2016. Different hydrogen isotope fractionations during lipid formation in higher plants: Implications for paleohydrology reconstruction at a global scale. Scientific reports, 6(1), p.19711.

Liu, M., Prentice, I.C., Ter Braak, C.J. and Harrison, S.P., 2020. An improved statistical approach for reconstructing past climates from biotic assemblages. Proceedings of the Royal Society A, 476(2243), p.20200346.

Liu, W. and Yang, H., 2008. Multiple controls for the variability of hydrogen isotopic compositions in higher plant *n*-alkanes from modern ecosystems. Global Change Biology, 14(9), pp.2166-2177.

Liu, W., Huang, Y., 2005. Compound specific D/H ratios and molecular distributions of higher plant leaf waxes as novel paleoenvironmental indicators in the Chinese Loess Plateau. Organic geochemistry, 36(6), pp.851-860.

Liu, W., Huang, Y., An, Z., Clemens, S.C., Li, L., Prell, W.L. and Ning, Y., 2005. Summer monsoon intensity controls C_4/C_3 plant abundance during the last 35 ka in the Chinese Loess Plateau: carbon isotope evidence from bulk organic matter and individual leaf waxes. Palaeogeography, Palaeoclimatology, Palaeoecology, 220(3-4), pp.243-254.

Lu, J., Zang, J., Meyers, P., Huang, X., Qiu, P., Yu, X., Yang, H. and Xie, S., 2020. Surface soil *n*-alkane molecular and δD distributions along a precipitation transect in northeastern China. Organic Geochemistry, 144, p.104015.

Ma, J.Y., Sun, W., Liu, X.N. and Chen, F.H., 2012. Variation in the stable carbon and nitrogen isotope composition of plants and soil along a precipitation gradient in northern China. PloS one, 7(12), p.e51894.

Majoube, M., 1971. Oxygen-18 and deuterium fractionation between water and steam (in French). Journal de Chimie Physique et de Physico-Chimie Biologique, 68, pp.1423-1436.

Managave, S., Huang, Y., Sutra, J.P., Anupama, K. and Prasad, S., 2023. Holocene precipitation hydrogen isotopic values on Nilgiri Plateau (southern India) suggest a combined effect of precipitation amount and transport paths. The Holocene, 33(10), pp.1186-1195.

Managave, S.R., 2014. Model evaluation of the coherence of a common source water oxygen isotopic signal recorded by tree-ring cellulose and speleothem calcite. Geochemistry, Geophysics, Geosystems, 15(4), pp.905-922.

Managave, S.R., Sheshshayee, M.S., Bhattacharyya, A. and Ramesh, R., 2011. Intra-annual variations of teak cellulose $\delta^{18}O$ in Kerala, India: implications to the reconstruction of past summer and winter monsoon rains. Climate dynamics, 37, pp.555-567.

Martinez-Ruiz, F., Kastner, M., Gallego-Torres, D., Rodrigo-Gámiz, M., Nieto-Moreno, V. and Ortega-Huertas, M., 2015. Paleoclimate and paleoceanography over the past 20,000 yr in the Mediterranean Sea Basins as indicated by sediment elemental proxies. Quaternary Science Reviews, 107, pp.25-46.

Mattey, D., Lowry, D., Duffet, J., Fisher, R., Hodge, E. and Frisia, S., 2008. A 53 year seasonally resolved oxygen and carbon isotope record from a modern Gibraltar speleothem: reconstructed drip water and relationship to local precipitation. Earth and Planetary Science Letters, 269(1-2), pp.80-95.

McDermott, F., 2004. Palaeo-climate reconstruction from stable isotope variations in speleothems: a review. Quaternary Science Reviews, 23(7-8), pp.901-918.

McGrath, S.M., Clemens, S.C., Huang, Y. and Yamamoto, M., 2021. Greenhouse gas and ice volume drive Pleistocene Indian summer monsoon precipitation isotope variability. Geophysical Research Letters, 48(4), p.e2020GL092249.

McInerney, F.A., Helliker, B.R. and Freeman, K.H., 2011. Hydrogen isotope ratios of leaf wax *n*-alkanes in grasses are insensitive to transpiration. Geochimica et Cosmochimica Acta, 75(2), pp.541-554.

McInerney, F.A., Helliker, B.R. and Freeman, K.H., 2011. Hydrogen isotope ratios of leaf wax *n*-alkanes in grasses are insensitive to transpiration. Geochimica et Cosmochimica Acta, 75(2), pp.541-554.

Mediavilla, S. and Escudero, A., 2003. Stomatal responses to drought at a Mediterranean site: a comparative study of co-occurring woody species differing in leaf longevity. Tree physiology, 23(14), pp.987-996.

Misra, P., Tandon, S.K. and Sinha, R., 2019. Holocene climate records from lake sediments in India: Assessment of coherence across climate zones. Earth-Science Reviews, 190, pp.370-397.

Mooley, D.A. and Parthasarathy, B., 1983. Variability of the Indian summer monsoon and tropical circulation features. Monthly Weather Review, 111(5), pp.967-978.

Morales, M.S., Christie, D.A., Villalba, R., Argollo, J., Pacajes, J., Silva, J.S., Alvarez, C.A., Llancabure, J.C. and Soliz Gamboa, C.C., 2012. Precipitation changes in the South American Altiplano since 1300 AD reconstructed by tree-rings. Climate of the Past, 8(2), pp.653-666.

Morrill, C., Overpeck, J.T. and Cole, J.E., 2003. A synthesis of abrupt changes in the Asian summer monsoon since the last deglaciation. The Holocene, 13(4), pp.465-476.

Murphy, B.P. and Bowman, D.M., 2009. The carbon and nitrogen isotope composition of Australian grasses in relation to climate. Functional Ecology, 23(6), pp.1040-1049.

Niedermeyer, E.M., Forrest, M., Beckmann, B., Sessions, A.L., Mulch, A. and Schefuß, E., 2016. The stable hydrogen isotopic composition of sedimentary plant waxes as quantitative proxy for rainfall in the West African Sahel. Geochimica et Cosmochimica Acta, 184, pp.55-70.

Niedermeyer, E.M., Schefuß, E., Sessions, A.L., Mulitza, S., Mollenhauer, G., Schulz, M. and Wefer, G., 2010. Orbital-and millennial-scale changes in the hydrologic cycle and vegetation in the western African Sahel: insights from individual plant wax δD and $\delta^{13}C$. Quaternary Science Reviews, 29(23-24), pp.2996-3005.

Nordt, L., Von Fischer, J., Tieszen, L. and Tubbs, J., 2008. Coherent changes in relative C_4 plant productivity and climate during the late Quaternary in the North American Great Plains. Quaternary Science Reviews, 27(15-16), pp.1600-1611.

Nusbaumer, J., Wong, T.E., Bardeen, C. and Noone, D., 2017. Evaluating hydrological processes in the C ommunity A tmosphere M odel V ersion 5 (C AM5) using stable isotope ratios of water. Journal of Advances in Modeling Earth Systems, 9(2), pp.949-977.

O'Connor, K.F., Berke, M.A. and Ziolkowski, L.A., 2020. Hydrogen isotope fractionation in modern plants along a boreal-tundra transect in Alaska. Organic Geochemistry, 147, p.104064.

O'Leary, M.H., 1988. Carbon isotopes in photosynthesis. Bioscience, 38(5), pp.328-336.

Ortiz, J.E., Torres, T., Delgado, A., Valle, M., Soler, V., Araujo, R., Rivas, M.R., Julià, R., Sánchez-Palencia, Y. and Vega-Panizo, R., 2021. Bulk and compound-specific $\delta^{13}C$ and *n*-alkane indices in a palustrine intermontane record for assessing environmental changes over the past 320 ka: the Padul Basin (Southwestern Mediterranean realm). Journal of Iberian Geology, 47, pp.625-639.

Pagani, M., Pedentchouk, N., Huber, M., Sluijs, A., Schouten, S., Brinkhuis, H., Sinninghe Damsté, J.S. and Dickens, G.R., 2006. Arctic hydrology during global warming at the Palaeocene/Eocene thermal maximum. Nature, 442(7103), pp.671-675.

Pai D.S., Latha Sridhar, Rajeevan M., Sreejith O.P., Satbhai N.S. and Mukhopadhyay B., 2014: Development of a new high spatial resolution (0.25° X 0.25°) Long period (1901-2010) daily gridded rainfall data set over India and its comparison with existing data sets over the region; MAUSAM, 65, 1(January 2014), pp1-18.

Pedentchouk, N., Sumner, W., Tipple, B. and Pagani, M., 2008. $\delta^{13}C$ and δD compositions of *n*-alkanes from modern angiosperms and conifers: an experimental set up in central Washington State, USA. Organic Geochemistry, 39(8), pp.1066-1071.

Poynter, J. and Eglinton, G., 2014. Molecular composition of three sediments from hole 717C: the Bengal FAN1. In Proceedings of the Ocean Drilling Program, Scientific Results, College Station, TX (Ocean Drilling Program) ,pp. 151-161.

Prasad, S., Anoop, A., Riedel, N., Sarkar, S., Menzel, P., Basavaiah, N., Krishnan, R., Fuller, D., Plessen, B., Gaye, B. and Röhl, U., 2014. Prolonged monsoon droughts and links to Indo-Pacific warm pool: A Holocene record from Lonar Lake, central India. Earth and Planetary Science Letters, 391, pp.171-182.

Prasad, V., Farooqui, A., Sharma, A., Phartiyal, B., Chakraborty, S., Bhandari, S., Raj, R. and Singh, A., 2014. Mid–late Holocene monsoonal variations from mainland Gujarat, India: A multi-proxy study for evaluating climate culture relationship. Palaeogeography, Palaeoclimatology, Palaeoecology, 397, pp.38-51.

Ramesh, R., 2001. High resolution Holocene monsoon records from different proxies: An assessment of their consistency. Current Science, pp.1432-1436.

Ramesh, R., Sinha, D.K., Tiwari, M., Chakraborty, S., Managave, S.R. and Yadava, M.G., 2010. Retrieval of south Asian monsoon variation during the Holocene from natural climate archives. Current Science, pp.1770-1786.

Rao, Z., Zhu, Z., Jia, G., Zhang, X. and Wang, S., 2011. Compound-specific hydrogen isotopes of long-chain *n*-alkanes extracted from topsoil under a grassland ecosystem in northern China. Science China Earth Sciences, 54, pp.1902-1911.

Risi, C., Bony, S., Vimeux, F. and Jouzel, J., 2010. Water-stable isotopes in the LMDZ4 general circulation model: Model evaluation for present-day and past climates and applications to climatic interpretations of tropical isotopic records. Journal of Geophysical Research: Atmospheres, 115(D12).

Roden, J.S. and Ehleringer, J.R., 1999. Observations of hydrogen and oxygen isotopes in leaf water confirm the Craig-Gordon model under wide-ranging environmental conditions. Plant physiology, 120(4), pp.1165-1174.

Roden, J.S., Lin, G. and Ehleringer, J.R., 2000. A mechanistic model for interpretation of hydrogen and oxygen isotope ratios in tree-ring cellulose. Geochimica et Cosmochimica Acta, 64(1), pp.21-35.

Roy, B. and Sanyal, P., 2022. Isotopic and molecular distribution of leaf-wax in plant-soil system of the Gangetic floodplain and its implication for paleorecords. Quaternary International, 607, pp.89-99.

Rozanski, K., Johnsen, S.J., Schotterer, U. and Thompson, L.G., 1997. Reconstruction of past climates from stable isotope records of palaeo-precipitation preserved in continental archives. Hydrological sciences journal, 42(5), pp.725-745.

Sachse, D., Billault, I., Bowen, G.J., Chikaraishi, Y., Dawson, T.E., Feakins, S.J., Freeman, K.H., Magill, C.R., McInerney, F.A., Van Der Meer, M.T. and Polissar, P., 2012. Molecular paleohydrology: interpreting the hydrogen-isotopic composition of lipid biomarkers from photosynthesizing organisms. Annual Review of Earth and Planetary Sciences, 40, pp.221-249.

Sachse, D., Dawson, T.E. and Kahmen, A., 2015. Seasonal variation of leaf wax *n*-alkane production and δ^2H values from the evergreen oak tree, Quercus agrifolia. Isotopes in environmental and health studies, 51(1), pp.124-142.

Sachse, D., Gleixner, G., Wilkes, H. and Kahmen, A., 2010. Leaf wax *n*-alkane δD values of field-grown barley reflect leaf water δD values at the time of leaf formation. Geochimica et Cosmochimica Acta, 74(23), pp.6741-6750.

Sachse, D., Kahmen, A. and Gleixner, G., 2009. Significant seasonal variation in the hydrogen isotopic composition of leaf-wax lipids for two deciduous tree ecosystems (Fagus sylvativa and Acerpseudoplatanus). Organic Geochemistry, 40(6), pp.732-742.

Sachse, D., Radke, J. and Gleixner, G., 2006. δD values of individual *n*-alkanes from terrestrial plants along a climatic gradient–Implications for the sedimentary biomarker record. Organic Geochemistry, 37(4), pp.469-483.

Sage, R.F., 2004. The evolution of C_4 photosynthesis. New phytologist, 161(2), pp.341-370.

Sánchez-Murillo, R., Birkel, C., Welsh, K., Esquivel-Hernández, G., Corrales-Salazar, J., Boll, J., Brooks, E., Roupsard, O., Sáenz-Rosales, O., Katchan, I. and Arce-Mesén, R., 2016. Key drivers controlling stable isotope variations in daily precipitation of Costa Rica: Caribbean Sea versus Eastern Pacific Ocean moisture sources. Quaternary Science Reviews, 131, pp.250-261.

Sarangi, V., Agrawal, S. and Sanyal, P., 2021. The disparity in the abundance of C_4 plants estimated using the carbon isotopic composition of paleosol components. Palaeogeography, Palaeoclimatology, Palaeoecology, 561, p.110068.

Sarkar, S., Prasad, S., Wilkes, H., Riedel, N., Stebich, M., Basavaiah, N. and Sachse, D., 2015. Monsoon source shifts during the drying mid-Holocene: Biomarker isotope based evidence from the core 'monsoon zone'(CMZ) of India. Quaternary Science Reviews, 123, pp.144-157.

Sarkar, S., Wilkes, H., Prasad, S., Brauer, A., Riedel, N., Stebich, M., Basavaiah, N. and Sachse, D., 2014. Spatial heterogeneity in lipid biomarker distributions in the catchment and sediments of a crater lake in central India. Organic Geochemistry, 66, pp.125-136.

Sessions, A.L., 2006. Seasonal changes in D/H fractionation accompanying lipid biosynthesis in Spartina alterniflora. Geochimica et Cosmochimica Acta, 70(9), pp.2153-2162.

Sessions, A.L., Sylva, S.P., Summons, R.E. and Hayes, J.M., 2004. Isotopic exchange of carbon-bound hydrogen over geologic timescales. Geochimica et Cosmochimica Acta, 68(7), pp.1545-1559.

Sharmila, S., Joseph, S., Sahai, A.K., Abhilash, S. and Chattopadhyay, R., 2015. Future projection of Indian summer monsoon variability under climate change scenario: An assessment from CMIP5 climate models. Global and Planetary Change, 124, pp.62-78.

Shen, C.C., Lee, T., Liu, K.K., Hsu, H.H., Edwards, R.L., Wang, C.H., Lee, M.Y., Chen, Y.G., Lee, H.J. and Sun, H.T., 2005. An evaluation of quantitative reconstruction of past precipitation records using coral skeletal Sr/Ca and $\delta^{18}O$ data. Earth and Planetary Science Letters, 237(3-4), pp.370-386.

Shepherd, T. and Wynne Griffiths, D., 2006. The effects of stress on plant cuticular waxes. New Phytologist, 171(3), pp.469-499.

Shuman, B., Huang, Y., Newby, P. and Wang, Y., 2006. Compound-specific isotopic analyses track changes in seasonal precipitation regimes in the Northeastern United States at ca 8200 cal yr BP. Quaternary Science Reviews, 25(21-22), pp.2992-3002.

Singh, A., Paul, D., Sinha, R., Thomsen, K.J. and Gupta, S., 2016. Geochemistry of buried river sediments from Ghaggar Plains, NW India: Multi-proxy records of variations in provenance, paleoclimate, and paleovegetation patterns in the Late Quaternary. Palaeogeography, Palaeoclimatology, Palaeoecology, 449, pp.85-100.

Sinha, A., Cannariato, K.G., Stott, L.D., Cheng, H., Edwards, R.L., Yadava, M.G., Ramesh, R. and Singh, I.B., 2007. A 900-year (600 to 1500 AD) record of the Indian summer monsoon precipitation from the core monsoon zone of India. Geophysical Research Letters, 34(16).

Smith, F.A. and Freeman, K.H., 2006. Influence of physiology and climate on δD of leaf wax *n*-alkanes from C3 and C4 grasses. Geochimica et Cosmochimica Acta, 70(5), pp.1172-1187.

Stein, R.A., Sheldon, N.D. and Smith, S.Y., 2021. Soil carbon isotope values and paleoprecipitation reconstruction. Paleoceanography and Paleoclimatology, 36(4), p.e2020PA004158.

Stevenson, B.A., Kelly, E.F., McDonald, E.V. and Busacca, A.J., 2005. The stable carbon isotope composition of soil organic carbon and pedogenic carbonates along a bioclimatic gradient in the Palouse region, Washington State, USA. Geoderma, 124(1-2), pp.37-47.

Sturm, C., Zhang, Q. and Noone, D., 2010. An introduction to stable water isotopes in climate models: benefits of forward proxy modelling for paleoclimatology. Climate of the Past, 6(1),

pp.115-129.Sun, D., Gagan, M.K., Cheng, H., Scott-Gagan, H., Dykoski, C.A., Edwards, R.L. and Su, R., 2005. Seasonal and interannual variability of the Mid-Holocene East Asian monsoon in coral $\delta^{18}O$ records from the South China Sea. Earth and planetary science letters, 237(1-2), pp.69-84.

Swap, R.J., Aranibar, J.N., Dowty, P.R., Gilhooly III, W.P. and Macko, S.A., 2004. Natural abundance of ^{13}C and ^{15}N in C_3 and C_4 vegetation of southern Africa: patterns and implications. Global Change Biology, 10(3), pp.350-358.

Tang, H. and Dubayah, R., 2017. Light-driven growth in Amazon evergreen forests explained by seasonal variations of vertical canopy structure. Proceedings of the National Academy of Sciences, 114(10), pp.2640-2644.

Terwilliger, V.J., Eshetu, Z., Colman, A., Bekele, T., Gezahgne, A. and Fogel, M.L., 2008. Reconstructing palaeoenvironment from $\delta^{13}C$ and $\delta^{15}N$ values of soil organic matter: A calibration from arid and wetter elevation transects in Ethiopia. Geoderma, 147(3-4), pp.197-210.

Thomas, E.K., McGrane, S., Briner, J.P. and Huang, Y., 2012. Leaf wax $\delta^{2}H$ and varve-thickness climate proxies from proglacial lake sediments, Baffin Island, Arctic Canada. Journal of paleolimnology, 48, pp.193-207.

Tierney, J.E., Russell, J.M., Huang, Y., Damsté, J.S.S., Hopmans, E.C. and Cohen, A.S., 2008. Northern hemisphere controls on tropical southeast African climate during the past 60,000 years. science, 322(5899), pp.252-255.

Tipple, B.J. and Pagani, M., 2010. A 35 Myr North American leaf-wax compound-specific carbon and hydrogen isotope record: Implications for C_4 grasslands and hydrologic cycle dynamics. Earth and Planetary Science Letters, 299(1-2), pp.250-262.

Tipple, B.J. and Pagani, M., 2013. Environmental control on eastern broadleaf forest species' leaf wax distributions and D/H ratios. Geochimica et Cosmochimica Acta, 111, pp.64-77.

Tipple, B.J., Berke, M.A., Doman, C.E., Khachaturyan, S. and Ehleringer, J.R., 2013. Leaf-wax *n*-alkanes record the plant–water environment at leaf flush. Proceedings of the National Academy of Sciences, 110(7), pp.2659-2664.

Tipple, B.J., Berke, M.A., Hambach, B., Roden, J.S. and Ehleringer, J.R., 2015. Predicting leaf wax n-alkane $^{2}H/^{1}H$ ratios: controlled water source and humidity experiments with hydroponically grown trees confirm predictions of Craig–Gordon model. Plant, Cell & Environment, 38(6), pp.1035-1047.

Tiwari, M., Ramesh, R., Somayajulu, B.L.K., Jull, A.J.T. and Burr, G.S., 2006. Paleomonsoon precipitation deduced from a sediment core from the equatorial Indian Ocean. Geo-Marine Letters, 26, pp.23-30.

Tremaine, D.M., Froelich, P.N. and Wang, Y., 2011. Speleothem calcite farmed in situ: Modern calibration of $\delta^{18}O$ and $\delta^{13}C$ paleoclimate proxies in a continuously-monitored natural cave system. Geochimica et Cosmochimica Acta, 75(17), pp.4929-4950.

Turgeon, R., 1989. The sink-source transition in leaves. Annual review of plant biology, 40(1), pp.119-138.

Van Bloem, S., Lugo, A. E., Murphy, P. G., 2004. Regional Forest Types-Tropical Dry Forests. https://tigerprints.clemson.edu/forestry_env_pub/20

Van Schaik, C.P., Terborgh, J.W. and Wright, S.J., 1993. The phenology of tropical forests: adaptive significance and consequences for primary consumers. Annual Review of ecology and Systematics, 24(1), pp.353-377.

Vidic, N.J. and Montañez, I.P., 2004. Climatically driven glacial-interglacial variations in C_3 and C_4 plant proportions on the Chinese Loess Plateau. Geology, 32(4), pp.337-340.

Vittal, H., Villarini, G. and Zhang, W., 2020. Early prediction of the Indian summer monsoon rainfall by the Atlantic Meridional Mode. Climate dynamics, 54, pp.2337-2346.

Wang, G., Feng, X., Han, J., Zhou, L., Tan, W. and Su, F., 2008. Paleovegetation reconstruction using $\delta^{13}C$ of soil organic matter. Biogeosciences, 5(5), pp.1325-1337.

Weiguo, L., Xiahong, F., Youfeng, N., Qingle, Z., Yunning, C. and Zhisheng, A.N., 2005. $\delta^{13}C$ variation of C_3 and C_4 plants across an Asian monsoon rainfall gradient in arid northwestern China. Global Change Biology, 11(7), pp.1094-1100.

Werner, M., Langebroek, P.M., Carlsen, T., Herold, M. and Lohmann, G., 2011. Stable water isotopes in the ECHAM5 general circulation model: Toward high-resolution isotope modeling on a global scale. Journal of Geophysical Research: Atmospheres, 116(D15).

White, J.W., Cook, E.R. and Lawrence, J.R., 1985. The D/H ratios of sap in trees: Implications for water sources and tree ring D/H ratios. Geochimica et Cosmochimica Acta, 49(1), pp.237-246.

Wynn, J.G. and Bird, M.I., 2008. Environmental controls on the stable carbon isotopic composition of soil organic carbon: implications for modelling the distribution of C_3 and C_4 plants, Australia. Tellus B: Chemical and Physical Meteorology, 60(4), pp.604-621.

Yadava, M.G., Ramesh, R. and Pandarinath, K., 2007. A positive 'amount effect' in the Sahayadri (Western Ghats) rainfall. Current science, pp.560-564.

Yang, B., Qin, C., Wang, J., He, M., Melvin, T.M., Osborn, T.J. and Briffa, K.R., 2014. A 3,500-year tree-ring record of annual precipitation on the northeastern Tibetan Plateau. Proceedings of the National Academy of Sciences, 111(8), pp.2903-2908.

Yang, S., Ding, Z., Li, Y., Wang, X., Jiang, W. and Huang, X., 2015. Warming-induced northwestward migration of the East Asian monsoon rain belt from the Last Glacial Maximum to the mid-Holocene. Proceedings of the National Academy of Sciences, 112(43), pp.13178-13183.

Yang, Y., Zhang, Y. and Huang, X., 2021. Comparison of δ^2H values of leaf wax *n*-alkanes and *n*-alkanoic acids in subtropical angiosperms. Palaeogeography, Palaeoclimatology, Palaeoecology, 577, p.110537.

Yoshimura, K., Kanamitsu, M., Noone, D. and Oki, T., 2008. Historical isotope simulation using reanalysis atmospheric data. Journal of Geophysical Research: Atmospheres, 113(D19).

Youfeng, N., Weiguo, L. and Zhisheng, A., 2008. A 130-ka reconstruction of precipitation on the Chinese Loess Plateau from organic carbon isotopes. Palaeogeography, Palaeoclimatology, Palaeoecology, 270(1-2), pp.59-63.

Zech, M., Zech, R., Rozanski, K., Gleixner, G. and Zech, W., 2015. Do *n*-alkane biomarkers in soils/sediments reflect the δ^2H isotopic composition of precipitation? A case study from Mt.

Kilimanjaro and implications for paleoaltimetry and paleoclimate research. Isotopes in environmental and health studies, 51(4), pp.508-524.

Zhang, Z., Zhao, M., Lu, H. and Faiia, A.M., 2003. Lower temperature as the main cause of C_4 plant declines during the glacial periods on the Chinese Loess Plateau. Earth and Planetary Science Letters, 214(3-4), pp.467-481.

PUBLICATIONS

1. **Saishree, A.**, Managave, S., Sarangi, V. and Sanyal, P., 2023. Experimental evidence suggests dominance of species effect on the variability in hydrogen isotope fractionation between leaf wax compounds and source water. Organic Geochemistry, 183, p.104656.

2. **Saishree, A.**, Managave, S., Yadava. M.G., Devi S.M., and Sanyal, P., 2024. The δD records of *n*-alkane and *n*-alkanoic acid of tropical trees reflect δD of precipitation during the early stages of the leaf growth. ESS Open Archive.

3. Calibration of plant-derived isotope proxies against precipitation along a precipitation gradient in western peninsular India.
   Saishree et al. (In preparation)